# Optimal Control of Tube Drawing Processes

**Azhar Iqbal Kashif Butt**

Vom Fachbereich Mathematik
der Technischen Universität Kaiserslautern
zur Verleihung des Akademischen Grades
Doktor der Naturwissenschaften
(Doktor rerum naturalium, Dr. rer. nat.)
genehmigte Dissertation

1. Gutachter: Prof. Dr. René Pinnau

2. Gutachter: Prof. Dr. Michael Herty

Datum der Disputation: 28 September 2009

D386

*To the memories of my late father*

# Acknowledgements

I would like to express my sincere gratitude to my supervisor, Prof. Dr. René Pinnau, whose guidance, continuous encouragement and support right from the start to the end enabled me to successfully complete this work. He was always there to listen and to give advice. His constructive comments and remarks during the meetings we held together, helped me in understanding the problem and the relevant concepts.

I am also thankful to Prof. Dr. Michael Herty for accepting the request to be the second referee. His early report on my thesis enabled me to finish the things early. I also wish to thank Prof. Axel Klar for his support about administrative and academic matters during my PhD.

Let me also give thank to my colleagues (past and present) with whom I had a wonderful time and had very helpful discussions. Special thanks to M. Kimathi for proof-reading the manuscript. I am also obliged to Dr. Sudarshan Tiwari for his very friendly and always ready-to-help attitude.

There are no words to thank my parents who supported me over the years and brought me up to what I am today. I am greatly indebted to my wife Kashifa Zia and to my daughters Eshal Azhar and Menaal Fatima for their love, support and patience.

I greatly acknowledge the financial support from Higher Education Commission (HEC) Pakistan and the German Academic Exchange Service (DAAD) for the pursuit of this research work. The partial support from International School for Graduate Studies (ISGS) and the Technical University of Kaiserslautern is also acknowledged.

Azhar Iqbal Kashif Butt

# Contents

# Chapter 1

# Introduction

Glass tubes are drawn from a source of molten glass by means of various processes. The most popular of which are the Danner process, the Vello process and the Down draw process (see Fig. 1.1). In each of these processes, with some variations in mechanism, the molten glass flows through a feeder channel on the surface of a cylindrical device (mandrel/needle) which is hollow such that air can be blown through it. Shaping of the tube takes place at and just below the end of the cylindrical device and is drawn off by the drawing machine. The shape of the drawn tube is characterized by the parameters: the wall thickness and the diameter or by the cross-sectional area of the tube. These parameters are influenced by variables such as the drawing speed, the air pressure in the cylindrical device, the composition of the raw materials and the room temperature. We remark that the drawing speed, as compared to the other variables, significantly affects the shaping parameters and hence can be utilized as a control variable to control the geometry of the tube.

In glass industry people are in particular interested in controlling the geometry of the tube which may be circular, square or rectangular in shape. Different techniques have been discussed in the literature to control the geometry of the tube during the drawing process. For example in [18], the manufacturing of non-axisymmetric capillary tubing via Vello process is considered with the aim of solving the inverse problem to determine the die shape required to achieve a given final shape (square or rectangular). The problem was solved analytically by considering the steady tube drawing. In [49], the control of a complex glass forming process (tube drawing) has been studied. The process modeled by four coupled and nonlinear partial differential equations is solved numerically by Finite Element Method (FEM). To control the process, a control methodology like Nonlinear Model Predictive Control (an

advanced method of process control used in the processing industries) was implemented. The Two-Degree-Of-Freedom Internal Model Control scheme was used in [15] for controlling the average external diameter and the aver-

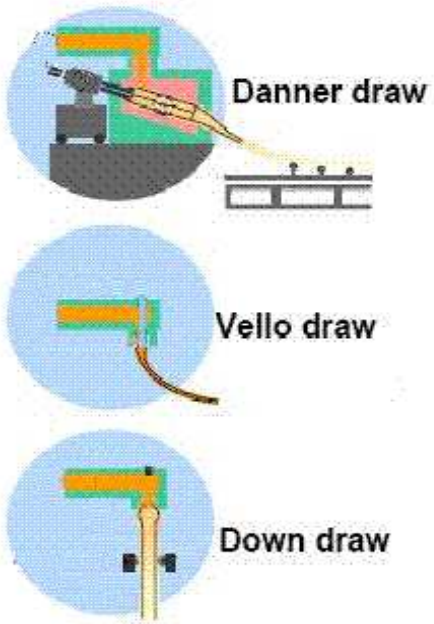


Figure 1.1: Tube Drawing Processes. Courtesy: SCHOTT-Rohrglas GmbH

age wall thickness of the tubes used for the production of the gas-discharge lamps. However, none of these has used the adjoint variable approach which is very robust and commonly used in solving the optimal control problems, see [7, 23, 24, 29, 30, 32, 34, 35, 36, 37, 38, 45] and the references therein.

This study is aimed at using the adjoint variable approach to control the circular cross-sectional area of a glass tube in the glass tube manufacturing process. This leads us to the formulation of an optimal control problem which requires a mathematical model for the physical process to be controlled, a specification of the performance index, and a specification of all boundary conditions on states.

Various types of mathematical models of the drawing processes, with varying level of description and needs, are available in the literature. We cite here some of them. The drawing of hollow optical fibers both for the isothermal

and the non-isothermal cases has been studied in [3] and [4] respectively. Therein the axisymmetric fiber is considered and the large aspect ratio of the fiber is exploited to obtain one-dimensional models. The main concern was the evolution in the size of the hole. A mathematical model of the drawing process of glass capillary tubes based on real, acceptable and critically analyzed assumptions is developed in [46]. In [28], for the considered non-axisymmetric fiber drawing with slow variations in the axial direction, the shape of the cross-section was found to satisfy a two dimensional time dependent Stokes flow problem when expressed in suitable scaled Lagrangian coordinates. Production of non-isothermal tubing has also been discussed in [10, 47, 50].

In Chapter 2, we derive a mathematical model for non-isothermal tube drawing processes. We begin the chapter with a presentation of the physical process involved and then write the Stokes equations along with the convection-diffusion equation which govern the axisymmetric slow flow of incompressible Newtonian fluid (molten glass). By considering the glass flow as thin layer flow, we exploit the large aspect ratio of the flow to obtain simplified model equations from the general Stokes and the convection-diffusion equations. A similar strategy is used in [3, 4, 10, 42] to derive the simplified model equations. We conclude the chapter by presenting he isothermal tube drawing model and proving the existence and uniqueness of the solutions to the stationary model equations.

In Chapter 3, we state the optimal control problem by defining the tracking type cost functional and the weak formulation of the state system. By assuming sufficient regularity and uniqueness of the solutions of the state equations, we define the reduced cost functional. Under some assumptions, the existence of minimizer of the optimal control problem is also proved. We derive the first-order optimality conditions by introducing the Lagrange functional. The existence and uniqueness of the solutions of the stationary adjoint equations are also proved. For more analysis, we also derive the second-order conditions to compute the Hessian of the reduced cost functional. The analytical information gathered in this chapter is then used in the Chapter 4 to solve the control problem numerically.

Solution algorithms and numerical implementation details are discussed in Chapter 4. We define the first and the second order optimization algorithms to respectively solve the first order and the second order optimality conditions derived in Chapter 3. These optimization algorithms are based on steepest descent (SD) [9, 22], nonlinear conjugate gradient (NCG) [9, 22],

BFGS [22, 33] and Newton-CG [22, 37] approaches. SD, NCG and BFGS based approaches use the first derivative information of the reduced cost functional whereas Newton-CG algorithm uses the second derivative information. In the Newton-CG method, the CG iterations are embedded in the Newton's method [33, 37] to solve the linear equations. The Newton-CG method unlike the Newton method does not require explicit knowledge of the Hessian, rather it requires only the matrix-vector products, e.g. see matrix-vector products form given in (3.33). To stop the embedded CG iterations, we use the stopping criterion as given in [33, 37]. With this criterion we get the linear, the superlinear and the quadratic convergence of the method for different values of the parameter used therein. In the second half of the chapter, we use the finite difference methods to discretize the first and the second order optimality conditions. The Newton's iterations are implemented to solve the nonlinear discretized equations. The consistency of the implemented schemes is also proved. Furthermore, we also illustrate the symmetry of the reduced Hessian by showing that the discretization of the linearized state and the adjoint equations yield transpose of each other.

In Chapter 5, the numerical results of the optimal control problems both for the isothermal and the non-isothermal models are presented and discussed. We discuss here the control of the cross-sectional area in the entire time domain and also at the final time $t_f$. We also compare the convergence results of the optimization algorithms defined in Chapter 4.

We summarize the results in Chapter 6 and give some concluding remarks.

Appendix A is devoted to definition of the optimal control problem for isothermal tube drawing model. We also define the weak formulation and derive the first and the second order optimality conditions for solving the control problem. Some basic definitions, lemmas and theorems related to this work are given in Appendix B.

# Chapter 2

# Modelling Tube Drawing Processes

This chapter is devoted to the derivation of mathematical models of the tube drawing process. We first briefly describe the industrial manufacturing process of the tube drawing and then derive the corresponding model equations.

The typical glass tube manufacturing processes are the Danner process and the Vello process. In these processes, the molten glass flows through a feeder channel into a bowl where the temperature is decreased so far that tubes can be drawn. In the bowl an inclined(Danner)/vertical(Vello) mandrel/needle is mounted which is hollow from inside such that air can be blown through it. Shaping of the tube takes place at, and just below the end of the mandrel. At this stage the shaped tube is like a thick-walled cylinder. This thick-walled cylinder is then fed with a low feeding speed $v_0$ into a hot-forming zone of length $L$, and is pulled by a drawing machine with a drawing speed $v_L\,(v_L > v_0)$. The change of temperature in the hot-forming zone determines whether to develop an isothermal or a non-isothermal model. We consider both the isothermal and the non-isothermal tube drawing processes and derive the corresponding model equations. (See the schematic diagram of the tube in figure 2.1).

## 2.1 Non-isothermal Tube Drawing

To model the tube drawing process, we consider a slow flow of incompressible Newtonian fluid (molten glass) and suppose that the temperature is not constant in the hot-forming zone. The flow is considered between two free

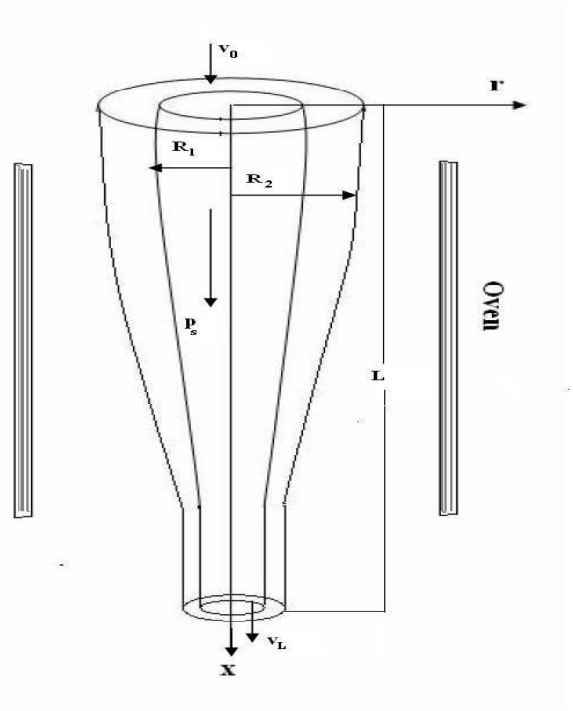


Figure 2.1: Schematic diagram of tube.

surfaces $r = R_1(x,t)$ and $r = R_2(x,t)$, where $R_1(x,t)$ and $R_2(x,t)$ are respectively the inner and the outer radii of the tube. Since the inertial force as well as the surface tension force acting upon the molten glass in the draw-down zone are insignificant, they can be neglected. The governing equations

| Parameters | Symbols | Approx. Values | Units |
|---|---|---|---|
| specific heat | $c_p$ | 770 | $Jkg^{-1}K^{-1}$ |
| density | $\rho$ | 2500 | $kg\ m^{-3}$ |
| thermal conductivity | $k$ | 1.1 | $Wm^{-1}K^{-1}$ |
| emissivity | $\epsilon$ | 0.9 | — |
| Stefan-Boltzmann const. | $\sigma$ | $5.67 \times 10^{-8}$ | $Wm^2K^{-4}$ |

Table 2.1: Typical parameter values taken from [16, 18, 39, 48, 46]

for such type of flow are given as:

$$\frac{1}{r}\left(rw\right)_r + v_x = 0, \tag{2.1a}$$

$$p_r = \mu\left(w_{rr} + \frac{w_r}{r} - \frac{w}{r^2}\right) + \left(\mu w_x\right)_x + \mu_x v_r + 2\mu_r w_r, \tag{2.1b}$$

$$p_x = \frac{1}{r}\left(\mu r v_r\right)_r + \left(2\mu v_x\right)_x + \frac{1}{r}\left(\mu r w_x\right)_r + \rho g, \tag{2.1c}$$

$$\rho c_p\left(T_t + vT_x + wT_r\right) = \left(kT_x\right)_x + \frac{1}{r}\left(krT_r\right)_r + \sigma\epsilon\left(T_{amb}^4 - T^4\right), \tag{2.1d}$$

Equations (2.1$a$)-(2.1$c$) are the standard equations for axisymmetric Stokes flow (see [4] for Navier-Stokes equations) where the first equation is the continuity equation given by the incompressibility condition, and the second and third equations are respectively the momentum equations in $r$ and $x$ directions. Equation (2.1$d$) is the energy conservation equation. Derivatives are denoted by subscripts $x$, $r$ and $t$ where $x$ measures the distance along the axis of the tube, $r$ denotes distance normal to it and $t$ denotes the time. The velocity $\mathbf{v}$ of the molten glass is denoted by $\mathbf{v} = (v, w)$, where $v$ is the component of velocity along $x$ direction and $w$ along $r$ direction. The acceleration due to gravity and the pressure are respectively denoted by $g$ and $p$. The parameters $\rho$, $k$, $c_p$, $\epsilon$ and $\sigma$ are respectively the density, thermal conductivity, specific heat, emissivity and Stefan-Boltzmann constant. $T$ is the glass temperature and $T_{amb}$ denotes the ambient temperature in the furnace. The temperature dependent viscosity $\mu$ is given by the relation

$$\mu\left(T\right) = \mu_0 e^{\beta\left(1-\frac{T}{T_0}\right)}, \tag{2.1e}$$

where $\mu_0$ is the viscosity at initial temperature $T_0$. The dimensionless parameter $\beta$ reflects the extreme sensitivity of $\mu$ to variations in $T$. The physical applicability of relation (2.1e) is considered in [39] and is used in mathematical models of tube drawing, for example see [46].

To close the problem, it is now necessary to specify the kinematic conditions, the stress conditions and the temperature conditions at the free surfaces. The kinematic conditions are

$$w = R_{1t} + R_{1x}v \qquad on \quad r = R_1, \tag{2.1f}$$

$$w = R_{2t} + R_{2x}v \qquad on \quad r = R_2. \tag{2.1g}$$

The stress conditions on the inner and the outer surfaces are respectively given as

$$\tau\hat{n}_{in} = -p_s\hat{n}_{in} \qquad on \quad r = R_1,$$

$$\tau\hat{n}_{out} = 0 \qquad on \quad r = R_2.$$

where $p_s$ is the pressure imposed on the inner surface of the tube, $\hat{n}_{in}$ and $\hat{n}_{out}$ are the unit normals on the inner and the outer surfaces defined respectively as:

$$\hat{n}_{in} = \frac{1}{\sqrt{1+(R_{1x})^2}}(1, -R_{1x}), \quad \text{and} \quad \hat{n}_{out} = \frac{-1}{\sqrt{1+(R_{2x})^2}}(1, -R_{2x})$$

The stress tensor $\tau$ is given as:

$$\tau = \begin{pmatrix} -p + 2\mu w_r & \mu(v_r + w_x) \\ \mu(v_r + w_x) & -p + 2\mu v_x \end{pmatrix}$$

The stress conditions can be written as

$$(-p + 2\mu w_r) - \mu(w_x + v_r) R_{1x} = -p_s \qquad on \quad r = R_1, \tag{2.1h}$$

$$\mu(v_r + w_x) - (-p + 2\mu v_x) R_{1x} = p_s R_{1x} \qquad on \quad r = R_1, \tag{2.1i}$$

$$-p + 2\mu w_r = \mu(w_x + v_r) R_{2x} \qquad on \quad r = R_2, \tag{2.1j}$$

$$\mu(v_r + w_x) = (-p + 2\mu v_x) R_{2x} \qquad on \quad r = R_2. \tag{2.1k}$$

Since the thermal conductivity of air is much lower than the thermal conductivity of glass, we assume that the glass is essentially insulated on its inner surface $r = R_1(x,t)$. At the outer surface $r = R_2(x,t)$, we also assume that the glass loses heat to the surrounding air in the furnace via the Newton-type cooling law. So boundary conditions for temperature are

$$T_r = 0 \qquad on \quad r = R_1, \tag{2.1l}$$

$$kT_r = \alpha(T_{amb} - T) \qquad on \quad r = R_2, \tag{2.1m}$$

where $\alpha$ is heat transfer coefficient and taken as a constant.

### 2.1.1 Nondimensionalisation and Scaling

It is now appropriate to non-dimensionalise (2.1) to take advantage of the small parameters that are present in the problem. The appropriate scalings for the dimensional quantities as defined in [4, 42] are

$$x = L\bar{x}, \qquad r = \varepsilon L\bar{r}$$

$$R_1 = \varepsilon L\bar{R}_1, \qquad R_2 = \varepsilon L\bar{R}_2$$

$$v = U\bar{v}, \qquad w = \varepsilon U\bar{w}$$

$$p = \frac{\mu_0 U}{L}\bar{p}, \qquad p_s = \frac{\mu_0 U}{L}\bar{p}_s$$

$$T = \theta\bar{T}, \qquad T_{amb} = \theta\bar{T}_{amb}$$

$$\mu = \mu_0\bar{\mu}, \qquad t = \frac{L}{U}\bar{t}$$

Here $L$ is the typical length of the hot-forming zone, $U$ denotes a typical draw speed, $\theta$ is the reference temperature of tube and $\mu_0$ denotes the typical glass viscosity. $\varepsilon = \dfrac{W}{L} \ll 1$ is the small parameter present in the problem where $W$ is the width of the tube.

The dimensionless system of governing equations, after dropping the bar for notational convenience, is then given as follows.

The continuity equation (2.1a) is

$$\frac{1}{r}\left(rw\right)_r + v_x = 0, \tag{2.2a}$$

The momentum equation (2.1b) in the $r$ direction becomes

$$p_r = \mu\left(w_{rr} + \frac{w_r}{r} - \frac{w}{r^2}\right) + \varepsilon^2\left(\mu w_x\right)_x + \mu_x v_r + 2\mu_r w_r, \tag{2.2b}$$

and in $x$ direction we have

$$\varepsilon^2 p_x = \frac{1}{r}\left(\mu r v_r\right)_r + \varepsilon^2\left(2\mu v_x\right)_x + \varepsilon^2\frac{1}{r}\left(\mu r w_x\right)_r + \varepsilon^2 St, \tag{2.2c}$$

The energy equation (2.1d) is given as

$$\begin{aligned}\varepsilon^2\left(T_t + vT_x + wT_r\right) = \frac{1}{PrRe}\left(\varepsilon^2\left(T_x\right)_x + \frac{1}{r}\left(rT_r\right)_r\right)\\ +\varepsilon^2\Gamma\left(T_{amb}^4 - T^4\right)\end{aligned} \tag{2.2d}$$

The kinematic conditions (2.1f), (2.1g) and the temperature conditions (2.1l), (2.1m) become

$$w = R_{1t} + R_{1x}v \qquad on \quad r = R_1, \tag{2.2e}$$
$$w = R_{2t} + R_{2x}v \qquad on \quad r = R_2, \tag{2.2f}$$
$$T_r = 0 \qquad on \quad r = R_1, \tag{2.2g}$$
$$T_r = \bar{\alpha}\varepsilon^2\left(T_{amb} - T\right) \qquad on \quad r = R_2, \tag{2.2h}$$

and the stress conditions (2.1h)-(2.1k) yield

$$\left(-p + 2\mu w_r\right) - \mu\left(\varepsilon^2 w_x + v_r\right)R_{1x} = -p_s \qquad on \quad r = R_1, \tag{2.2i}$$
$$\mu\left(v_r + \varepsilon^2 w_x\right) - \varepsilon^2\left(-p + 2\mu v_x\right)R_{1x} = \varepsilon^2 p_s R_{1x} \qquad on \quad r = R_1, \tag{2.2j}$$
$$-p + 2\mu w_r = \mu\left(\varepsilon^2 w_x + v_r\right)R_{2x} \qquad on \quad r = R_2, \tag{2.2k}$$
$$\mu\left(v_r + \varepsilon^2 w_x\right) = \varepsilon^2\left(-p + 2\mu v_x\right)R_{2x} \qquad on \quad r = R_1 \tag{2.2l}$$

where

$$\bar{\alpha} = \frac{L\alpha}{k\varepsilon}, \quad \Gamma = \frac{L\theta^3\sigma\epsilon}{Uc_p\rho}$$

and the other dimensionless numbers are given as

$$St = \frac{\rho g L^2}{\mu_0 U}, \quad Pr = \frac{c_p\mu_0}{k}, \quad Re = \frac{LU\rho}{\mu_0},$$

which are respectively the Stokes number, the Prandtl number and the Reynolds number.

### 2.1.2 Asymptotic Expansions

In this section, we exploit the small parameter $\varepsilon$ present in the system of governing equations (2.2) to simplify them. Since the small parameter appears there in even powers of $\varepsilon$ only, the obvious choice to expand the dependent variables, as given in [4, 42], is:

$$\begin{aligned} v &= v_0 + \varepsilon^2 v_1 + \mathcal{O}(\varepsilon^4) \\ w &= w_0 + \varepsilon^2 w_1 + \mathcal{O}(\varepsilon^4) \\ p &= p_0 + \varepsilon^2 p_1 + \mathcal{O}(\varepsilon^4) \\ T &= T_0 + \varepsilon^2 T_1 + \mathcal{O}(\varepsilon^4) \end{aligned}$$

We substitute these expansions into equations (2.2) and collect the coefficients of like powers of $\varepsilon$.

The leading-order contributions from equations (2.2a)-(2.2d) are respectively given as

$$\frac{1}{r}\left(rw_0\right)_r + v_{0x} = 0, \tag{2.3a}$$

$$p_{0r} = \mu\left(w_{0rr} + \frac{w_{0r}}{r} - \frac{w_0}{r^2}\right) + \mu_x v_{0r} + 2\mu_r w_{0r}, \tag{2.3b}$$

$$\left(\mu r v_{0r}\right)_r = 0, \tag{2.3c}$$

$$\left(rT_{0r}\right)_r = 0, \tag{2.3d}$$

The kinematic and the temperature conditions (2.2e)-(2.2h) and the stress conditions (2.2i)-(2.2l) respectively give the following leading-order contribu-

tions.

$$w_0 = R_{1t} + R_{1x} v_0 \qquad on \quad r = R_1, \tag{2.3e}$$

$$w_0 = R_{2t} + R_{2x} v_0 \qquad on \quad r = R_2, \tag{2.3f}$$

$$T_{0r} = 0 \qquad on \quad r = R_1 \quad and \quad r = R_2, \tag{2.3g}$$

$$-p_0 + 2\mu w_{0r} = -p_{s0} \qquad on \quad r = R_1, \tag{2.3h}$$

$$v_{0r} = 0 \qquad on \quad r = R_1, \tag{2.3i}$$

$$-p_0 + 2\mu w_{0r} = 0, \qquad on \quad r = R_2, \tag{2.3j}$$

$$v_{0r} = 0, \qquad on \quad r = R_2. \tag{2.3k}$$

From equation (2.3d) and the boundary condition (2.3g), we find that

$$T_0 = T_0(x, t)$$

which means that leading order temperature $T_0$ is independent of $r$ and hence the viscosity $\mu$ is also independent of $r$.

Similarly, the leading-order momentum equation (2.3c) and the leading-order conditions (2.3i), (2.3k) yield

$$v_0 = v_0(x, t)$$

Thus the leading-order axial velocity $v_0$ is also independent of $r$.

From the continuity equation (2.3a), we obtain

$$w_0 = -\frac{r}{2} v_{0x} + \frac{C(x, t)}{r}, \tag{2.4}$$

where the function $C(x, t)$ is to be determined.

The equation (2.4) along with the normal stress boundary conditions (2.3h) and (2.3j) give

$$-p_0 - \frac{2\mu}{R_1^2} C(x, t) - \mu v_{0x} + p_{s0} = 0, \tag{2.5a}$$

$$-p_0 - \frac{2\mu}{R_2^2} C(x, t) - \mu v_{0x} = 0. \tag{2.5b}$$

We solve the equations (2.5) for $p_0$ and $C(x, t)$ by considering that these equations are linear in the variables $p_0$ and $C$. That is

$$p_0 = -\frac{p_{s0} R_1^2}{R_2^2 - R_1^2} - \mu v_{0x}, \tag{2.6}$$

$$C(x, t) = \frac{p_{s0} R_1^2 R_2^2}{2\mu (R_2^2 - R_1^2)}. \tag{2.7}$$

Equation (2.4) at boundary $r = R_1$ is written as

$$-\frac{R_1}{2}v_{0x} + \frac{C\,(x,t)}{R_1} = R_{1t} + R_{1x}v_0, \tag{2.8}$$

where we have also used the kinematic boundary condition (2.3e). Now using (2.7), we obtain

$$\left(R_1^2\right)_t + \left(v_0 R_1^2\right)_x = \frac{p_{s0}R_1^2R_2^2}{\mu\left(R_2^2 - R_1^2\right)}, \tag{2.9a}$$

Similarly at boundary $r = R_2$, equation (2.4) gives us

$$\left(R_2^2\right)_t + \left(v_0 R_2^2\right)_x = \frac{p_{s0}R_1^2R_2^2}{\mu\left(R_2^2 - R_1^2\right)}. \tag{2.9b}$$

Equations (2.9) give the inner radius $R_1$ and the outer radius $R_2$ of the tube. To get the equation for mean radius $R$, we do some simple manipulations with the equations (2.9) and arrive at the below equation in dimensional from

$$\left(R^2\right)_t + \left(vR^2\right)_x = \frac{p_s}{16\pi\mu(T)A}\left(16\pi^2R^4 - A^2\right) \tag{2.10}$$

where $A = 2\pi RW$ is the cross-sectional area of the tube, $R$ and $W$ are respectively the mean radius and the width of the tube which in terms of $R_1$ and $R_2$ are given by the relations

$$R = \frac{R_1 + R_2}{2}, \quad W = R_2 - R_1.$$

Equations (2.9) also lead us to the equation of continuity:

$$\left(R_2^2 - R_1^2\right)_t + \left(v_0\left(R_2^2 - R_1^2\right)\right)_x = 0$$

or in dimensional form

$$(A)_t + (vA)_x = 0, \tag{2.11}$$

Since $\mu$ and $v_0$ are independent of $r$, the leading-order $r$-momentum equation (2.3b) yields

$$p_{0r} = 0, \Rightarrow p_0 = p_0\,(x,t)\,.$$

which means that leading-order pressure is also independent of $r$.

To get the closed system of equations for the tube drawing process, we consider the $x$-momentum equation and the energy equation of $\mathcal{O}(\varepsilon^2)$

$$p_{0x} = \frac{\mu}{r}(rv_{1r})_r + (2\mu v_{0x})_x + \frac{\mu}{r}(rw_{0x})_r + St, \tag{2.12a}$$

$$T_{0t} + v_0 T_{0x} = \frac{1}{PrRe}\left((T_{0x})_x + \frac{1}{r}(rT_{1r})_r\right) + \Gamma\left(T_{amb}^4 - T_0^4\right). \tag{2.12b}$$

We multiply the equations (2.12) by $r$ and then integrate them from $r = R_1$ to $r = R_2$ to yield

$$\begin{aligned}\frac{R_2^2 - R_1^2}{2}&\left(p_{0x} - (2\mu v_{0x})_x + \mu v_{0xx} - St\right)\\ &= \mu\left((rv_{1r})\,|_{r=R_2} - (rv_{1r})\,|_{r=R_1}\right),\end{aligned} \tag{2.13a}$$

$$\begin{aligned}\frac{R_2^2 - R_1^2}{2}&\left(T_{0t} + v_0 T_{0x} - \frac{1}{PrRe}(T_{0x})_x - \Gamma\left(T_{amb}^4 - T_0^4\right)\right)\\ &= \frac{1}{PrRe}\left((rT_{1r})\,|_{R_2} - (rT_{1r})\,|_{R_1}\right).\end{aligned} \tag{2.13b}$$

The normal stress boundary conditions of order $\varepsilon^2$ are

$$\mu(v_{1r} + w_{0x}) - (-p_0 + 2\mu v_{0x})R_{1x} = p_{s0}R_{1x} \quad on \quad r = R_1, \tag{2.14a}$$

$$\mu(v_{1r} + w_{0x}) = (-p_0 + 2\mu v_{0x})R_{2x} \quad on \quad r = R_2, \tag{2.14b}$$

Taking $x$-derivative of equation (2.4) and then substituting $w_{0x}$ in the stress conditions (2.14), we have

$$\mu v_{1r}|_{r=R_1} = \frac{\mu R_1}{2}v_{0xx} - \frac{\mu C_x}{R_1} + (-p_0 + 2\mu v_{0x})R_{1x} + p_{s0}R_{1x},$$

$$\mu v_{1r}|_{r=R_2} = \frac{\mu R_2}{2}v_{0xx} - \frac{\mu C_x}{R_2} + (-p_0 + 2\mu v_{0x})R_{2x}.$$

Using these conditions and the $x$-derivative of $p_0$, the momentum equation (2.13a), after certain simplifications, reduces to

$$\left[3\mu\left(R_2^2 - R_1^2\right)v_{0x}\right]_x + \left(R_2^2 - R_1^2\right)St = 0$$

and in dimensional form we get

$$(3\mu A v_x)_x + \rho g A = 0 \tag{2.15}$$

To $\mathcal{O}(\varepsilon^2)$, the temperature boundary conditions are

$$T_{1r} = 0 \qquad on \quad r = R_1, \tag{2.16a}$$

$$T_{1r} = \bar{\alpha}(T_{amb} - T_0) \qquad on \quad r = R_2. \tag{2.16b}$$

Using the boundary conditions (2.16) in equation (2.13b), we get the energy equation in dimensionless form as

$$\frac{R_2^2 - R_1^2}{2}\left(T_{0t} + v_0 T_{0x} - \frac{1}{PrRe}\left(T_{0x}\right)_x - \Gamma\left(T_{amb}^4 - T_0^4\right)\right) = \frac{R_2\bar{\alpha}}{PrRe}\left(T_{amb} - T_0\right).$$

and in dimensional form as

$$\rho c_p\left(T_t + vT_x\right) = kT_{xx} + \sigma\varepsilon\left(T_{amb}^4 - T^4\right) + \alpha\left(\frac{2\pi R}{A} + \frac{1}{2R}\right)\left(T_{amb} - T\right). \tag{2.17}$$

For the sake of clarity, we have dropped the zero-subscript referring to the leading-order quantities in the derived equations (2.10), (2.11), (2.15) and (2.17). Furthermore, we need to supplement these derived equations with boundary and initial conditions. The boundary conditions are:

$$A\left(x=0,t\right) = A_0, \qquad R\left(x=0,t\right) = R_0, \tag{2.18a}$$
$$v\left(x=0,t\right) = v_0, \qquad v\left(x=L,t\right) = v_L, \tag{2.18b}$$
$$T\left(x=0,t\right) = T_0, \qquad T\left(x=L,t\right) = T_L, \tag{2.18c}$$

and the initial conditions read as:

$$A\left(x,t=0\right) = A_0,\ R\left(x,t=0\right) = R_0,\ T\left(x,t=0\right) = T_0,\ \ for\ x \in [0,L] \tag{2.19}$$

The derived model equations (2.10), (2.11), (2.15) (2.17) along with the boundary conditions (2.18) and the initial conditions (2.19) are strongly coupled, nonlinear and describe the non-isothermal tube drawing process.

Before moving to the next chapter where we, on the basis of this model, will define the optimal control problem and derive the first order and the second order conditions, it is necessary to transform the simplified model into dimensionless form. For that we do the rescaling and use the simple scales

$$\tilde{x} = \frac{x}{L}, \quad \tilde{A} = \frac{A}{A_0}, \quad \tilde{R} = \frac{R}{R_0}, \quad \tilde{v} = \frac{v}{v_0}, \quad \tilde{t} = \frac{v_0 t}{L},$$

$$\tilde{\mu} = \frac{\mu}{\mu_0}, \quad \tilde{T} = \frac{T}{T_0}, \quad \tilde{T_a} = \frac{T_{amb}}{T_0}, \quad \tilde{p} = \frac{Lp_s}{\mu_0 v_0}$$

Dropping the tilde notation, we get the following dimensionless system of equations (also given by [49]):

$$(A)_t + (vA)_x = 0, \tag{2.20a}$$

$$(3\mu(T)Av_x)_x + (St)\,A = 0, \tag{2.20b}$$

$$\left(R^2\right)_t + \left(vR^2\right)_x = \frac{\pi c_1 p}{\mu(T)A}\left(R^4 - \frac{A^2}{(4\pi c_1)^2}\right), \tag{2.20c}$$

$$T_t + vT_x = aT_{xx} + c_2\left(T_a^4 - T^4\right) + \left(\frac{b_1 R}{A} + \frac{b_2}{2R}\right)(T_a - T). \tag{2.20d}$$

where

$$St = \frac{\rho g L^2}{v_0 \mu_0},$$

is the Stokes number and the other parameters are

$$a = \frac{k}{\rho c_p v_0 L},\ c_1 = \frac{R_0^2}{A_0},\ c_2 = \frac{\sigma\varepsilon L T_0^3}{\rho v_0 c_p},\ b_1 = \frac{2\pi\alpha R_0 L}{\rho c_p v_0 A_0},\ b_2 = \frac{\alpha L}{\rho c_p v_0 R_0},$$

The initial and the boundary conditions are respectively given as:

$$A(x, t=0) = 1,\ R(x, t=0) = 1,\ T(x, t=0) = 1,\ for\ x \in [0,1] \tag{2.20e}$$

and

$$A(x=0,t) = 1, \qquad R(x=0,t) = 1, \qquad T(x=0,t) = 1, \tag{2.20f}$$

$$v(x=0,t) = 1, \qquad v(x=1,t) = v_d, \tag{2.20g}$$

where $v_d = \dfrac{v_L}{v_0} > 1$ is the draw ratio.

The viscosity-temperature relationship, which couples the energy equation (2.20d) with the other equations, in dimensionless form is:

$$\mu(T) = e^{\beta(1-T)}. \tag{2.20h}$$

**Remark 2.1** *For the sake of simplicity when performing the numerical simulations, we will neglect the diffusion term $T_{xx}$ in* (2.20d) *as the coefficient* '$a$' *is of order* $10^{-4}$ *for typical process parameters (see tables 2.1 and 5.1).*

## 2.2 Isothermal Tube Drawing

Now we assume that the temperature remains constant throughout the hot-forming zone of the tube drawing process. Then the model (2.20) can be

simplified to get the mathematical model for the isothermal tube drawing process (also given by [10, 42]) which reads as

$$(A)_t + (vA)_x = 0, \tag{2.21a}$$
$$(3\mu A v_x)_x + \rho g A = 0, \tag{2.21b}$$
$$\left(R^2\right)_t + \left(vR^2\right)_x = \frac{p}{16\pi\mu A}\left(16\pi^2 R^4 - A^2\right). \tag{2.21c}$$

with the boundary conditions

$$A\left(x=0,t\right) = A_0, \qquad R\left(x=0,t\right) = R_0, \tag{2.21d}$$
$$v\left(x=0,t\right) = v_0, \qquad v\left(x=L,t\right) = v_L. \tag{2.21e}$$

and the initial conditions

$$A\left(x,t=0\right) = A_0,\ R\left(x,t=0\right) = R_0,\ for\ x \in [0,L] \tag{2.21f}$$

Equations (2.21) give us the circular cross-sectional area $A$, velocity $v$ and the mean radius $R$ of the tube. The width $W$ of the tube is obtained from the relation $A = 2\pi RW$.

### 2.2.1 Existence and Uniqueness

In this section, we give the existence and uniqueness results for the stationary isothermal tube drawing model

$$\frac{d}{dx}\left(vA\right) = 0, \tag{2.22a}$$
$$\frac{d}{dx}\left(A\frac{dv}{dx}\right) + A = 0, \tag{2.22b}$$
$$\frac{d}{dx}\left(vR^2\right) - \frac{1}{A}\left(R^4 - A^2\right) = 0. \tag{2.22c}$$

$$A\left(x=0\right) = A_0, \qquad R\left(x=0\right) = R_0, \tag{2.22d}$$
$$v\left(x=0\right) = v_0, \qquad v\left(x=1\right) = v_d. \tag{2.22e}$$

where for the sake of simplicity we have ignored the constant coefficients.

Equation (2.22a) implies that

$$A(x) = \frac{1}{v(x)}, \quad v(x) > 0, \quad x \in \Omega \tag{2.23}$$

Now equation (2.22b) can be written as

$$\frac{d^2}{dx^2} ln(v) = -v^{-1}, \quad v(0) = v_0, \quad v(1) = v_d.$$

Using the transformation $w = ln(v)$, we have

$$\begin{aligned} -\frac{d^2 w}{dx^2} - e^{-w} &= 0, \qquad \text{on } \Omega, \\ w(0) &= ln(v_0), \\ w(1) &= ln(v_d). \end{aligned}$$

To transform the boundary conditions to homogeneous boundary conditions, we define a function

$$g(x) = ln(v_0) + (ln(v_d) - ln(v_0))x, \quad \text{for } x \in \Omega$$

and then introduce the variable $\psi(x) = w(x) - g(x)$ to get

$$-\frac{d^2 \psi}{dx^2} - m(x)e^{-\psi} = 0, \qquad \text{on } \Omega, \tag{2.24a}$$

$$\psi = 0 \qquad \text{on } \partial\Omega. \tag{2.24b}$$

where $m(x) = e^{-g(x)} > 0$.

**Definition 2.1** *The nonlinear variational problem corresponding to the equation* (2.24) *is defined as:*

*Find* $\psi \in H_0^1(\Omega)$ *such that*

$$(\mathcal{A}\psi, \varphi) = 0, \qquad \textit{for all } \varphi \in H_0^1(\Omega). \tag{2.25}$$

*where the operator* $\mathcal{A} : H_0^1(\Omega) \to H_0^1(\Omega)$ *is defined as*

$$(\mathcal{A}\psi, \varphi) = \int_\Omega \left( \frac{d\psi}{dx}\frac{d\varphi}{dx} - m(x)e^{-\psi}\varphi \right) dx, \ \varphi \in H_0^1(\Omega). \tag{2.26}$$

**Lemma 2.2** *The operator* $\mathcal{A} : H_0^1(\Omega) \to H_0^1(\Omega)$ *defined by* (2.26) *is strongly monotone, i.e., there exists a* $\Theta > 0$ *s.t.*

$$(\mathcal{A}\psi_1 - \mathcal{A}\psi_2, \psi_1 - \psi_2) \geq \Theta \|\psi_1 - \psi_2\|^2,$$

*for all* $\psi_1, \psi_2 \in H_0^1$.

*Proof:* For $\psi_1, \psi_2 \in H_0^1(\Omega)$

$$\begin{aligned}(\mathcal{A}\psi_1 - \mathcal{A}\psi_2, \psi_1 - \psi_2) &= \int_\Omega \Bigg[\frac{d}{dx}(\psi_1 - \psi_2)\frac{d}{dx}(\psi_1 - \psi_2) \\ &\qquad - m(x)\underbrace{(e^{-\psi_1} - e^{-\psi_2})(\psi_1 - \psi_2)}_{\leq 0}\Bigg]dx \\ &\geq \int_\Omega \frac{d}{dx}(\psi_1 - \psi_2)\frac{d}{dx}(\psi_1 - \psi_2)dx \\ &= \int_\Omega |\frac{d}{dx}(\psi_1 - \psi_2)|^2 dx \\ &= \|\frac{d}{dx}(\psi_1 - \psi_2)\|^2 \\ &\geq \Theta\|\psi_1 - \psi_2\|^2, \quad \text{where } \Theta = \frac{1}{c(\Omega)} > 0.\end{aligned}$$

Hence the operator $\mathcal{A}$ is strongly monotone. □

**Lemma 2.3** *Function $\psi(x) \in H_0^1(\Omega)$ defined in equation (2.24) is positive for $x \in \Omega$.*

*Proof:* $\psi(x) \neq 0$ for $x \in \Omega$ otherwise it does not satisfy the equation (2.24a). Let $\psi(x) < 0$ for $x \in \Omega$. The weak formulation of the equation (2.24) is written as

$$\int_\Omega \frac{d\psi}{dx}\frac{d\psi}{dx}dx - \int_\Omega m(x)e^{-\psi}\psi dx = 0, \text{ for } \psi \in H_0^1(\Omega) \text{ with } \psi < 0 \text{ in } \Omega,$$

or $$\int_\Omega \underbrace{|\frac{d\psi}{dx}|^2}_{>0} dx - \int_\Omega \underbrace{m(x)e^{-\psi}}_{>0}\underbrace{\psi}_{<0} dx = 0,$$

Both the terms on the left hand side are positive and thus give a non-zero number which is a contradiction. Therefore, $\psi(x) > 0$ for $x \in \Omega$. □

**Remark 2.4** *For $0 < \psi_1, \psi_2 \in H_0^1$ the relation*

$$|e^{-\psi_1} - e^{-\psi_2}| \leq n|\psi_1 - \psi_2|, \text{ for } n > 0.$$

*holds. We will use it in proving the Lemma 2.5 below.*

**Lemma 2.5** *The operator $\mathcal{A} : H_0^1(\Omega) \to H_0^1(\Omega)$ defined by (2.26) is Lipschitz continuous, i.e., there exists $L > 0$ s.t.*

$$\|\mathcal{A}\psi_1 - \mathcal{A}\psi_2\| \leq L\|\psi_1 - \psi_2\|,$$

*for all $\psi_1, \psi_2 \in H_0^1(\Omega)$.*

*Proof:* For $\varphi \in H_0^1(\Omega)$,

$$\begin{aligned}
|\,(\mathcal{A}\psi_1,\varphi)-(\mathcal{A}\psi_2,\varphi)\,| &= |\int_\Omega \Big[\frac{d}{dx}(\psi_1-\psi_2)\frac{d\varphi}{dx} \\
&\qquad + m(x)(e^{-\psi_2}-e^{-\psi_1})\varphi\Big]dx| \\
&\le |\int_\Omega \left(\frac{d}{dx}(\psi_1-\psi_2)\frac{d\varphi}{dx}\right)dx| \\
&\qquad + |\int_\Omega m(x)(e^{-\psi_2}-e^{-\psi_1})\varphi dx| \\
&\le \|\frac{d}{dx}(\psi_1-\psi_2)\|_{L_2}\|\frac{d\varphi}{dx}\|_{L_2} \\
&\qquad + n\|\psi_1-\psi_2\|_{L_2}\|\varphi\|_{L_2}\|m\|_{L^\infty}, \\
&\le \|\frac{d}{dx}(\psi_1-\psi_2)\|_{L_2}\|\frac{d\varphi}{dx}\|_{L_2} \\
&\qquad + cnK\|\frac{d}{dx}(\psi_1-\psi_2)\|_{L_2}\|\frac{d\varphi}{dx}\|_{L_2} \\
&= L\|\psi_1-\psi_2\|_{H_0^1}\|\varphi\|_{H_0^1},\ L=(1+nKc(\Omega))>0.
\end{aligned}$$

Therefore the operator $\mathcal{A}$ is Lipschitz continuous. □

**Lemma 2.6** *[6] Let $V$ be a Hilbert space with scalar product $(.,.)$ and let $B : V \to V$ be a monotone and Lipschitz continuous operator. Then the operator equation*

$$Bu = 0.$$

*has a unique solution $u \in V$. This solution is a fixed point of the auxiliary operator $T_r : V \to V$ defined by*

$$T_r v := v - rBv, \qquad v \in V,$$

*which is contractive when the parameter $r$ lies in $\left(0, \frac{2\Theta}{L^2}\right)$ where $\Theta > 0$ is a monotonicity constant and $L > 0$ is a Lipschitz constant.* □

**Lemma 2.7** *If the operator $\mathcal{A} : H_0^1 \to H_0^1$ defined in (2.26) is monotone and Lipschitz continuous, then the operator equation defined in (2.25) has a unique solution $\psi \in H_0^1$.*

*Proof:* By Lemmata 2.2 and 2.5, the operator $\mathcal{A}$ is strongly monotone and Lipschitz continuous. Therefore by Lemma 2.6, there exists a unique solution to the equation (2.25). □

Incorporating equation (2.23), equation (2.22c) can be written as

$$\frac{d}{dx}(vR^2) = A\left((vR^2)^2 - 1\right). \tag{2.27}$$

Let $z(x) = v(x)R^2(x)$, then the equation (2.27) is transformed to

$$\frac{dz}{dx} = f(x, z, A), \quad \text{for } x \in \Omega \text{ and with } z(x_0) = z_0. \tag{2.28}$$

where $f(x, z, A) = A(z^2 - 1)$ and $x_0 = 0,\ z_0 = v_0 R_0^2$.

**Lemma 2.8** *Let $A$ and $z$ be continuous functions of $x$. Then if the functions $f$ and $\dfrac{\partial f}{\partial z}$ are continuous in some rectangle $\alpha < x < \beta,\ \gamma < z < \delta$ containing the point $(x_0, z_0)$, then there exists a unique solution $z(x)$ to the initial value problem* (2.28) *in some neighbourhood of $(x_0, z_0)$.*

*Proof:* Since both $A$ and $z$ are continuous functions of $x$, therefore

$$f = A(z^2 - 1) \quad \text{and } \frac{\partial f}{\partial z} = 2zA, \tag{2.29}$$

are also continuous functions of $x$. Therefore by Theorem B.8, there exists a unique solution to the equation (2.28) in some neighbourhood of $(x_0, z_0)$. □

**Remark 2.9** *Existence and uniqueness of the solution of the differential equation* (2.22a) *follows from the Lemma 2.7 and the equation* (2.23).

# Chapter 3

# Optimal Control Problem

In this chapter, we study an optimal control problem of the non-isothermal tube drawing process (for isothermal see Appendix A) with the aim to control the cross-sectional area $A$ of the tube to the desired state $A_d$. The cross-sectional area is related to the mean radius $R$ and the width $W$ by the relation $A = 2\pi RW$. Since the cross-sectional area is mainly influenced by the pulling speed $v_d$ of the drawing machine, we choose it as the control variable for our control problem and define the cost functional of tracking-type

$$J(A, v_d) = \frac{w_1}{2} \int_0^{t_f} \int_\Omega (A(x,t) - A_d)^2 dxdt + \frac{w_2}{2} \int_\Omega (A(x,t_f) - A_d)^2 dx + \frac{\lambda}{2} \int_0^{t_f} (v_d)^2 dt \qquad (3.1)$$

where the first and second terms in the cost functional measure the distance between area $A$ and the desired state $A_d$, and the third term measures the size of the control. The parameter $\lambda > 0$ is the cost of the control and the weighting coefficients $w_1, w_2 \geq 0$ allow to adjust the cost functional to different scenarios.

We have to minimize the cost functional (3.1) with respect to the constraints given by system (2.20) (w.r.t. (A.1) in case of isothermal tube drawing), i.e.

$$\text{minimize } J(A, v_d) \text{ with respect to } (A, v_d) \text{ subject to system (2.20).} \qquad (3.2)$$

The problem defined in (3.2) belongs to the class of constrained optimization problems where the constraints are partial differential equations. We address this problem by the adjoint variable approach which has been studied by [14, 24, 31, 35, 38, 45].

## 3.1 Weak Formulation

In this section we state the weak formulation of the state system (2.20). Later on we shall use this formulation to derive the adjoint equations, the gradient equation, and also to collect the second derivative information for the implementation of the Newton's algorithm.

The integration domain used in the weak formulation is defined as

$$Q := \Omega \times (0, t_f),\ \Sigma_0 := 0 \times (0, t_f),\ \Sigma_1 := 1 \times (0, t_f)$$

where $\Omega = (0, 1)$ is the space domain and the model equations (2.20) are solved in the time interval $(0, t_f)$. The appropriately chosen spaces are the Hilbert space $U$ and the Banach spaces $Y$ and $Z$. The Hilbert space $U$ is the space of controls $u = (v_d)$, $Y$ is the space of states $y = (A, v, R, T)$ and $Z$ is the space of test functions.

Weak formulation of the state system (2.20) is defined as follows.

**Definition 3.1** *The weak formulation of the state system* (2.20) *is given by*

$$e(y, u) = 0 \tag{3.3a}$$

*where the operator*

$$e := (e_1, e_2, e_3, e_4, e_5, e_6, e_7) : Y \times U \to Z^*,\ Z^* \text{ is the dual space of } Z,$$

*is defined as*

$$\begin{aligned}\langle e_1(y,u), \xi_A\rangle := &\int_0^{t_f} \langle A_t, \xi_A\rangle dt - \int_Q vA(\xi_A)_x dxdt - \int_{\Sigma_0} \xi_A dt \\ &+ \int_{\Sigma_1} v_d(t) A \xi_A dt = 0, \end{aligned} \tag{3.3b}$$

$$\begin{aligned}\langle e_2(y,u), \xi_v\rangle := &\int_Q (St) A \xi_v dxdt + \int_Q (3\mu A(\xi_v)_x)_x v dxdt \\ &+ \int_{\Sigma_0} 3(\xi_v)_x dt - \int_{\Sigma_1} 3\mu A v_d(t)(\xi_v)_x dt \\ &- \int_{\Sigma_0} 3 v_x \xi_v dt + \int_{\Sigma_1} 3\mu A v_x \xi_v dt = 0, \end{aligned} \tag{3.3c}$$

$$\begin{aligned}\langle e_3(y,u),\xi_R\rangle := &\int_0^{t_f}\langle (R^2)_t,\xi_R\rangle dt - \int_Q vR^2(\xi_R)_x dxdt\\ &- \int_Q \frac{\pi c_1 p}{\mu A}\left(R^4 - \frac{A^2}{(4\pi c_1)^2}\right)\xi_R dxdt\\ &- \int_{\Sigma_0}\xi_R dt + \int_{\Sigma_1} v_d(t)R^2\xi_R dt = 0, \qquad (3.3d)\\ \langle e_4(y,u),\xi_T\rangle := &\int_0^{t_f}\langle T_t,\xi_T\rangle dt - \int_Q (v\xi_T)_x T dxdt\\ &- \int_Q \left[c_2(T_a^4 - T^4) + \left(\frac{b_1 R}{A} + \frac{b_2}{R}\right)(T_a - T)\right]\xi_T dxdt\\ &+ \int_{\Sigma_1} v_d T\xi_T dt - \int_{\Sigma_0}\xi_T dt = 0 \qquad (3.3e)\end{aligned}$$

*with*

$$e_5 = A(0) - 1, \quad e_6 = R(0) - 1, \quad e_7 = T(0) - 1 \qquad (3.3f)$$

*for all test functions* $(\xi_A, \xi_v, \xi_R, \xi_T) \in Z$.

Now the minimization problem (3.2) can be re-written as

$$\min_{(y,u)\in Y\times U} \quad J(y,u) \qquad \text{subject to} \quad e(y,u) = 0, \quad y \in Y,\ u \in U_{ad}. \qquad (3.4)$$

where $Y$ is space of states and $U_{ad} \subset U$ is the set consisting of admissible controls.

**Remark 3.1** *The minimization problem for isothermal tube drawing is defined in appendix A.*

## 3.2 Derivatives

In this section we give the Fréchet derivatives of the operator $e$ defined in section 3.1 and of the cost functional (3.1).

**Lemma 3.2** *Let the mapping* $e : Y \times U \to Z^*$ *be twice continuously Fréchet differentiable. Then the action of the first two derivatives of* $e = (e_1, e_2, e_3, e_4)$ *at* $z = (y,u) \in Y \times U$ *in directions* $\tilde{z} = (\tilde{y},\tilde{u}) = (\tilde{A}, \tilde{v}, \tilde{R}, \tilde{T}, \tilde{v}_d) \in Y \times U$ *and*

*$(\tilde{z}, \hat{z}) \in (Y \times U)^2$ are respectively given by*

$$\begin{aligned}\langle e_{1z}(z)\tilde{z}, \xi_A\rangle = &\int_0^{t_f} \langle (\tilde{A})_t, \xi_A\rangle dt - \int_Q (v\tilde{A} + \tilde{v}A)(\xi_A)_x dxdt + \int_{\Sigma_1} v_d \tilde{A}\xi_A dt \\ &+ \int_{\Sigma_1} \tilde{v}_d A\xi_A dt,\end{aligned}$$

$$\begin{aligned}\langle e_{2z}(z)\tilde{z}, \xi_v\rangle = &\int_{\Sigma_1} 3\mu \left(\tilde{A}v_x + A\tilde{v}_x - \beta\tilde{T}Av_x\right)\xi_v dt + \int_Q St\tilde{A}\xi_v dxdt \\ &- \int_{\Sigma_1} 3\mu \left(\tilde{A}v_d + A\tilde{v}_d - \beta\tilde{T}Av_d\right)(\xi_v)_x dt - \int_{\Sigma_0} 3\tilde{v}_x\xi_v dt \\ &+ \int_Q \left(3\mu\tilde{A}(\xi_v)_x\right)_x v dxdt + \int_Q \left(3\mu A(\xi_v)_x\right)_x \tilde{v} dxdt \\ &- \int_Q \left(3\beta\mu\tilde{T}A(\xi_v)_x\right)_x v dxdt,\end{aligned}$$

$$\begin{aligned}\langle e_{3z}(z)\tilde{z}, \xi_R\rangle = &\int_0^{t_f} \langle (2R\tilde{R})_t, \xi_R\rangle dt - \int_Q 2vR\tilde{R}(\xi_R)_x dxdt \\ &- \int_Q \frac{4\pi c_1 p R^3 \tilde{R}\xi_R}{\mu A} dxdt + \int_Q \frac{\pi c_1 p\tilde{A}}{\mu}\left(\frac{R^4}{A^2} + \frac{1}{(4\pi c_1)^2}\right)\xi_R dxdt \\ &- \int_Q \tilde{v}R^2(\xi_R)_x dxdt - \int_Q \frac{\pi c_1 p\beta\tilde{T}}{\mu A}\left(R^4 - \frac{A^2}{(4\pi c_1)^2}\right)\xi_R dxdt \\ &+ \int_{\Sigma_1} 2v_d R\tilde{R}\xi_R dt + \int_{\Sigma_1} \tilde{v}_d R^2\xi_R dt,\end{aligned}$$

$$\begin{aligned}\langle e_{4z}(z)\tilde{z}, \xi_T\rangle = &\int_0^{t_f} \langle \tilde{T}_t, \xi_T\rangle dt - \int_Q (v\xi_T)_x \tilde{T} dxdt + \int_Q \left[4c_2 T^3 + \frac{b_1 R}{A}\right. \\ &\left. + \frac{b_2}{R}\right]\tilde{T}\xi_T dxdt - \int_Q (\tilde{v}\xi_T)_x T dxdt - \int_Q \tilde{R}(T_a - T) \\ &\times \left(\frac{b_1}{A} - \frac{b_2}{R^2}\right)\xi_T dxdt + \int_Q \frac{b_1 R(T_a - T)\tilde{A}}{A^2}\xi_T dxdt \\ &+ \int_{\Sigma_1} (v_d\tilde{T} + \tilde{v}_d T)\xi_T dt,\end{aligned}$$

*and*

$$\langle e_{1zz}(z)(\tilde{z},\hat{z}),\xi_A\rangle = -\int_Q(\tilde{v}\hat{A}+\hat{v}\tilde{A})(\xi_A)_x dxdt+\int_{\Sigma_1}(\tilde{u}\hat{A}+\hat{u}\tilde{A})\xi_A dt,$$

$$\begin{aligned}\langle e_{2zz}(z)(\tilde{z},\hat{z}),\xi_v\rangle = &\int_{\Sigma_1} 3\mu\Big[\hat{A}\tilde{v}_x-\beta\tilde{T}\hat{A}v_x+\tilde{A}\hat{v}_x-\beta\tilde{T}A\hat{v}_x-\beta\hat{T}\tilde{A}v_x\\ &-\beta\hat{T}A\tilde{v}_x+\beta^2\tilde{T}\hat{T}Av_x\Big]\xi_v dt-\int_{\Sigma_1}3\mu\Big[\hat{A}\tilde{v}_d-\beta\tilde{T}\hat{A}v_d\\ &+\tilde{A}\hat{v}_d-\beta\tilde{T}A\hat{v}_d-\beta\hat{T}\tilde{A}v_d-\beta\hat{T}A\tilde{v}_d+\beta^2\tilde{T}\hat{T}Av_d\Big]\\ &\times(\xi_v)_x dt-\int_Q\Big[\Big(3\beta\mu\tilde{T}\hat{A}(\xi_v)_x\Big)_x+\Big(3\beta\mu\hat{T}\tilde{A}(\xi_v)_x\Big)_x\\ &-\Big(3\beta^2\mu\tilde{T}\hat{T}A(\xi_v)_x\Big)_x\Big]vdxdt+\int_Q\Big[\Big(3\mu\hat{A}(\xi_v)_x\Big)_x\\ &-\Big(3\beta\mu\hat{T}A(\xi_v)_x\Big)_x\Big]\tilde{v}dxdt+\int_Q\Big(3\mu\tilde{A}(\xi_v)_x\Big)_x\hat{v}dxdt\\ &-\int_Q\Big(3\beta\mu\tilde{T}A(\xi_v)_x\Big)_x\hat{v}dxdt,\end{aligned}$$

$$\begin{aligned}\langle e_{3zz}(z)(\tilde{z},\hat{z}),\xi_R\rangle = &\int_0^{t_f}\langle(2\hat{R}\tilde{R})_t,\xi_R\rangle dt-\int_Q 2\tilde{v}R\hat{R}(\xi_R)_x dxdt\\ &+\int_Q\frac{4\pi c_1 pR^3\tilde{A}\hat{R}}{\mu A^2}\xi_R dxdt-\int_Q\frac{12\pi c_1 pR^2\hat{R}\tilde{R}}{\mu A}\xi_R dxdt\\ &-\int_Q\frac{4\pi c_1 p\beta R^3\hat{R}\tilde{T}}{\mu A}\xi_R dxdt-\int_Q\frac{4\pi c_1 p\beta R^3\tilde{R}\hat{T}}{\mu A}\xi_R dxdt\\ &-\int_Q 2v\hat{R}\tilde{R}(\xi_R)_x dxdt-\int_Q\frac{\pi c_1 p\beta^2}{\mu A}\left(R^4-\frac{A^2}{(4\pi c_1)^2}\right)\\ &\times\tilde{T}\hat{T}\xi_R dxdt+\int_Q\frac{\pi c_1 p\beta\hat{T}\tilde{A}}{\mu}\left(\frac{R^4}{A^2}+\frac{1}{(4\pi c_1)^2}\right)\xi_R dxdt\\ &+\int_Q\frac{4\pi c_1 pR^3\tilde{R}\hat{A}}{\mu A^2}\xi_R dxdt-\int_Q\frac{2\pi c_1 pR^4\tilde{A}\hat{A}}{\mu A^3}\xi_R dxdt\\ &+\int_Q\frac{\pi c_1 p\beta\tilde{T}\hat{A}}{\mu}\left(\frac{R^4}{A^2}+\frac{1}{(4\pi c_1)^2}\right)\xi_R dxdt\end{aligned}$$

$$- \int_Q 2R\tilde{R}\hat{v}(\xi_R)_x dxdt + \int_{\Sigma_1} 2v_d\hat{R}\tilde{R}\xi_R dt$$
$$+ \int_{\Sigma_1} 2R\left(\tilde{v}_d\hat{R} + \hat{v}_d\tilde{R}\right)\xi_R dt,$$

$$\langle e_{4zz}(z)(\tilde{z},\hat{z}),\xi_T\rangle = \int_Q \frac{b_1(T_a-T)\hat{A}\tilde{R}}{A^2}\xi_T dxdt - \int_Q \frac{2b_1R(T_a-T)\tilde{A}\hat{A}}{A^3}$$
$$\times \xi_T dxdt - \int_Q \frac{b_1R\tilde{T}\hat{A}}{A^2}\xi_T dxdt - \int_Q (\hat{v}\xi_T)_x\tilde{T}dxdt$$
$$+ \int_Q \frac{b_1(T_a-T)\tilde{A}\hat{R}}{A^2}\xi_T dxdt - \int_Q \frac{2b_2(T_a-T)\tilde{R}\hat{R}}{R^3}\xi_T$$
$$\times dxdt + \int_Q \left(\frac{b_1}{A} - \frac{b_2}{R^2}\right)\tilde{T}\hat{R}\xi_T dxdt - \int_Q \frac{b_1R\tilde{A}\hat{T}}{A^2}\xi_T$$
$$\times dxdt - \int_Q (\tilde{v}\xi_T)_x\hat{T}dxdt + \int_Q \left(\frac{b_1}{A} - \frac{b_2}{R^2}\right)\tilde{R}\hat{T}\xi_T$$
$$\times dxdt + \int_Q 12c_2T^2\tilde{T}\hat{T}\xi_T dxdt + \int_{\Sigma_1}\left(\hat{v}_d\tilde{T} + \tilde{v}_d\hat{T}\right)\xi_T dt.$$

□

**Lemma 3.3** *The cost functional* (3.1) *has the first and the second derivatives respectively given by*

$$J_A(y,u)\tilde{A} = w_1\int_Q (A-A_d)\tilde{A}dxdt + w_2\int_\Omega (A-A_d)\tilde{A}dx$$
$$J_u(y,u)\tilde{u} = \lambda\int_{\Sigma_1} v_d\tilde{v}_d dt$$

*and*

$$J_{AA}(y,u)[\tilde{A},\hat{A}] = w_1\int_Q \hat{A}\tilde{A}dxdt + w_2\int_\Omega \hat{A}(x,t_f)\tilde{A}(x,t_f)dx$$
$$J_{uu}(y,u)[\tilde{u},\hat{u}] = \int_{\Sigma_1}\hat{v}_d\tilde{v}_d dt$$

□

## 3.3 Existence of Optimal Control

To prove the existence of minimizer of the optimal control problem (3.4), we follow the idea given in [37] and make the following assumption.

**Assumption 3.1**

(*i*) *$Y$ and $U$ are reflexive.*

(*ii*) *$U_{ad} \subset U$ is convex, bounded and closed such that the control problem* (3.4) *has a feasible point.*

(*iii*) *The state equation $e(y,u) = 0$ has a unique bounded solution operator $u \in U_{ad} \mapsto y(u) \in Y$.*

(*iv*) *$(y,u) \in Y \times U \mapsto e(y,u) \in Z^*$ is continuous under weak convergence, i.e., if $(y_k, u_k) \rightharpoonup (y,u)$ in $Y \times U$ then $e(y_k,u_k) \rightharpoonup e(y,u)$ in $Z^*$.*

(*v*) *$J$ is sequentially weakly lower semicontinuous.*

**Definition 3.2** *[37] A state-control pair $(\bar{y}, \bar{u}) \in Y \times U_{ad}$ is called optimal for the control problem* (3.4)*, if it is feasible i.e., $e(\bar{y}, \bar{u}) = 0$ and*

$$J(\bar{y}, \bar{u}) \leq J(y,u) \quad \forall (y,u) \in Y \times U_{ad}, \quad e(y,u) = 0.$$

**Theorem 3.4** *Let assumption 3.1 holds. Then the control problem* (3.4) *has an optimal solution $(\bar{y}, \bar{u})$.*

**Proof:** Let the feasible set be

$$F_{ad} := \{(y,u) \in Y \times U : u \in U_{ad},\ e(y,u) = 0\}.$$

By the assumption that (3.4) has a feasible point, $F_{ad}$ is nonempty. Since $J \geq 0$, the infimum

$$J^* := \inf_{(y,u) \in F_{ad}} J(y,u)$$

exists and we can find a minimizing sequence $(y_k, u_k)_{k \in \mathbb{N}} \subset F_{ad}$ with

$$\lim_{k \to \infty} J(y_k, u_k) = J^*.$$

Due to the assumption 3.1($ii$), the sequence $(u_k)_{k\in\mathbb{N}}$ is bounded. Since $u \in U_{ad} \mapsto y(u) \in Y$ is continuous and bounded by assumption 3.1($iii$), we have $(y_k)_{k\in\mathbb{N}} = (y(u_k)) \subset Y$ is bounded. Therefore by Theorem B.5, there exists a weakly convergent subsequence $(y_{k_n}, u_{k_n})_{n\in\mathbb{N}} \subset (y_k, u_k)$ and some $(\bar{y}, \bar{u}) \in Y \times U$ with $(y_{k_n}, u_{k_n}) \rightharpoonup (\bar{y}, \bar{u})$ as $n \to \infty$. By assumption 3.1($ii$), $(\bar{y}, \bar{u}) \in Y \times U_{ad}$ and by assumption 3.1($iv$),

$$e(y_{k_n}, u_{k_n}) \rightharpoonup e(\bar{y}, \bar{u})$$

and thus $e(\bar{y}, \bar{u}) = 0$. Therefore, $(\bar{y}, \bar{u}) \in F_{ad}$.

Next assumption 3.1($v$) implies that

$$\begin{aligned} J^* &= \lim_{k\to\infty} J(y_k, u_k) = \lim_{n\to\infty} (y_{k_n}, u_{k_n}) \geq J(\bar{y}, \bar{u}) \geq J^*. \\ &\Rightarrow \; J(\bar{y}, \bar{u}) = J^*. \end{aligned}$$

Therefor, $(\bar{y}, \bar{u})$ is the optimal solution of the control problem (3.4). □

## 3.4 First Order Optimality Conditions

To derive the first order optimality system, we define the Lagrange functional $L : Y \times U \times Z \to \mathbb{R}$ associated with the minimization problem (3.4) as

$$L\,(y, u, \xi) = J\,(y, u) + \langle e(y, u), \xi\rangle_{Z^*,Z} \tag{3.5}$$

where $\xi = (\xi_A, \xi_v, \xi_R, \xi_T, \xi_{A_0}, \xi_{R_0}, \xi_{T_0}) \in Z$ are the adjoint variables and $\langle ., . \rangle_{Z^*,Z}$ denotes the duality pairing between $Z^*$ and $Z$.

The first order optimality conditions are then computed by setting the directional derivatives of $L$ with respect to $(y, \xi, u)$ equal to zero in the admissible directions $(\tilde{y}, \tilde{\xi}, \tilde{u})$, i.e.

$$\bigtriangledown_{(y,\xi,u)} L(y, u, \xi)[\tilde{y}, \tilde{\xi}, \tilde{u}] = 0.$$

or in more expressive way

$$J_y(y, u)\tilde{y} + \langle e_y(y, u)\tilde{y}, \xi\rangle_{Z^*,Z} = 0, \quad \forall\ \tilde{y} \in Y \tag{3.6}$$

$$\langle e(y, u), \tilde{\xi}\rangle_{Z^*,Z} = 0, \quad \forall\ \tilde{\xi} \in Z \tag{3.7}$$

$$J_u(y, u)\tilde{u} + \langle e_u(y, u)\tilde{u}, \xi\rangle_{Z^*,Z} = 0, \quad \forall\ \tilde{u} \in U \tag{3.8}$$

The linearized equations (3.6)-(3.8) will respectively lead us to the adjoint equations, the state equations (2.20) and the optimality condition. We derive the adjoint equations and the gradient equation respectively in the subsections 3.4.1 and 3.4.2.

### 3.4.1 Adjoint Equations

We write the linearized equation (3.6) in a more concise way as

$$\langle \frac{\partial e(y,u)}{\partial A}\tilde{A}, \xi\rangle = -\frac{\partial J(y,u)}{\partial A}\tilde{A}, \quad \forall\ \tilde{A} \in Y \tag{3.9}$$

$$\langle \frac{\partial e(y,u)}{\partial v}\tilde{v}, \xi\rangle = -\frac{\partial J(y,u)}{\partial v}\tilde{v}, \quad \forall\ \tilde{v} \in Y \tag{3.10}$$

$$\langle \frac{\partial e(y,u)}{\partial R}\tilde{R}, \xi\rangle = -\frac{\partial J(y,u)}{\partial R}\tilde{R}, \quad \forall\ \tilde{R} \in Y \tag{3.11}$$

$$\langle \frac{\partial e(y,u)}{\partial T}\tilde{T}, \xi\rangle = -\frac{\partial J(y,u)}{\partial T}\tilde{T}, \quad \forall\ \tilde{T} \in Y. \tag{3.12}$$

where each equation will yield us an adjoint equation which we derive formally in strong form in the sequel.

After taking derivatives of $e$ and $J$ with respect to $v$ in the direction $\tilde{v}$, the linearization (3.10) is written as

$$\begin{aligned}\int_Q \left[\frac{\partial}{\partial x}\left(3\mu A\frac{\partial \xi_v}{\partial x}\right) - A\frac{\partial \xi_A}{\partial x} - R^2\frac{\partial \xi_R}{\partial x} + \xi_T\frac{\partial T}{\partial x}\right]\tilde{v}dxdt \\ + \int_{\Sigma_1} 3\mu A\xi_v\frac{\partial \tilde{v}}{\partial x}dt + \int_{\Sigma_1}\left[-\xi_T T - 3\mu A\frac{\partial \xi_v}{\partial x}\right]\tilde{v}dt \\ - \int_{\Sigma_0} 3\xi_v\frac{\partial \tilde{v}}{\partial x}dt + \int_{\Sigma_0}\left[\xi_T + 3\frac{\partial \xi_v}{\partial x}\right]\tilde{v}dt = 0,\end{aligned}$$

From this expression we get the strong form of the adjoint equation for $\xi_v$ as

$$(3\mu A(\xi_v)_x)_x = A(\xi_A)_x + R^2(\xi_R)_x - \xi_T T_x,$$

with boundary conditions

$$\xi_v(x=1,t) = 0,\ \xi_v(x=0,t) = 0, \quad t \in (0,t_f)$$

Equation (3.9), after taking derivatives and rearranging the terms, is written as

$$\begin{aligned}\int_0^{t_f}\langle -\frac{\partial \xi_A}{\partial t}, \tilde{A}\rangle dt + \int_Q \Bigg[ - v\frac{\partial \xi_A}{\partial x} - 3\mu\frac{\partial v}{\partial x}\frac{\partial \xi_v}{\partial x} + St\xi_v + \frac{b_1 R\xi_T}{A^2}(T_a - T) \\ + \frac{p\pi c_1\xi_R}{\mu}\left(\frac{R^4}{A^2} + \frac{1}{(4\pi c_1)^2}\right)\Bigg]\tilde{A}dxdt + \int_{\Sigma_1}\left[v_d\xi_A + 3\mu v_x\xi_v\right]\tilde{A}dt \\ - \int_0^1 \xi_A(x,0)\tilde{A}(x,0)dx + \int_0^1 \xi_A(x,t_f)\tilde{A}(x,t_f)dx \\ = - w_1\int_Q (A - A_d)\tilde{A}dxdt - w_2\int_0^1 \left(A(x,t_f) - A_d\right)\tilde{A}(x,t_f)dx.\end{aligned}$$

This leads us to the following strong form

$$\begin{aligned}-(\xi_A)_t - v(\xi_A)_x =& 3\mu v_x(\xi_v)_x - \frac{\pi c_1 p \xi_R}{\mu}\left(\frac{R^4}{A^2} + \frac{1}{(4\pi c_1)^2}\right) \\ & - St(\xi_v) - \frac{b_1 R \xi_T}{A^2}(T_a - T) - w_1(A - A_d).\end{aligned}$$

with the boundary and terminal conditions

$$\begin{aligned}\xi_A(x=1,t) &= 0, \qquad t \in (0,t_f) \\ \xi_A(x,t_f) &= -w_2\left(A(x,t_f) - A_d\right), \quad x \in (0,1).\end{aligned}$$

Linearization (3.11) reduces to

$$\begin{aligned}\int_0^{t_f} \langle -2R\frac{\partial \xi_R}{\partial t}, \tilde{R}\rangle dt + \int_Q \Bigg[ & -2vR\frac{\partial \xi_R}{\partial x} - \frac{4\pi c_1 p R^3}{\mu A}\xi_R - \left(\frac{b_1}{A} - \frac{b_2}{R^2}\right) \\ & \times (T_a - T)\xi_T\Bigg]\tilde{R}dxdt + \int_0^1 2R(x,t_f)\xi_R(x,t_f)\tilde{R}(x,t_f)dx \\ & + \int_{\Sigma_1} 2v_d R \xi_R \tilde{R}(1,t)dt - \int_0^1 2\xi_R(x,0)\tilde{R}(x,0)dx = 0.\end{aligned}$$

which gives us the adjoint equation

$$-(\xi_R)_t - v(\xi_R)_x - \frac{2\pi c_1 p R^2}{\mu A}\xi_R = \frac{\xi_T}{2R}\left(\frac{b_1}{A} - \frac{b_2}{R^2}\right)(T_a - T),$$

with the following terminal and boundary conditions

$$\begin{aligned}\xi_R(x, t = t_f) &= 0, \qquad x \in (0,1) \\ \xi_R(x=1,t) &= 0, \qquad t \in (0,t_f)\end{aligned}$$

Similarly from (3.12), we have

$$\begin{aligned}\int_0^{t_f} \langle -\frac{\partial \xi_T}{\partial t}, \tilde{T}\rangle dt + \int_Q \Bigg[ & -\frac{\partial}{\partial x}(v\xi_T) + \left(4c_2 T^3 + \frac{b_1 R}{A} + \frac{b_2}{R}\right)\xi_T \\ & + 3\beta\mu A\frac{\partial v}{\partial x}\frac{\partial \xi_v}{\partial x} - \frac{\beta\pi c_1 p \xi_R}{\mu A}\left(R^4 - \frac{A^2}{(4\pi c_1)^2}\right)\Bigg]\tilde{T}dxdt - \int_0^1 \xi_T(x,0) \\ & \times \tilde{T}(x,0)dx + \int_0^1 \xi_T(x,t_f)\tilde{T}(x,t_f)dx + \int_{\Sigma_1} v_d \xi_T \tilde{T}dt = 0.\end{aligned}$$

That leads us to the following strong form of the adjoint equation along with the terminal condition and the boundary condition

$$-(\xi_T)_t - (v\xi_T)_x + \left(4c_2T^3 + \frac{b_1R}{A} + \frac{b_2}{R}\right)\xi_T = -3\beta\mu A v_x(\xi_v)_x + \frac{\beta\pi c_1 p\xi_R}{\mu A}\left(R^4 - \frac{A^2}{(4\pi c_1)^2}\right),$$

$$\xi_T(x, t = t_f) = 0,\ x \in (0,1)$$
$$\xi_T(x = 1, t) = 0,\ t \in (0, t_f)$$

Putting together all the adjoint equations along with the terminal and the boundary conditions, we have

$$-(\xi_A)_t - v(\xi_A)_x = 3\mu v_x(\xi_v)_x - \frac{\pi c_1 p\xi_R}{\mu}\left(\frac{R^4}{A^2} + \frac{1}{(4\pi c_1)^2}\right) - St(\xi_v) - \frac{b_1R\xi_T}{A^2}(T_a - T) - w_1(A - A_d), \tag{3.13a}$$

$$(3\mu A(\xi_v)_x)_x = A(\xi_A)_x + R^2(\xi_R)_x - \xi_T T_x, \tag{3.13b}$$

$$-(\xi_R)_t - v(\xi_R)_x - \frac{2\pi c_1 pR^2}{\mu A}\xi_R = \frac{\xi_T}{2R}\left(\frac{b_1}{A} - \frac{b_2}{R^2}\right)(T_a - T), \tag{3.13c}$$

$$-(\xi_T)_t - (v\xi_T)_x + \left(4c_2T^3 + \frac{b_1R}{A} + \frac{b_2}{R}\right)\xi_T = -3\beta\mu A v_x(\xi_v)_x + \frac{\beta\pi c_1 p\xi_R}{\mu A}\left(R^4 - \frac{A^2}{(4\pi c_1)^2}\right). \tag{3.13d}$$

$$\xi_A(x = 1, t) = 0,\ \xi_R(x = 1, t) = 0,\ \xi_T(x = 1, t) = 0, \tag{3.13e}$$

$$\xi_v(x = 1, t) = 0,\ \xi_v(x = 0, t) = 0, \quad t \in (0, t_f) \tag{3.13f}$$

$$\xi_A(x, t_f) = -w_2\left(A(x, t_f) - A_d\right),\ \xi_R(x, t_f) = 0,\ \xi_T(x, t_f) = 0,\ x \in (0,1) \tag{3.13g}$$

Adjoint equations (3.13) are linear in the adjoint variables $(\xi_A, \xi_v, \xi_R, \xi_T)$. Information travels backwards in time in case of adjoint equations.

#### 3.4.1.1 Existence and Uniqueness

In this section we consider the stationary adjoint equations

$$-v\frac{d\xi_A}{dx} - 3\frac{dv}{dx}\frac{d\xi_v}{dx} + St\xi_v + \pi p c_1 \xi_R \left(\frac{R^4}{A^2} + \frac{1}{(4\pi c_1)^2}\right) = f_A(x), \tag{3.14a}$$

$$-\frac{d^2\xi_v}{dx^2} - \frac{1}{A}\frac{dA}{dx}\frac{d\xi_v}{dx} + \frac{1}{3}\frac{d\xi_A}{dx} + \frac{R^2}{3A}\frac{d\xi_R}{dx} = f_v(x), \tag{3.14b}$$

$$-\frac{d\xi_R}{dx} - \frac{2\pi c_1 p R^2}{vA}\xi_R = f_R(x). \tag{3.14c}$$

with

$$\xi_A(1) = 0,\ \xi_R(1) = 0,\ \xi_v(1) = 0,\ \xi_v(0) = 0 \tag{3.14d}$$

for isothermal tube drawing and prove the existence and uniqueness of the solutions. The functions $f_A$, $f_v$, $f_R$ are supposed to be continuous functions of $x$.

By letting

$$\bar{x} = 1 - x, \tag{3.15}$$

the equation (3.14c) is transformed into an Initial Value Problem (IVP)

$$\frac{d\xi_R}{dx} + b(x)\xi_R = f_R, \text{ with } \xi_R(x_0) = 0, \tag{3.16}$$

where $b(x) = -\dfrac{2\pi c_1 p R^2(x)}{v(x)A(x)}$, $x_0 = 0$ and the bar has been omitted for the sake of simplicity.

**Lemma 3.5** *If $b(x)$, $f_R(x)$ are continuous functions in some interval $I$ containing $x_0$, then there exists a unique solution $\xi_R(x)$ for $x \in I$ to the initial value problem* (3.16)

*Proof*: We have already proved in subsection 2.2.1 that the stationary equations (2.22) has a unique solution $(A, v, R)$ where $A$, $v$, $R$ are continuous functions of $x$. Therefore, we can find an interval $I$ containing the point $x_0$ where $b(x)$ is also continuous. $f_R$ is continuous by its construction. Therefore by Theorem B.7, there exists a unique solution to the IVP (3.16) and hence to the equation (3.14c) with boundary condition $\xi_R(1) = 0$. □

Incorporating equations (3.14a) and (3.14c) in equation (3.14b) and then rearranging the terms, we write the equation for $\xi_v$ as

$$-\frac{d^2\xi_v}{dx^2} - \left(\frac{d}{dx}ln|vA|\right)\frac{d\xi_v}{dx} + \frac{St}{3v}\xi_v - \frac{\pi p c_1}{3v}\left(\frac{R^4}{A^2} - \frac{1}{(4\pi c_1)^2}\right)\xi_R = f_v + \frac{1}{3v}f_A + \frac{R^2}{3A}f_R. \tag{3.17}$$

Equation (2.22a) implies that the flow rate is constant i.e., $vA = constant$, therefore

$$\frac{d}{dx}\ln|vA| = 0$$

Then the equation (3.17) can be written as

$$-\frac{d^2\xi_v}{dx^2} + c(x)\xi_v = g(x), \qquad \text{in } \Omega \tag{3.18a}$$

$$\xi_v = 0, \qquad \text{on } \partial\Omega \tag{3.18b}$$

where

$$c(x) = \frac{St}{3v}, \quad g(x) = f_v + \frac{1}{3v}f_A + \frac{R^2}{3A}f_R + \frac{\pi p c_1}{3v}\left(\frac{R^4}{A^2} - \frac{1}{(4\pi c_1)^2}\right)\xi_R.$$

**Definition 3.3** *The Variational Boundary Value Problem (VBVP) corresponding to equation* (3.18) *is defined as:*

*Find* $\xi_v \in H_0^1(\Omega)$ *such that*

$$\mathfrak{a}(\xi_v, \varphi) = G(\varphi), \qquad \varphi \in H_0^1(\Omega). \tag{3.19}$$

*where*

$$\mathfrak{a}(\xi_v, \varphi) := \int_\Omega \left[\frac{d\xi_v}{dx}\frac{d\varphi}{dx} + c(x)\xi_v\varphi\right] dx \tag{3.20}$$

$$G(\varphi) := \int_\Omega g\varphi dx \tag{3.21}$$

*and* $c(x)$ *is continuous on* $\Omega$.

**Definition 3.4** *[5] Let* $U_1$, $V_1$ *be linear spaces. An operator* $b : U_1 \times V_1 \to R$ *is a bilinear form if*

$$b(\alpha_0 u_1 + \beta_0 w_1, v_1) = \alpha_0 b(u_1, v_1) + \beta_0 b(w_1, v_1), \quad u_1, w_1 \in U_1,\ v_1 \in V_1,$$
$$b(u_1, \alpha_0 v_1 + \beta_0 w_1) = \alpha_0 b(u_1, v_1) + \beta_0 b(u_1, w_1), \quad u_1 \in U_1,\ v_1, w_1 \in V_1,$$

*where* $\alpha_0, \beta_0 \in R$.

**Lemma 3.6** *The operator* $\mathfrak{a} : H_0^1 \times H_0^1 \to \mathbb{R}$ *defined by* (3.20) *defines a bilinear form.*

*Proof*: For $\alpha_0, \beta_0 \in R$, and $(\xi_v)_1,\ (\xi_v)_2,\ \varphi_1\ \varphi_2 \in H_0^1$, we have

$$\begin{aligned}\mathfrak{a}(\alpha_0(\xi_v)_1 + \beta_0(\xi_v)_2, \varphi_1) &= \int_\Omega \Bigg[\frac{d}{dx}(\alpha_0(\xi_v)_1 + \beta_0(\xi_v)_2)\frac{d\varphi_1}{dx} + c(x)(\alpha_0(\xi_v)_1 \\ &\qquad + \beta_0(\xi_v)_2)\varphi_1\Bigg]dx \\ &= \alpha_0 \int_\Omega \left[\frac{d(\xi_v)_1}{dx}\frac{d\varphi_1}{dx} + c(x)(\xi_v)_1\varphi_1\right]dx \\ &\quad + \beta_0 \int_\Omega \left[\frac{d(\xi_v)_2}{dx}\frac{d\varphi_1}{dx} + c(x)(\xi_v)_2\varphi_1\right]dx \\ &= \alpha_0\mathfrak{a}((\xi_v)_1, \varphi_1) + \beta_0\mathfrak{a}((\xi_v)_2, \varphi_1).\end{aligned}$$

Similarly we can show that

$$\mathfrak{a}((\xi_v)_1, \alpha_0\varphi_1 + \beta_0\varphi_2) = \alpha_0\mathfrak{a}((\xi_v)_1, \varphi_1) + \beta_0\mathfrak{a}((\xi_v)_1, \varphi_2).$$

□

**Definition 3.5** *[5](continuous bilinear form)*
*A bilinear form* $b : U_1 \times V_1 \to R$ *where* $U_1$ *and* $V_1$ *are normed linear spaces, is called a continuous bilinear form if there exists a positive number* $K$ *such that*

$$|b(u_1, v_1)| \le K\|u_1\|\|v_1\| \qquad \text{for all } u_1 \in U_1,\ v \in V_1.$$

**Definition 3.6** *[5] ($V_1$-elliptic bilinear form)*
*A bilinear form* $b : V_1 \times V_1 \to R$ *where* $V_1$ *is an inner product space, is called* $V_1$*-elliptic if there exists a constant* $\alpha_0 > 0$ *such that*

$$b(v_1, v_1) \ge \alpha_0\|v_1\|_{V_1}^2 \qquad \text{for all } v_1 \in V_1.$$

**Lemma 3.7** *Bilinear form* $\mathfrak{a} : H_0^1 \times H_0^1 \to R$ *defined by* (3.20) *is both continuous and* $H_0^1$*-elliptic.*

*Proof*:*Continuity of* $\mathfrak{a}(.,.)$*:*

$$|\mathfrak{a}(\xi_v, \varphi)| = |\int_\Omega \left[\frac{d\xi_v}{dx}\frac{d\varphi}{dx} + c(x)\xi_v\varphi\right]dx|$$

Let $c(x)$ be bounded positive function, i.e. $0 < c_1 \leq c(x) \leq c_2$, then

$$\begin{aligned}
|\mathfrak{a}(\xi_v, \varphi)| &\leq |\int_\Omega \left[\frac{d\xi_v}{dx}\frac{d\varphi}{dx} + c_2\xi_v\varphi\right] dx| \\
&\leq |\int_\Omega \frac{d\xi_v}{dx}\frac{d\varphi}{dx}dx| + c_2|\int_\Omega \xi_v\varphi dx| \\
&\leq \|\frac{d\xi_v}{dx}\|_{L^2(\Omega)}\|\frac{d\varphi}{dx}\|_{L^2(\Omega)} + c_2\|\xi_v\|_{L^2(\Omega)}\|\varphi\|_{L^2(\Omega)} \\
&\leq \|\xi_v\|_{H^1(\Omega)}\|\varphi\|_{H^1(\Omega)} + c_2\|\xi_v\|_{H^1(\Omega)}\|\varphi\|_{H^1(\Omega)} \\
&= C\|\xi_v\|_{H^1(\Omega)}\|\varphi\|_{H^1(\Omega)}, \qquad \text{where } C = 1 + c_2.
\end{aligned}$$

$\Rightarrow$ $\mathfrak{a}(.,.)$ is continuous.

*$H_0^1$-ellipticity of $\mathfrak{a}(.,.)$:*

$$\begin{aligned}
\mathfrak{a}(\xi_v, \xi_v) &= \int_\Omega \left[\frac{d\xi_v}{dx}\frac{d\xi_v}{dx} + c(x)(\xi_v)^2\right] dx \\
&\geq \int_\Omega \left[(\frac{d\xi_v}{dx})^2 + c_1(\xi_v)^2\right] dx \\
&\geq \gamma \int_\Omega \left[(\frac{d\xi_v}{dx})^2 + (\xi_v)^2\right] dx, \text{ where } \gamma = min(1, c_1) \\
&= \gamma\|\xi_v\|_{H^1}^2 \geq \gamma\|\xi_v\|_{H_0^1}^2
\end{aligned} \tag{3.22}$$

$\Rightarrow$ $\mathfrak{a}(.,.)$ is $H_0^1$-elliptic. □

**Lemma 3.8** *The linear functional $G : H_0^1 \to \mathbb{R}$ defined by (3.21) is continuous.*

*Proof*: We prove boundedness of $G$ by using the Schwarz inequality.

$$|G(\varphi)| = |\int_\Omega g\varphi dx| \;\leq\; \|g\|_{L^2(\Omega)}\|\varphi\|_{L^2(\Omega)} \;\leq\; \|g\|_{L^2(\Omega)}\|\varphi\|_{H^1(\Omega)},$$

Let $\|g\|_{L^2(\Omega)} = K$, then

$$|G(\varphi)| \leq K\|\varphi\|_{H^1(\Omega)}$$

$\Rightarrow$ $G$ is bounded and hence continuous. □

**Theorem 3.9** *The VBVP defined in Definition 3.3 has a unique solution. Moreover, the solution depends continuously on the data, i.e.,*

$$\|\xi_v\|_{H^1} \leq \frac{1}{\gamma}\|G\|_{(H^1)^*}.$$

*where $(H^1)^*$ is the dual space of $H^1$.*

*Proof*: Due to Lemmata 3.6 - 3.8, we have the bilinearity, continuity and coercivity of the operator $\mathfrak{a} : H_0^1(\Omega) \times H_0^1(\Omega) \to R$ and the continuity of the linear functional $G : H_0^1(\Omega) \to R$. Therefore by the Lax-Milgram Lemma B.9, we have the existence and uniqueness of the solution of the variational problem defined in 3.3.

Now set $\varphi = \xi_v$ in (3.19) and using coercivity relation (3.22) and the boundedness of $G$, we have

$$\begin{aligned} &\gamma\|\xi_v\|_{H^1}^2 \leq \mathfrak{a}(\xi_v, \xi_v) = G(\xi_v) \leq \|G\|_{(H^1)^*}\|\xi_v\|_{H^1} \\ &\Rightarrow \|\xi_v\|_{H^1}^2 \leq \frac{1}{\gamma}\|G\|_{(H^1)^*}. \end{aligned}$$

which proves the continuous dependence of the solution on data. □

Again using the transformation (3.15), the equation (3.14a) is transformed to IVP

$$\frac{d\xi_A}{dx} = \mathcal{F}(x), \text{ with } \xi_A(x_0) = \xi_{A_0}, \tag{3.23a}$$

where $x_0 = 0$, $\xi_{A_0} = 0$ and

$$\mathcal{F}(x) = \frac{1}{v}\left(f_A(x) + 3\frac{dv}{dx}\frac{d\xi_v}{dx} - St\xi_v - \pi p c_1\left(\frac{R^4}{A^2} + \frac{1}{(4\pi c_1)^2}\right)\xi_R\right), \tag{3.23b}$$

**Lemma 3.10** *If $\mathcal{F}(x)$ is continuous function of $x \in \Omega$, then there exists a unique solution $\xi_A(x) \in C^1(\Omega)$ to the initial value problem* (3.23).

*Proof:* $\mathcal{F}(x)$ is continuous by its definition as $A(x)$, $v(x)$, $R(x)$, $\xi_v(x)$, $\xi_R(x)$, $f_A(x)$ are all continuous functions of $x \in \Omega$. So by the fundamental theorem of calculus, there exists a unique solution

$$\xi_A(x) = \xi_{A_0} + \int_{x_0}^{x} \mathcal{F}(t)dt.$$

to the problem (3.23). □

### 3.4.2 Gradient Equation

By Assumption 3.1(*iii*), the system $e(y, u) = 0$ is uniquely solvable. Thus we reformulate the minimization problem (3.4) as

$$\min_{u \in U_{ad}} \hat{J}(u) := J(y(u), u) \quad \text{subject to} \quad e(y(u), u) = 0 \tag{3.24}$$

where $\hat{J}$ is the reduced cost functional and $y(u) \in Y$.

We assume that $e_y(y(u), u) \in \mathcal{L}(Y, Z^*)$ is continuously invertible, then by Lemma 3.2 and by the implicit function Theorem B.3 the derivative of $y(u)$ in a direction $\tilde{u}$ is given as

$$y'(u)\tilde{u} = -e_y(y(u), u)^{-1} e_u(y(u), u)\tilde{u}. \tag{3.25}$$

And using the chain rule we get

$$\langle \hat{J}'(u), \tilde{u} \rangle = \langle J_u(y(u), u) - e_u(y(u), u)^* e_y(y(u), u)^{-*} J_y(y(u), u), \tilde{u} \rangle.$$

Now defining the adjoint variable

$$\xi = -e_y(y(u), u)^{-*} J_y(y(u), u) \in Z$$

and assuming sufficient regularity of the solution we get the Riesz representative of the derivative

$$\hat{J}'(u) = J_u(y(u), u) + e_u(y(u), u)^* \xi \tag{3.26}$$

Linearization (3.8) will lead us to

$$\int_{\Sigma_1} \lambda u(t)\tilde{u} dt + \int_{\Sigma_1} \Big[ A\xi_A - 3\mu A(\xi_v)_x + R^2 \xi_R + T\xi_T \Big] \tilde{u} dt = 0.$$

Since $\xi_A = 0,\ \xi_R = 0,\ \xi_T = 0$ on $\Sigma_1$, we obtain the following optimality condition

$$\lambda u - 3\mu A(\xi_v)_x = 0, \qquad on \quad \Sigma_1 \tag{3.27}$$

From (3.26) and (3.27), the gradient of the reduced cost functional $\hat{J}'(u)$ is written as

$$\hat{J}'(u) = \lambda u - 3\mu A(\xi_v)_x, \qquad on \quad \Sigma_1 \tag{3.28}$$

Gradient of $\hat{J}$ given in (3.28) gives the optimal direction to the control variable $u$ to move in order to reduce the cost functional (3.1). For the evaluation of this gradient, we first need to solve the non-linear state system (2.20) and then the linear coupled adjoint system (3.13).

After having derived the first order optimality conditions, we are now in a position to solve the minimization problem (3.24). The optimization algorithms for solving these conditions will be dealt with in the next chapter.

## 3.5 Second Order Conditions

The minimization problem (3.4) can be solved more efficiently by collecting the second derivative information of the reduced cost functional $\hat{J}$. In the next subsection we derive the second derivative of $\hat{J}$ and describe there the procedure to compute it.

### 3.5.1 Second Derivatives

We write the Lagrange functional (3.5), for arbitrary $\xi \in Z$, as

$$L\left(y(u), u, \xi\right) = J\left(y(u), u\right) + \left\langle e\left(y(u), u\right), \xi \right\rangle_{Z^*,Z} = J\left(y(u), u\right) = \hat{J}(u). \tag{3.29}$$

Then differentiating (3.29) in the direction $\delta u_1 \in U$, we obtain

$$\langle \hat{J}'(u), \delta u_1 \rangle_{U^*,U} = \left\langle L_y\left(y(u), u, \xi\right), y'(u)\delta u_1 \right\rangle_{Y^*,Y} + \left\langle L_u\left(y(u), u, \xi\right), \delta u_1 \right\rangle_{U^*,U}.$$

where the linearization $y'(u)\delta u_1$ of $e(y(u), u) = 0$ in the direction $\delta u_1 \in U$ is given by (3.25).

Differentiating again in the direction $\delta u_2 \in U$, we have

$$\begin{aligned}
\langle \hat{J}''(u)\delta u_2, \delta u_1 \rangle_{U^*,U} =& \langle L_y(y(u), u, \xi), y''(u)(\delta u_1, \delta u_2) \rangle_{Y^*,Y} \\
&+ \langle L_{yy}(y(u), u, \xi)y'(u)\delta u_2, y'(u)\delta u_1 \rangle_{Y^*,Y} \\
&+ \langle L_{yu}(y(u), u, \xi)\delta u_2, y'(u)\delta u_1 \rangle_{Y^*,Y} \\
&+ \langle L_{uy}(y(u), u, \xi)y'(u)\delta u_2, \delta u_1 \rangle_{U^*,U} \\
&+ \langle L_{uu}(y(u), u, \xi)\delta u_2, \delta u_1 \rangle_{U^*,U}.
\end{aligned}$$

Choosing $\xi = \xi(u)$, i.e., $L_y\left(y(u), u, \xi(u)\right) = 0$, we reach at

$$\begin{aligned}
\langle \hat{J}''(u)\delta u_2, \delta u_1 \rangle_{U^*,U} =& \langle y'(u)^* L_{yy}(y(u), u, \xi(u))y'(u)\delta u_2, \delta u_1 \rangle_{U^*,U} \\
&+ \langle y'(u)^* L_{yu}(y(u), u, \xi(u))\delta u_2, \delta u_1 \rangle_{U^*,U} \\
&+ \langle L_{uy}(y(u), u, \xi(u))y'(u)\delta u_2, \delta u_1 \rangle_{U^*,U} \\
&+ \langle L_{uu}(y(u), u, \xi(u))\delta u_2, \delta u_1 \rangle_{U^*,U}.
\end{aligned}$$

This gives us

$$\begin{aligned}
\hat{J}''(u)\delta u =& y'(u)^* L_{yy}\left(y(u), u, \xi(u)\right) y'(u)\delta u + y'(u)^* L_{yu}\left(y(u), u, \xi(u)\right)\delta u \\
&+ L_{uy}\left(y(u), u, \xi(u)\right) y'(u)\delta u + L_{uu}\left(y(u), u, \xi(u)\right)\delta u.
\end{aligned} \tag{3.30a}$$

The reduced Hessian $\hat{J}''(u) \in \mathcal{L}(U)$ can also be written as

$$\hat{J}''(u) := T^*(u) L_{ww} T(u) \tag{3.30b}$$

where

$$L_{ww} = \begin{pmatrix} L_{yy} & L_{yu} \\ L_{uy} & L_{uu} \end{pmatrix}, \tag{3.31}$$
$$T(u) := \begin{pmatrix} y'(u) \\ Id \end{pmatrix} \in \mathcal{L}(U, Y \times U),$$

and $w = (y, u)$, $y = (A, R, T, v)$ and $u = (v_d)$.

In the sequel we describe the step by step procedure to compute $\hat{J}''(u)\delta u$ given by (3.30)

1. compute the solution

$$V = y'(u)\delta u = -e_y(y(u), u)^{-1} e_u(y(u), u)\delta u$$

where $V := (V_A, V_v, V_R, V_T)$ are the linearized state variables. (Derivations of the linearized state equations in strong form are given in subsection 3.5.1.1).
2. compute

$$\begin{pmatrix} d_1 \\ d_2 \end{pmatrix} = \begin{pmatrix} (J_{yy} + \langle e_{yy}, \xi \rangle)(V, .) + (J_{yu} + \langle e_{yu}, \xi \rangle)(\delta u, .) \\ (J_{uy} + \langle e_{uy}, \xi \rangle)(V, .) + (J_{uu} + \langle e_{uu}, \xi \rangle)(\delta u, .) \end{pmatrix}$$

where $d_2$ after some computations and simplifications is given as

$$d_2 = 3\mu(\xi_v)_x (\beta A V_T - V_A) + \lambda \delta u, \quad on \quad \Sigma_1$$

3. compute the solution

$$W = e_y(y(u), u)^{-*} d_1 \tag{3.32}$$

where $W := (W_A, W_v, W_R, W_T)$. (Equations for $W$ in the strong form are derived in subsection 3.5.1.2)
4. then compute

$$\begin{aligned} s_3 &= -e_u(y(u), u)^* W, \\ &= 3\mu A (W_v)_x, \quad on \quad \Sigma_1 \end{aligned}$$

5. set

$$\hat{J}''(u)\delta u = d_2 + d_3$$

such that

$$\hat{J}''(u)\delta u = 3\mu \{A(W_v)_x + (\xi_v)_x (\beta V_T A - V_A)\} + \lambda \delta u, \quad on \quad \Sigma_1 \tag{3.33}$$

The operator-vector product computed in this procedure will later be used in implementations of the Newton-CG algorithm.

#### 3.5.1.1 Linearized State Equations

We do linearization of the state equations $e\left(y(u),u\right)=0$ to get the solution

$$V = y'(u)\delta u = -e_y(y(u),u)^{-1}e_u(y(u),u)\delta u \tag{3.34}$$

where $V := (V_A, V_v, V_R, V_T)$ are the linearized state variables.

For $V_A$, we write (3.34) as

$$\langle e_y(y(u),u)V, \xi_A\rangle = -\langle e_u(y(u),u)\delta u, \xi_A\rangle$$

Using derivatives of $e$ with respect to $y$ and $u$ and after some simplifications we get

$$\int_0^{t_f}\langle (V_A)_t, \xi_A\rangle dt + \int_Q \Big[(vV_A)_x + (AV_v)_x\Big]\xi_A dxdt - \int_{\Sigma_1} V_v A\xi_A dt + \int_{\Sigma_0}\Big[V_A + V_v\Big]\xi_A dt = -\int_{\Sigma_1} A\xi_A\delta u dt.$$

Hence we write down the linearized state equation for $V_A$ as

$$(V_A)_t + (vV_A)_x + (AV_v)_x = 0,$$

with

$$V_A(x,0) = 0, \quad V_A(0,t) = -V_v(0,t) \tag{3.35}$$

For the linearized state variable $V_v$, equation (3.34) is written as

$$\langle e_y(y(u),u)V, \xi_v\rangle = -\langle e_u(y(u),u)\delta u, \xi_v\rangle$$

and in classical form, after some simplifications, we have

$$\int_Q\Big[(3\mu V_A v_x)_x + (3\mu A(V_v)_x)_x - (3\beta\mu V_T A v_x)_x + StV_A\Big]\xi_v dxdt + \int_{\Sigma_1} 3\mu A(\xi_v)_x V_v dt - \int_{\Sigma_0} 3V_v(\xi_v)_x dt - \int_{\Sigma_0} 3V_A(\xi_v)_x dt + \int_{\Sigma_0} 3\beta V_T(\xi_v)_x dt = \int_{\Sigma_1} 3\mu A\delta u(\xi_v)_x dt.$$

which yields

$$(3\mu A(V_v)_x)_x = (3\beta\mu V_T A v_x)_x - (3\mu V_A v_x)_x - StV_A$$

with

$$V_v(0,t) = \beta V_T(0,t) - V_A(0,t), \quad V_v(1,t) = \delta u \tag{3.36}$$

Next we consider

$$\langle e_y(y(u),u)V, \xi_R\rangle = -\langle e_u(y(u),u)\delta u, \xi_R\rangle$$

which lead us to

$$\begin{aligned}\int_0^{t_f} \langle (2RV_R)_t, \xi_R\rangle dt + \int_Q \Bigg[(2vRV_R)_x - \frac{4\pi c_1 p R^3 V_R}{\mu A} + (R^2 V_v)_x \\ + \frac{\pi c_1 p V_A}{\mu}\left(\frac{R^4}{A^2} + \frac{1}{(4\pi c_1)^2}\right) - \frac{\beta \pi c_1 p V_T}{\mu A}\left(R^4 - \frac{A^2}{(4\pi c_1)^2}\right)\Bigg]\xi_R dx dt \\ + \int_{\Sigma_0}\Big[2V_R + V_v\Big]\xi_R dt - \int_{\Sigma_1} R^2 V_v \xi_R dt = -\int_{\Sigma_1} R^2 \xi_R \delta u dt.\end{aligned}$$

$$\begin{aligned}(RV_R)_t + (vRV_R)_x - \frac{2\pi c_1 p R^3}{\mu A} V_R =& \frac{\beta \pi c_1 p V_T}{2\mu A}\left(R^4 - \frac{A^2}{(4\pi c_1)^2}\right) \\ & - \frac{1}{2}(R^2 V_v)_x - \frac{\pi c_1 p V_A}{2\mu}\left(\frac{R^4}{A^2} + \frac{1}{(4\pi c_1)^2}\right).\end{aligned}$$

with

$$V_R(x,0) = 0, \quad V_R(0,t) = -V_v(0,t). \tag{3.37}$$

Finally, from (3.34) we write the equation

$$\langle e_y(y(u),u)V, \xi_T\rangle = -\langle e_u(y(u),u)\delta u, \xi_T\rangle$$

which yield us

$$\begin{aligned}\int_0^{t_f} \langle (V_T)_t, \xi_T\rangle dt + \int_Q \Bigg[v(V_T)_x + V_v T_x + \frac{b_1 R V_A (T_a - T)}{A^2} - (T_a - T) \\ \times \left(\frac{b_1 V_R}{A} - \frac{b_2 V_R}{R^2}\right) + \left(4c_2 T^3 + \frac{b_1 R}{A} + \frac{b_2}{R}\right) V_T\Bigg]\xi_T dx dt \\ - \int_{\Sigma_1} T V_v \xi_T dt + \int_{\Sigma_0}\Big[V_v + V_T\Big]\xi_T dt = -\int_{\Sigma_1} T \delta u \xi_T dt.\end{aligned}$$

This will lead us to the following linearized state equation for $V_T$

$$\begin{aligned}(V_T)_t + v(V_T)_x + (4c_2 T^3 + \frac{b_1 R}{A} + \frac{b_2}{R})V_T \\ = (T_a - T)\left(\frac{b_1 V_R}{A} - \frac{b_1 R V_A}{A^2} - \frac{b_2 V_R}{R^2}\right) - V_v T_x.\end{aligned}$$

with initial and boundary conditions

$$V_T(x,0)=0, \quad V_T(0,t)=-V_v(0,t) \tag{3.38}$$

After some manipulations, the boundary conditions (3.35)-(3.38) can be written as

$$V_A(0,t)=0,\ V_v(0,t)=0,\ V_v(1,t)=\delta u,\ V_R(0,t)=0,\ V_T(0,t)=0.$$

Putting together the derived equations we have the following system of linearized state equations

$$(V_A)_t+(vV_A)_x+(AV_v)_x=0, \tag{3.39a}$$

$$(3\mu A(V_v)_x)_x+(3\mu V_A v_x)_x-(3\beta\mu V_T A v_x)_x+StV_A=0, \tag{3.39b}$$

$$\begin{aligned}(RV_R)_t+(vRV_R)_x-\frac{2\pi c_1 pR^3}{\mu A}V_R=&\frac{\beta\pi c_1 pV_T}{2\mu A}\left(R^4-\frac{A^2}{(4\pi c_1)^2}\right)\\&-\frac{1}{2}(R^2V_v)_x-\frac{\pi c_1 pV_A}{2\mu}\left(\frac{R^4}{A^2}+\frac{1}{(4\pi c_1)^2}\right),\end{aligned} \tag{3.39c}$$

$$\begin{aligned}(V_T)_t+v(V_T)_x+&(4c_2T^3+\frac{b_1R}{A}+\frac{b_2}{R})V_T\\=&(T_a-T)\left(\frac{b_1V_R}{A}-\frac{b_1RV_A}{A^2}-\frac{b_2V_R}{R^2}\right)-V_vT_x.\end{aligned} \tag{3.39d}$$

with initial conditions

$$V_A(x,0)=0,\ V_R(x,0)=0,\ V_T(x,0)=0\ V_v(x,0)=0. \tag{3.39e}$$

and the boundary conditions

$$V_A(0,t)=0,\ V_R(0,t)=0,\ V_T(0,t)=0,\ V_v(0,t)=0,\ V_v(1,t)=\delta u. \tag{3.39f}$$

#### 3.5.1.2 Linearized Adjoint Equations

Equation (3.32) will lead us to the linearized state equations for the variables $(W_A, W_v, W_R, W_T)$ which will be solved backward in time. For $W_v$ we have

$$e_v(y(u),u)^*W=s_1 \tag{3.40}$$

where

$$s_1 = (J_{vA} + \langle e_{vA}, \xi\rangle)(V_A, .) + (J_{vv} + \langle e_{vv}, \xi\rangle)(V_v, .) + (J_{vR} + \langle e_{vR}, \xi\rangle)(V_R, .) + (J_{vT} + \langle e_{vT}, \xi\rangle)(V_T, .) + (J_{vu} + \langle e_{vu}, \xi\rangle)(\delta u, .).$$

Taking derivatives and then rearranging the terms we have

$$s_1 = \int_Q \Big[ -(\xi_A)_x V_A + (3\mu V_A(\xi_v)_x)_x - 2RV_R(\xi_R)_x - (3\beta\mu V_T A(\xi_v)_x)_x + \xi_T(V_T)_x \Big]\tilde{v}dxdt + \int_{\Sigma_1} 3\mu V_A \xi_v \tilde{v}_x dt - \int_{\Sigma_1} 3\beta\mu V_T A \xi_v \tilde{v}_x dt. \quad (3.41)$$

The left hand side of (3.40) is expressed as

$$\begin{aligned} e_v(y(u), u)^* W &= \langle e_v \tilde{v}, W\rangle \\ &= \int_Q \Big[ -A(W_A)_x + (3\mu A(W_v)_x)_x - R^2(W_R)_x + W_T T_x \Big] \\ &\quad \times \tilde{v}dxdt + \int_{\Sigma_1} W_T T\tilde{v}dt - \int_{\Sigma_0} 3W_v \tilde{v}_x dt + \int_{\Sigma_0} W_T \tilde{v}dt \\ &\quad + \int_{\Sigma_1} 3\mu A W_v \tilde{v}_x dt. \end{aligned} \quad (3.42)$$

Therefore (3.40) will lead us to the following adjoint equation

$$\begin{aligned} (3\mu A(W_v)_x)_x =& A(W_A)_x + R^2(W_R)_x - W_T T_x - V_A(\xi_A)_x + (V_T)_x \xi_T \\ & - 2RV_R(\xi_R)_x + (3\mu V_A(\xi_v)_x)_x - (3\beta\mu V_T A(\xi_v)_x)_x, \end{aligned}$$

with terminal and boundary conditions

$$W_v(x, t_f) = 0,\ W_v(1, t) = 0. \quad (3.43)$$

Again from (3.32) we have

$$e_A(y(u), u)^* W = s_1 \quad (3.44)$$

where

$$s_1 = (J_{AA} + \langle e_{AA}, \xi\rangle)(V_A, .) + (J_{Av} + \langle e_{Av}, \xi\rangle)(V_v, .) + (J_{AR} + \langle e_{AR}, \xi\rangle)(V_R, .) + (J_{AT} + \langle e_{AT}, \xi\rangle)(V_T, .) + (J_{Au} + \langle e_{Au}, \xi\rangle)(\delta u, .).$$

After taking derivatives of $J$ and $e$ and then rearranging the terms, we have

$$\begin{aligned} s_1 = \int_Q \Bigg[ & w_1 V_A - \frac{2\pi c_1 p R^4 V_A \xi_R}{\mu A^3} - \frac{2 b_1 R V_A \xi_T}{A^3}(T_a - T) - V_v (\xi_A)_x - 3\mu (\xi_v)_x (V_v)_x \\ & + \frac{4\pi c_1 p R^3 V_R \xi_R}{\mu A^2} + \frac{b_1 V_R \xi_T}{A^2}(T_a - T) + 3\beta\mu V_T v_x (\xi_v)_x - \frac{b_1 R V_T \xi_T}{A^2} \\ & + \frac{\beta \pi c_1 p V_T \xi_R}{\mu}\left(\frac{R^4}{A^2} + \frac{1}{(4\pi c_1)^2}\right)\Bigg] \tilde{A} dx dt - \int_{\Sigma_1} 3\beta\mu V_T v_x \xi_v \tilde{A} dt \\ & + \int_{\Sigma_1} \xi_A \delta u \tilde{A} dt + \int_{\Sigma_1} 3\xi_v (V_v)_x \mu \tilde{A} dt + w_2 \int_0^1 V_A(x, t_f)\tilde{A}(x, t_f) dx. \end{aligned} \tag{3.45}$$

Left hand side of (3.44) can be written as

$$\begin{aligned} e_A(y(u), u)^* W &= \langle e_A \tilde{A}, W \rangle \\ &= \int_0^{t_f} \langle -(W_A)_t, \tilde{A} \rangle dt + \int_Q \Bigg[ - v(W_A)_x - 3\mu (W_v)_x v_x + S t W_v \\ &\quad + \frac{\pi c_1 p W_R}{\mu}\left(\frac{R^4}{A^2} + \frac{1}{(4\pi c_1)^2}\right) + \frac{b_1 R W_T}{A^2}(T_a - T)\Bigg] \tilde{A} dx dt \\ &\quad + \int_0^1 W_A(x, t_f)\tilde{A}(x, t_f) dx + \int_{\Sigma_1} \Big[ v_d W_A + 3\mu v_x W_v \Big] \tilde{A} dt \\ &\quad - \int_{\Sigma_0} 3(W_v)_x \tilde{A} dt. \end{aligned} \tag{3.46}$$

From (3.45) and (3.46), we get the following equation for $W_A$

$$\begin{aligned} -(W_A)_t - v(W_A)_x = & 3\mu \left\{ (W_v)_x v_x - (\xi_v)_x (V_v)_x + \beta V_T v_x (\xi_v)_x \right\} - V_v (\xi_A)_x \\ & - (St) W_v - \frac{b_1 (Ta - T)}{A^2}\left\{ R W_T + \xi_T \left( \frac{2 R V_A}{A} - V_R \right) \right\} \\ & + \frac{\pi c_1 p}{\mu}\Bigg[ (\beta V_T \xi_R - W_R)\left(\frac{R^4}{A^2} + \frac{1}{(4\pi c_1)^2}\right) + \frac{2 R^3 \xi_R}{A^3} \\ & \qquad \times (2 A V_R - R V_A) \Bigg] + w_1 V_A - \frac{b_1 R V_T \xi_T}{A^2} \end{aligned}$$

with terminal and boundary conditions

$$W_A(x, t_f) = w_2 V_A(x, t_f), \; W_A(1, t) = 0.$$

Following the same procedure, we can derive the other adjoint equations.

Therefore, the whole system is written as

$$-(W_A)_t - v(W_A)_x = 3\mu\left\{(W_v)_x v_x - (\xi_v)_x(V_v)_x + \beta V_T v_x(\xi_v)_x\right\} - V_v(\xi_A)_x + \frac{\pi c_1 p}{\mu}\left\{(\beta V_T\xi_R - W_R)\left(\frac{R^4}{A^2} + \frac{1}{(4\pi c_1)^2}\right) + \frac{2R^3\xi_R}{A^3}(2AV_R - RV_A)\right\} + w_1 V_A - (St)W_v - \frac{b_1 R V_T \xi_T}{A^2} - \frac{b_1(Ta - T)}{A^2}\left\{RW_T + \xi_T\left(\frac{2RV_A}{A} - V_R\right)\right\} \tag{3.47a}$$

$$(3\mu A(W_v)_x)_x = A(W_A)_x + R^2(W_R)_x - W_T T_x - V_A(\xi_A)_x + (V_T)_x\xi_T - 2RV_R(\xi_R)_x + (3\mu V_A(\xi_v)_x)_x - (3\beta\mu V_T A(\xi_v)_x)_x, \tag{3.47b}$$

$$-R(W_R)_t - vR(W_R)_x - \frac{2\pi c_1 p R^3}{\mu A}W_R = \frac{2\pi c_1 p R^2\xi_R}{\mu A}\left(\frac{RV_A}{A} - 2V_R - \beta RV_T\right) + \frac{1}{2}\left(\frac{b_1}{A} - \frac{b_2}{R^2}\right)\left\{(T_a - T)W_T + V_T\xi_T + \frac{(T_a - T)V_R\xi_T}{R}\right\} + \frac{(T_a - T)\xi_T}{2}\left(\frac{b_1 V_A}{A^2} - \frac{2b_2 V_R}{R^3}\right) - RV_v(\xi_R)_x, \tag{3.47c}$$

$$-(W_T)_t - (vW_T)_x + \left(4c_2T^3 + \frac{b_1 R}{A} + \frac{b_2}{R}\right)W_T = -(V_v\xi_T)_x + 3\beta\mu \times\left\{(V_A(\xi_v)_x - A(W_v)_x - \beta AV_T(\xi_v)_x)\,v_x + A(\xi_v)_x(V_v)_x\right\} + \frac{\beta\pi c_1 p}{\mu A} \times\left\{(W_R - \beta V_T\xi_R)\left(R^4 - \frac{A^2}{(4\pi c_1)^2}\right) + AV_A\xi_R\left(\frac{R^4}{A^2} + \frac{1}{(4\pi c_1)^2}\right)\right\} - \frac{4\beta\pi c_1 p R^3 V_R\xi_R}{\mu A} + \left\{12c_2T^2V_T + \left(\frac{b_1}{A} - \frac{b_2}{R^2}\right)V_R - \frac{b_1 RV_A}{A^2}\right\}\xi_T. \tag{3.47d}$$

with the boundary conditions

$$W_A(x=1,t) = 0,\ W_R(x=1,t) = 0,\ W_T(x=1,t) = 0, \tag{3.47e}$$

$$W_v(x=1,t) = 0,\ W_v(x=0,t) = 0 \tag{3.47f}$$

and the terminal conditions

$$W_A(x,t_f) = w_2 V_A(x,t_f),\ W_R(x,t_f) = 0,\ W_T(x,t_f) = 0 \tag{3.47g}$$

# Chapter 4

# Numerical Implementations

In the previous chapter, we presented the optimal control problem analytically by defining the cost functional and deriving the first order and the second order optimality conditions. Since the optimality conditions are to be solved numerically so we, in this chapter, explain the numerical implementation details first by defining some solution algorithms and then by describing the discretization strategies.

## 4.1 Optimization Algorithms

To solve the first and the second order optimality conditions, we need to describe some optimization algorithms. Optimization algorithms are iterative and start their iterations with an initial guess of the optimal values of the variables and generate a sequence of improved estimates until a solution is reached. These algorithms can be distinguished on the basis of the strategy which they use to move from one iterate to the next. Most strategies make use of the values of the objective function, the constraints, and the first and the second derivatives of these functions. In this section, we explain the gradient-type first order optimization algorithms as well as the second order optimization algorithm that will help us to solve the optimality conditions. Later on, in the next chapter we will compare the performance of these algorithms on the basis of the obtained numerical results.

### 4.1.1 First Order Algorithms

**Steepest Descent**

We first present the steepest descent (SD) algorithm to solve the control problem. This algorithm is globally convergent but quite slow in practice. (For global convergence see the theorem due to Zoutendijk given in [22])

**Algorithm 4.1** *[22, 45] (Steepest Descent)*

1. *set* $k = 0$ *and choose an initial control* $u_0 \in U_{ad}$.
2. *given* $u_k$, *solve the state* (2.20) *and the adjoint equations* (3.13)
3. *compute the gradient* $\hat{J}'(u_k)$ *from* (3.28)
4. *set* $p_k = -\hat{J}'(u_k)$
5. *find step length* $\alpha_k > 0$ *(see remark 4.2), and set* $u_{k+1} = u_k + \alpha_k p_k$ *to update the control*
6. if $\dfrac{\| \hat{J}'(u_k) \|}{\| \hat{J}'(u_0) \|} \leq tol$ *then*
   *STOP*
   else
   $k \to k+1$ *and goto 2*

**Remark 4.1** *Throughout the section 4.1* $tol = 10^{-4}$ *and the norm is* $L_2$ *except otherwise stated.*

**Remark 4.2** *The step length* $\alpha_k$ *is very crucial for the convergence of the optimization algorithms. It is line search parameter that determines how far to go in the given direction. To find an optimal step length in the direction of gradient we use strong Wolfe conditions which ensure the convergence of the optimization algorithm. The strong Wolfe conditions [22] require* $\alpha_k$ *to satisfy*

$$\hat{J}(u_k + \alpha_k p_k) - \hat{J}(u_k) \leq s_1 \alpha_k \hat{J}'(u_k)^T p_k, \tag{4.1a}$$

$$|\hat{J}'(u_k + \alpha_k p_k)^T p_k| \leq s_2 |\hat{J}'(u_k)^T p_k|, \tag{4.1b}$$

*with* $0 < s_1 < s_2 < 1$. *The first condition is the sufficient decrease condition also called as Armijo condition and the second condition is called as curvature condition. Implementation details of strong Wolfe conditions can be seen in [22]. There are many other approaches as well for finding a step length* $\alpha_k$. *Among them are the Armijo line search [26] and the Goldstein line search [1]. A couple of techniques to find the approximations to the optimal step length* $\alpha_k$ *has also been given and discussed in [33].*

### Nonlinear Conjugate Gradient

Next we present the nonlinear conjugate gradient (NCG) algorithm which is very well-known and efficient technique for solving nonlinear optimization problems [2, 19, 22, 52]. The key feature of this algorithm is that it requires no matrix storage and can be viewed as an acceleration of the steepest descent method.

**Algorithm 4.2** *[22] (nonlinear conjugate gradient)*

1. *given* $u_0 \in U_{ad}$.
2. *solve the state system* (2.20) *to evaluate* $\hat{J}_0 = \hat{J}(u_0)$
3. *solve the adjoint system* (3.13) *to evaluate* $\hat{J}'_0 = \hat{J}'(u_0)$
4. *set* $p_0 = -\hat{J}'_0, \quad k \leftarrow 0, \quad tol > 0$
5. while $\dfrac{\| \hat{J}'_k \|}{\| \hat{J}'_0 \|} > tol$ *then*
   - *compute step length* $\alpha_k$ *(see remark 4.2), and set* $u_{k+1} = u_k + \alpha_k p_k$
   - *solve the state system* (2.20) *and the adjoint system* (3.13)
   - *evaluate* $\hat{J}'_{k+1}$ *using the gradient equation* (3.28)
   - *then compute* $\beta^{PR}_{k+1} = \dfrac{\hat{J}'_{k+1}\left(\hat{J}'_{k+1} - \hat{J}'_k\right)}{\| \hat{J}'_k \|^2}$
   - $p_{k+1} = -\hat{J}'_{k+1} + \beta^{PR}_{k+1} p_k$
   - $k \leftarrow k + 1$

   end

where the parameter $\beta^{PR}_k$ is defined by Polak and Ribiére [12]. There are some other variants of the Algorithm 4.2 as well, that differ from each other in the choice of the parameter $\beta_k$, for details see [11, 40, 43]. None of these choices of $\beta_k$ proved to be significantly more efficient than the PR choice [22], e.g. we experienced more optimization iterations (66) when Fletcher-Reeves (FR) formula [43]

$$\beta^{FR}_{k+1} = \frac{\| \hat{J}'_{k+1} \|^2}{\| \hat{J}'_k \|^2} \tag{4.2}$$

was used as compared to the iterations (36) under the PR method. However the algorithm 4.2 with FR formula (4.2) gives the following convergence result.

**Theorem 4.3** *[9] Assume that the set*

$$\mathcal{N} = \left\{ u | \hat{J}(u) \leq \hat{J}(u_0) \right\}$$

*is bounded and that $\hat{J}$ is Lipschitz continuously differentiable in a neighbourhood of $\mathcal{N}$. Let the algorithm 4.2 be implemented with Fletcher-Reeves formula* (4.2) *and a line search that satisfies the strong Wolfe conditions* (4.1). *Then*

$$\lim_{k \to \infty} inf \|\nabla \hat{J}_k\| = 0.$$

□

In [19], this result has been generalized to allow for any choice of $\beta_k$ such that $|\beta_k| \leq \beta_k^{FR}$. A similar result for the Polak-Ribière method with more complex conditions on the line search has been proved in [27].

### 4.1.2 Second Order Algorithms

In the previous subsection we presented the steepest descent and the nonlinear conjugate gradient algorithms to solve the optimization problem (3.4). The drawback of these first order methods is their slow convergence which results in large number of functional and gradient evaluations.

In this subsection we describe the Newton method and the BFGS method to solve the optimization problem. These methods respectively give the quadratic and the superlinear convergence.

#### Newton-CG Method

The Newton method uses the second derivative information of the reduced cost functional $\hat{J}$ computed in the subsection 3.5.1 to solve the optimization problem (3.4) numerically. The method reads

**Algorithm 4.3** *[33] (Newton Algorithm)*

1. *choose an initial control $u_0 \in U_{ad}$.*

2. *for* $k = 0, 1, 2, ...$

   (a) *solve* $\hat{J}''(u_k)\delta u_k = -\hat{J}'(u_k)$,

   (b) *set* $u_{k+1} = u_k + \delta u_k$ *to update the control.*

The convergence of the algorithm is given by the following theorems.

**Theorem 4.4** *[22](Second-Order Sufficient Conditions) Suppose that* $\hat{J}''(u_k)$ *is continuous in an open neighbourhood of* $u^*$ *and that* $\hat{J}'(u^*) = 0$ *and* $\hat{J}''(u^*)$ *is positive definite. Then* $u^*$ *is a strict local minimizer of* $\hat{J}$. □

**Theorem 4.5** *[22] Suppose that* $\hat{J}$ *is twice differentiable and that the Hessian* $\hat{J}''(u_k)$ *is Lipschitz continuous in a neighbourhood of a solution* $u^*$ *at which the sufficient conditions (Theorem 4.4) are satisfied. Consider the Algorithm 4.3, where* $\delta u_k$ *is computed as* $\hat{J}''(u_k)\delta u_k = -\hat{J}'(u_k)$. *Then*

1. *if the starting point* $u_0$ *is sufficiently close to* $u^*$*, the sequence of iterates converges to* $u^*$*;*
2. *the rate of convergence of* $\{u_k\}$ *is quadratic; and*
3. *the sequence of gradient norms* $\left\{\|\hat{J}'(u_k)\|\right\}$ *converges quadratically to zero.* □

The computation of the reduced Hessian $\hat{J}''(u_k)$ as a matrix in the Newton equation $(2a)$ looks infeasible because of its size and the numerical effort involved. In this case, $(2a)$ must be solved iteratively, e.g. by a conjugate gradient method. The sequence of iterates (of CG method) for the linear equation is referred to as the inner iteration and the sequence of Newton steps as the outer iteration. The algorithm thus formed is called the Newton-CG (see [8, 21] for naming convention) method and it does not require explicit knowledge of the reduced Hessian. Rather it only requires that we can supply matrix-vector product of the form $\hat{J}''(u_k)\delta u_k$ for any given vector $\delta u_k$. Furthermore, by making the termination tolerance of this inner CG algorithm dependent on the convergence of the outer algorithm, the number of CG iterations can be reduced (see the stopping criterion of the inner CG loop as defined in [33, 37, 44]).

The CG method is designed to solve positive definite systems but the Hessian $\hat{J}''(u_k)$ may not always be positive definite. This problem is resolved by the

algorithm defined below where the CG iterations are terminated as soon as a direction of negative curvature is encountered. This adaption will ensure that the direction $\delta u_k$ is a descent direction.

**Algorithm 4.4** *[22, 33](Newton-CG)*

1. *choose an initial control* $u_0 \in U_{ad}$.
2. **for** $k = 0, 1, 2, ...$

   $(a)$ *solve the state system* (2.20) *and the adjoint system* (3.13)

   $(b)$ *using* (3.28) *evaluate* $\hat{J}'(u_k)$ *and set* $\delta u_k^j = 0$

   $(c)$ *set remainder* $r_k^j = \hat{J}'(u_k)$ *and* $p_k^j = -r_k^j$

   $(d)$ **for** $j = 0, 1, 2, ...$*terminate when*

$$\frac{\|r_k^j\|}{\|\hat{J}'(u_0)\|} < min\left\{\left(\frac{\|\hat{J}'(u_k)\|}{\|\hat{J}'(u_0)\|}\right)^{p_1}, q_1\frac{\|\hat{J}'(u_k)\|}{\|\hat{J}'(u_0)\|}\right\}$$

   $(i)$ *evaluate* $q_k^j = \hat{J}''(u_k)p_k^j$ *using procedure given in section* (3.5.1)

   $(ii)$ **if** $sp(p_k^j, q_k^j) \leq 0$ *and if it is first CG iteration then*

   - *compute* $\gamma_k^j = \dfrac{sp(r_k^j, r_k^j)}{sp(p_k^j, q_k^j)}$
   - *set* $\delta u_k^{j+1} = \delta u_k^j + \gamma_k^j p_k^j$
   - *break inner CG-loop, return* $\delta u_k^{j+1}$ *as* $\delta u_k$

   $(iii)$ **if** $sp(p_k^j, q_k^j) \leq 0$ *and if not the first CG iteration then*

   - *break inner CG-loop, return* $\delta u_k^{j+1}$ *as* $\delta u_k$

   $(iv)$ **if** $sp(p_k^j, q_k^j) > 0$

   - *compute* $\gamma_k^j = \dfrac{sp(r_k^j, r_k^j)}{sp(p_k^j, q_k^j)}$
   - *set* $\delta u_k^{j+1} = \delta u_k^j + \gamma_k^j p_k^j$

- *set* $r_k^{j+1} = r_k^j + \gamma_k^j q_k^j$
- *compute* $\beta_k^{j+1} = \dfrac{sp(r_k^{j+1}, r_k^{j+1})}{sp(r_k^j, r_k^j)}$
- *set* $p_k^{j+1} = -r_k^{j+1} + \beta_k^{j+1} p_k^j$

(*e*) **end** *of inner CG-loop, return* $\delta u_k^{j+1}$ *as* $\delta u_k$

(*f*) *set* $u_{k+1} = u_k + \alpha_k \delta u_k$ *to update the control.*

3. **end** *of outer Newton-loop*

where $\alpha_k$ is the step length and is chosen to satisfy the strong Wolfe conditions defined in remark 4.2. *sp* is the function that computes the scalar product of vectors and $p_1$, $q_1$ are the parameters used to tune the termination criterion in the inner CG-loop. The value of parameter $p_1$ decides the order of convergence of the outer iteration and it is chosen from the interval $(1, 2)$. The value of parameter $q_1$ is important for controlling termination of the first iteration of the Newton-CG method as the norm quotients in the first iteration are all 1. In our implementations of the algorithm, we have chosen $p_1 = 1.5$ and $q_1 = 0.1$. We will also discuss the convergence of the Newton-CG algorithm in Chapter 5 by choosing $p_1 = 1$ and $p_1 = 2$ as done in [35].

### BFGS Method

To avoid tedious work of computing the second derivative of the objective function, one can use the quasi-Newton methods which like steepest descent require only the gradient of the objective function. Since second derivatives are not required, quasi-Newton methods are sometimes more efficient than the Newton's method. We consider here the BFGS method which is one of the quasi-Newton method.

**Algorithm 4.5** *[22](BFGS)*

1. *given* $u_0 \in U_{ad}$,
2. *solve the state system* (2.20)
3. *solve the adjoint system* (3.13)

4. *evaluate* $\hat{J}'_0$

5. *set* $B_0 = I$, $k \leftarrow 0$

6. *while* $\dfrac{\|\hat{J}'_k\|}{\|\hat{J}'_0\|} > tol$

   (a) *solve* $B_k p_k = -\hat{J}'_k$ *for search direction* $p_k$

   (b) *compute* $\alpha_k$ *by strong Wolfe conditions (see remark 4.2)*

   (c) *set* $u_{k+1} = u_k + \alpha_k p_k$

   (d) *solve the state system* (2.20)

   (e) *solve the adjoint system* (3.13)

   (f) *using* (3.28) *evaluate* $\hat{J}'_{k+1}$

   (g) *define* $s_k = u_{k+1} - u_k,\ y_k = \hat{J}'_{k+1} - \hat{J}'_k$

   (h) *update* $B_{k+1} = B_k - \dfrac{B_k s_k s_k^T B_k}{s_k^T B_k s_k} + \dfrac{y_k y_k^T}{y_k^T s_k}$

   (i) $k \leftarrow k + 1$

7. *end*

For the first iteration $B_0$ is initialized with the identity matrix $I$, which means that the search direction is the steepest descent but further iterations are more and more refined by updating $B_k$. There are some other strategies as well to initialize the matrix $B_0$ (see [22]).

The BFGS method is robust and its rate of convergence is superlinear, e.g., see the following convergence result by [22].

**Assumption 4.1** *The Hessian matrix* $\nabla^2 \hat{J}$ *is Lipschitz continuous at* $u^* \in U_{ad}$*, that is,*

$$\|\nabla^2 \hat{J}(u) - \nabla^2 \hat{J}(u^*)\| \leq K\|u - u^*\|,$$

*for all* $u \in U_{ad}$ *near* $u^*$*, where* $K$ *is a positive constant.*

**Theorem 4.6** *[22] Suppose that $\hat{J}$ is twice continuously differentiable and that the iterates generated by the BFGS algorithm converge to a minimizer $u^*$ at which Assumption 4.1 holds. Suppose also that $\sum_{k=1}^{\infty} \|u_k - u^*\| < \infty$ holds. Then $u_k$ converges to $u^*$ at a superlinear rate.* □

## 4.2 Discretization

For numerical simulations, we discretize the continuous equations in the $x-t$ plane by choosing a uniform mesh width $h, k > 0$ where $h = \frac{1}{N}$, $k = \frac{1}{M}$. We define the discrete mesh points as $(x_i, t_j) = (ih, jk),\ i = 0, ..., N,\ j = 0, ..., M$ and use the notation $u_i^j$ to denote the value of the function $u(x,t)$ at these mesh points.

We use standard finite differences for space discretization. Hyperbolic type equations are discretized by the upwind scheme and the elliptic type equations by the central differences. The time derivative is treated in a semi-implicit way. Same numerical strategy is used for the state, the adjoint and the linearized state equations. However to solve the discretized nonlinear state equations, Newton's iterations are used.

### 4.2.1 State Equations

In the following we discretize the state equations (2.20). Discretization of the equation (2.20a) is give as

$$\frac{A_i^{j+1} - A_i^j}{k} + \frac{v_i^j A_i^{j+1} - v_{i-1}^j A_{i-1}^{j+1}}{h} = 0, \tag{4.3}$$

for $i = 1, ..., N$ and $j = 0, ..., M-1$, with

$$A_0^j = 1,\ A_i^0 = 1, \quad j = 0, ..., M,\ i = 0, ..., N.$$

State equation (2.20c) is nonlinear hyperbolic type equation. We discretize it by the upwind scheme

$$\frac{(R^2)_i^{j+1} - (R^2)_i^j}{k} + \frac{v_i^j (R^2)_i^{j+1} - v_{i-1}^j (R^2)_{i-1}^{j+1}}{h} - \frac{\pi c_1 p}{\mu(T_i^j) A_i^j} \left( (R^4)_i^{j+1} - \frac{(A^2)_i^j}{(4\pi c_1)^2} \right) = 0. \tag{4.4}$$

for $i = 1, ..., N$ and $j = 0, ..., M-1$, with

$$R_0^j = 1, \qquad j = 0, ..., M, \quad R_i^0 = 1, \qquad i = 0, ..., N.$$

Then we write the discretized equation in the form

$$f(R) = 0,$$

where

$$f = (f_1, f_2, ..., f_n)^T$$
$$R = (R_1, R_2, ..., R_n)^T.$$

and implement the following Newton's iterations to solve it.

1. set an initial guess $R^0$,
2. for $m = 0, 1, ...$ until convergence do
   - solve Newton equation $J(R^m)\, d^m = -f(R^m)$ for $d^m$,
   - set $R^{m+1} = R^m + d^m$ to update $R$

where $d^m$ is the correction vector and $J(R^m)$ is the Jacobian matrix which is defined as

$$[J(R^m)]_{ij} = \begin{cases} 2\left(1 + \dfrac{k}{h} v_i\right) R_i - \dfrac{4k\pi p c_1}{\mu(T_i) A_i} (R^3)_i, & \text{for } j = i \\ -\dfrac{2k}{h} v_{i-1} R_{i-1}, & \text{for } j = i-1 \\ 0, & \text{otherwise} \end{cases}$$

where $R_i^{j+1} = R_i, \quad A_i^j = A_i, \quad v_i^j = v_i, \quad T_i^j = T_i.$

The nonlinear state equation (2.20d) is discretized as

$$\frac{T_i^{j+1} - T_i^j}{k} + v_i^j \frac{T_i^{j+1} - T_{i-1}^{j+1}}{h} - \left(\frac{b_1 R_i^j}{A_i^j} + \frac{b_2}{R_i^j}\right)\left(T_a - T_i^{j+1}\right) - c_2\left(T_a^4 - (T^4)_i^{j+1}\right) = 0. \qquad (4.5)$$

To solve it we again apply the Newton's iterations where the Jacobian matrix for the Newton's iterations is defined as

$$[J(T^m)]_{ij} = \begin{cases} 1 + \dfrac{k}{h}v_i + k\left(\dfrac{b_1 R_i}{A_i} + \dfrac{b_2}{R_i}\right) + 4kc_2(T^3)_i, & \text{for } j = i \\ -\dfrac{k}{h}v_i, & \text{for } j = i-1 \\ 0, & \text{otherwise} \end{cases}$$

where $T_i^{j+1} = T_i, \quad A_i^j = A_i, \quad v_i^j = v_i, \quad R_i^j = R_i.$

**Remark 4.7** *The Jacobian matrices $[J(R^m)]_{ij}$ and $[J(T^m)]_{ij}$ are nonsingular and hence invertible.*

For the discretization of the elliptic type equation (2.20b), we use the central difference for spatial derivatives

$$\begin{aligned} &\frac{3}{h^2}\Bigg[\mu\left(\frac{T_{i+1}^j + T_i^j}{2}\right)\frac{A_{i+1}^j + A_i^j}{2}\left(v_{i+1}^j - v_i^j\right) \\ &- \mu\left(\frac{T_i^j + T_{i-1}^j}{2}\right)\frac{A_i^j + A_{i-1}^j}{2}\left(v_i^j - v_{i-1}^j\right)\Bigg] + StA_i^j = 0, \end{aligned} \tag{4.6}$$

for $i = 1, ..., N-1$ and with boundary conditions

$$v_0^j = 1, \; v_N^j = (v_d)^j, \qquad for \; j = 0, ..., M.$$

### 4.2.2 Adjoint Equations

Using the upwind scheme, the linear adjoint equation (3.13a) is discretized as

$$\begin{aligned} -\frac{(\xi_A)_i^{j+1} - (\xi_A)_i^j}{k} - v_i^j\frac{(\xi_A)_{i+1}^j - (\xi_A)_i^j}{h} &= \frac{3\mu(T_i^j)}{h^2}(v_{i+1}^j - v_i^j)\left((\xi_v)_{i+1}^{j+1} - (\xi_v)_i^{j+1}\right) - w_1(A_i^j - Ad) \\ &- \frac{\pi c_1 p}{\mu(T_i^j)}\left(\frac{(R^4)_i^j}{(A^2)_i^j} + \frac{1}{(4\pi c_1)^2}\right)(\xi_R)_i^{j+1} - St(\xi_v)_i^{j+1} \\ &- \frac{b_1 R_i^j}{(A^2)_i^j}(T_a - T_i^j)(\xi_T)_i^{j+1}. \end{aligned}$$

for $i = N-1, ..., 0$ and $j = M-1, ..., 0$, with conditions

$$(\xi_A)_N^j = 0,\ (\xi_A)_i^M = -w_2(A_i^M - A_d), \quad j = M, ..., 0,\ i = N, ..., 0.$$

and the discretization of the adjoint equation (3.13b) is given as

$$\frac{3}{h^2}\Bigg[\mu\left(\frac{T_{i+1}^j + T_i^j}{2}\right)\frac{A_{i+1}^j + A_i^j}{2}\left((\xi_v)_{i+1}^j - (\xi_v)_i^j\right) - \mu\left(\frac{T_i^j + T_{i-1}^j}{2}\right)\frac{A_i^j + A_{i-1}^j}{2}\left((\xi_v)_i^j - (\xi_v)_{i-1}^j\right)\Bigg] = \frac{1}{2h} \times \left[A_i^j((\xi_A)_{i+1}^j - (\xi_A)_{i-1}^j) + (R^2)_i^j((\xi_R)_{i+1}^j - (\xi_R)_{i-1}^j) - (\xi_T)_i^j(T_{i+1}^j - T_{i-1}^j)\right].$$

for $i = 1, ..., N-1$ and with boundary conditions

$$(\xi_v)_0^j = 0,\ (\xi_v)_N^j = 0, \qquad for\ j = M, ..., 0.$$

Similarly we can discretize the other adjoint equations for the adjoint variables $\xi_R$ and $\xi_T$.

### 4.2.3 Linearized State Equations

While discretizing the linearized state equations (3.39), the derivatives are discretized in a similar way as for the state equations. Semi-implicit discretization of (3.39a) is given as

$$\frac{(V_A)_i^{j+1} - (V_A)_i^j}{k} + \frac{(vV_A)_i^{j+1} - (vV_A)_{i-1}^{j+1}}{h} + \frac{A_i^{j+1}(V_v)_i^j - A_{i-1}^{j+1}(V_v)_{i-1}^j}{h} = 0. \tag{4.7}$$

for $i = 1, ..., N$ and $j = 0, ..., M-1$, and with

$$(V_A)_0^j = 0,\ (V_A)_i^0 = 0, \quad j = 0, ..., M,\ i = 0, ..., N.$$

Equations (3.39c) and (3.39d) are respectively discretized as

$$\frac{(RV_R)_i^{j+1} - (RV_R)_i^j}{k} + \frac{(vRV_R)_i^{j+1} - (vRV_R)_{i-1}^{j+1}}{h} - \frac{2\pi c_1 p(R^3)_i^{j+1}}{(\mu A)_i^j}(V_R)_i^{j+1} = \frac{\pi c_1 p}{2\mu(T_i^j)}\Bigg[\frac{\beta(V_T)_i^j}{A_i^j}\left((R^4)_i^j - \frac{(A^2)_i^j}{(4\pi c_1)^2}\right) - (V_A)_i^j \times \left(\frac{(R^4)_i^j}{(A^2)_i^j} + \frac{1}{(4\pi c_1)^2}\right)\Bigg] - \frac{1}{2h}\left((R^2V_v)_i^j - (R^2V_v)_{i-1}^j\right), \tag{4.8}$$

for $i = 1, ..., N$ and $j = 0, ..., M-1$, and with

$$(V_R)_0^j = 0, \quad j = 0, ..., M, \quad (V_R)_i^0 = 0, \qquad i = 0, ..., N.$$

$$\frac{(V_T)_i^{j+1} - (V_T)_i^j}{k} + v_i^{j+1}\frac{(V_T)_i^{j+1} - (V_T)_{i-1}^{j+1}}{h} + \left(4c_2(T^3)_i^j + \frac{b_1 R_i^j}{A_i^j} + \frac{b_2}{R_i^j}\right) \times (V_T)_i^{j+1} = \left[\frac{b_1(V_R)_i^{j+1}}{A_i^j} - \frac{b_1 R_i^j (V_A)_i^{j+1}}{(A^2)_i^j} - \frac{b_2(V_R)_i^{j+1}}{(R^2)_i^j}\right] \times (T_a - T_i^j) - (V_v)_i^j \frac{T_i^j - T_{i-1}^j}{h}, \tag{4.9}$$

for $i = 1, ..., N$ and $j = 0, ..., M-1$, and

$$(V_T)_0^j = 0, \quad j = 0, ..., M, \quad (V_T)_i^0 = 0, \quad i = 0, ..., N.$$

The discretization of equation (3.39b) is

$$\begin{aligned}
&\frac{3}{h^2}\left[\mu\left(\frac{T_{i+1}^j + T_i^j}{2}\right)\frac{A_{i+1}^j + A_i^j}{2}\left((V_v)_{i+1}^j - (V_v)_i^j\right)\right. \\
&\qquad \left. - \mu\left(\frac{T_i^j + T_{i-1}^j}{2}\right)\frac{A_i^j + A_{i-1}^j}{2}\left((V_v)_i^j - (V_v)_{i-1}^j\right)\right] \\
&= \frac{3\beta}{h^2}\left[\mu\left(\frac{T_{i+1}^j + T_i^j}{2}\right)\left(\frac{(V_T)_{i+1}^j + (V_T)_i^j}{2}\right)\left(\frac{A_{i+1}^j + A_i^j}{2}\right)\left(v_{i+1}^j - v_i^j\right)\right. \\
&\qquad \left. - \mu\left(\frac{T_i^j + T_{i-1}^j}{2}\right)\left(\frac{(V_T)_i^j + (V_T)_{i-1}^j}{2}\right)\left(\frac{A_i^j + A_{i-1}^j}{2}\right)\left(v_i^j - v_{i-1}^j\right)\right] \\
&\quad - \frac{3}{h^2}\left[\mu\left(\frac{T_{i+1}^j + T_i^j}{2}\right)\frac{(V_A)_{i+1}^j + (V_A)_i^j}{2}\left(v_{i+1}^j - v_i^j\right)\right. \\
&\qquad \left. - \mu\left(\frac{T_i^j + T_{i-1}^j}{2}\right)\frac{(V_A)_i^j + (V_A)_{i-1}^j}{2}\left(v_i^j - v_{i-1}^j\right)\right] - StA_i^j
\end{aligned} \tag{4.10}$$

for $i = 1, ..., N-1$ and with boundary conditions

$$(V_v)_0^j = 0, \ (V_v)_N^j = (\delta u)^j, \qquad for\ j = 0, ..., M.$$

### 4.2.4 Linearized Adjoint Equations

Discretization of the equations (3.47) are given as

$$
\begin{aligned}
&-\frac{(W_A)_i^{j+1}-(W_A)_i^j}{k}-v_i^j\frac{(W_A)_{i+1}^j-(W_A)_i^j}{h}=-(V_v)_i^j\frac{(\xi_A)_{i+1}^j-(\xi_A)_i^j}{h}\\
&+\frac{3\mu_i^j}{h^2}\Big[\left((W_v)_{i+1}^{j+1}-(W_v)_i^{j+1}\right)(v_{i+1}^j-v_i^j)+\beta(V_T)_i^j\left((\xi_v)_{i+1}^j-(\xi_v)_i^j\right)\\
&\times(v_{i+1}^j-v_i^j)-\left((\xi_v)_{i+1}^j-(\xi_v)_i^j\right)\left((V_v)_{i+1}^j-(V_v)_i^j\right)\Big]-\frac{b_1(RV_T\xi_T)_i^j}{(A^2)_i^j}\\
&+\frac{\pi c_1 p}{\mu_i^j}\Big[\left(\beta(V_T\xi_R)_i^j-(W_R)_i^{j+1}\right)\left(\frac{(R^4)_i^j}{(A^2)_i^j}+\frac{1}{(4\pi c_1)^2}\right)+\frac{2(R^3\xi_R)_i^j}{(A^3)_i^j}\\
&\times\left(2(AV_R)_i^j-(RV_A)_i^j\right)\Big]-\frac{b_1(T_a-T_i^j)}{(A^2)_i^j}\Big[(\xi_T)_i^j\left(\frac{2(RV_A)_i^j}{A_i^j}-(V_R)_i^j\right)\\
&+(R)_i^j(W_T)_i^{j+1}\Big]-St(W_v)_i^{j+1}+w_1(V_A)_i^j \qquad (4.11)
\end{aligned}
$$

for $i=N-1,...,0$ and $j=M-1,...,0$, and with conditions

$$(W_A)_N^j=0,\ (W_A)_i^M=w_2(V_A)_i^M,\quad j=M,...,0,\ i=N,...,0.$$

$$
\begin{aligned}
&-R_i^j\frac{(W_R)_i^{j+1}-(W_R)_i^j}{k}-v_i^jR_i^j\frac{(W_R)_{i+1}^j-(W_R)_i^j}{h}-\frac{2\pi c_1 p(R^3)_i^j}{(\mu A)_i^j}(W_R)_i^j\\
&=\frac{2\pi c_1 p(R^2)_i^j(\xi_R)_i^j}{(\mu A)_i^j}\left(\frac{(RV_A)_i^j}{A_i^j}-2(V_R)_i^j-\beta(RV_T)_i^j\right)+\frac{1}{2}\Big[(V_T\xi_T)_i^j\\
&+(T_a-T_i^j)(W_T)_i^j+\frac{(V_R\xi_T)_i^j}{R_i^j}(T_a-T_i^j)\Big]\left(\frac{b_1}{A_i^j}-\frac{b_2}{(R^2)_i^j}\right)+\frac{1}{2}(\xi_T)_i^j\\
&\times(T_a-T_i^j)\left(\frac{b_1(V_A)_i^j}{(A^2)_i^j}-\frac{2b_2(V_R)_i^j}{(R^3)_i^j}\right)-(RV_v)_i^j\frac{(\xi_R)_{i+1}^j-(\xi_R)_i^j}{h}, \qquad (4.12)
\end{aligned}
$$

for $i=N-1,...,0$ and $j=M-1,...,0$, with

$$(W_R)_N^j=0,\ (W_R)_i^M=0,\quad j=M,...,0,\ i=N,...,0.$$

$$
\begin{aligned}
-\frac{(W_T)_i^{j+1}-(W_T)_i^j}{k}-\frac{(vW_T)_{i+1}^j-(vW_T)_i^j}{h}+\left(4c_2(T^3)_i^j+\frac{b_1R_i^j}{A_i^j}+\frac{b_2}{R_i^j}\right)\\
\times(W_T)_i^j=\frac{3\beta\mu_i^j}{h^2}\Bigg[\left\{(V_A)_i^j\left((\xi_v)_{i+1}^j-(\xi_v)_i^j\right)-A_i^j\left((W_v)_{i+1}^j-(W_v)_i^j\right)\right\}\\
\times\left(v_{i+1}^j-v_i^j\right)-\beta(V_TA)_i^j\left(v_{i+1}^j-v_i^j\right)\left((\xi_v)_{i+1}^j-(\xi_v)_i^j\right)+A_i^j\\
\times\left((\xi_v)_{i+1}^j-(\xi_v)_i^j\right)\left((V_v)_{i+1}^j-(V_v)_i^j\right)\Bigg]+\frac{\beta\pi c_1p}{(\mu A)_i^j}\Bigg[-4(V_R\xi_R)_i^j\\
\times(R^3)_i^j+\left((W_R)_i^j-\beta(V_T\xi_R)_i^j\right)\left((R^4)_i^j-\frac{(A^2)_i^j}{(4\pi c_1)^2}\right)+(AV_A)_i^j\\
\times(\xi_R)_i^j\left(\frac{(R^4)_i^j}{(A^2)_i^j}+\frac{1}{(4\pi c_1)^2}\right)\Bigg]+\Bigg[12c_2(T^2)_i^j(V_T)_i^j-\frac{b_1(RV_A)_i^j}{(A^2)_i^j}\\
+(V_R)_i^j\left(\frac{b_1}{A_i^j}-\frac{b_2}{(R^2)_i^j}\right)\Bigg](\xi_T)_i^j-\frac{1}{h}\left((V_v\xi_T)_{i+1}^j-(V_v\xi_T)_i^j\right),
\end{aligned}
\tag{4.13}
$$

for $i=N-1,...,0$ and $j=M-1,...,0$, with

$$
(W_T)_N^j=0,\ (W_T)_i^M=0,\quad j=M,...,0,\ i=N,...,0.
$$

Adjoint equation (3.47b) can be discretized exactly the same way as the equation (3.13b) was discretized.

Discretized state equations are solved forward in time and the discretized adjoint equations are solved backward in time.

**Remark 4.8** *Discretized equations given in subsections 4.2.3 and 4.2.4 respectively yield transpose of each other. For example, if we write the discretized equations* (4.7) *and* (4.11) *in matrix form respectively as*

$$
\begin{bmatrix}
1+\frac{k}{h}v_1^{j+1} & 0 & \dots & 0\\
-\frac{k}{h}v_1^{j+1} & 1+\frac{k}{h}v_2^{j+1} & & 0\\
\vdots & \ddots & \ddots & \vdots\\
0 & \dots & -\frac{k}{h}v_{N-1}^{j+1} & 1+\frac{k}{h}v_N^{j+1}
\end{bmatrix}
\begin{bmatrix}
(V_A)_1^{j+1}\\(V_A)_2^{j+1}\\\vdots\\(V_A)_N^{j+1}
\end{bmatrix}=
\begin{bmatrix}
(f_A)_1\\(f_A)_2\\\vdots\\(f_A)_N
\end{bmatrix}
\tag{4.14}
$$

*where*

$$(f_A)_i = (V_A)_i^j - \frac{k}{h}\left(A_i^{j+1}(V_v)_i^j - A_{i-1}^{j+1}(V_v)_{i-1}^j\right),\ i = 1, ..., N, j = 0, ..., M-1.$$

*and*

$$\begin{bmatrix} 1+\frac{k}{h}v_0^j & -\frac{k}{h}v_0^j & \dots & 0 \\ 0 & 1+\frac{k}{h}v_1^j & \ddots & \vdots \\ \vdots & & \ddots & -\frac{k}{h}v_{N-2}^j \\ 0 & 0 & \dots & 1+\frac{k}{h}v_{N-1}^j \end{bmatrix} \begin{bmatrix} (W_A)_0^j \\ (W_A)_1^j \\ \vdots \\ (W_A)_{N-1}^j \end{bmatrix} = \begin{bmatrix} (g_A)_0 \\ (g_A)_2 \\ \vdots \\ (g_A)_{N-1} \end{bmatrix} \tag{4.15}$$

*where*

$(g_A)_i = (W_A)_i^{j+1} + \frac{k}{h}v_i^j(W_A)_{i+1}^j + k$ *times terms on RHS of equation* (4.11)
$i = N-1, ..., 0,\ j = M-1, ..., 0.$

*then we observe that the coefficient matrices in* (4.14) *and* (4.15) *yield transpose of each other. Similar results can be shown for the others discretized equations. On the basis of this we conclude that the reduced Hessian matrix* (3.30b) *is symmetric provided that the matrix* $L_{ww}$ *given by* (3.31) *is symmetric.*

### 4.2.5 Consistency of Schemes

We check the consistency and the order of accuracy of the discretized equations given in sections 4.2.1 and 4.2.3 with the help of truncation error.

**Definition 4.1** *[20] A finite difference scheme* $P_{h,k}R_{h,k}(u) = f$ *is consistent with the partial differential equation* $Pu = f$ *if for any smooth function* $\phi(x,t)$

$$P\phi - P_{h,k}\phi \to 0 \quad as\ h, k \to 0,$$

*the convergence being pointwise convergence at each point* $(x,t)$.

**Definition 4.2** *[20] A scheme* $P_{h,k}R_{h,k}(u) = R_{h,k}f$ *that is consistent with the differential equation* $Pu = f$ *is accurate of order* $p$ *in space and order* $q$ *in time if for any smooth function* $\phi(x,t)$

$$P_{h,k}\phi - R_{h,k}(P\phi) = \mathcal{O}(h^p) + \mathcal{O}(k^q).$$

*We say that such a scheme is accurate of order* $(p,q)$.

**Remark 4.9** *The quantity $P_{h,k}\phi - R_{h,k}(P\phi)$ is called the truncation error of the scheme. $R_{h,k}$ is the restriction operator that transforms the continuous functions to the grid functions.*

A simple way to compute the local truncation error is to replace the approximate solution, say, $U_i^j$ in the difference equation by the true solution, say, $u(x_i, t_j) := u(ih, jk)$ and then to use the Taylor series expansions about the point $(x_i, t_j)$.

**Theorem 4.10** *(grid consistency of state equations) Let $A, v, R, T$ are sufficiently smooth functions of independent variables $x$ and $t$. Then the finite difference methods* (4.3)-(4.6) *are consistent with the partial differential equations* (2.20a)-(2.20d) *respectively. Furthermore, the schemes* (4.3)-(4.5) *are accurate of order* 1 *both in time and space and the scheme* (4.6) *is accurate of order* 2 *in space.*

*Proof*: To prove consistency, we need to determine the truncation error of each of the finite difference schemes (4.3)-(4.5). First, we consider the finite difference equation (4.3) and replace the approximate solutions with the true solutions, e.g. $A_i^j$ with $A(x_i, t_j)$, to get

$$TE_{h,k}^A = \frac{A(x_i, t_{j+1}) - A(x_i, t_j)}{k} + \frac{v(x_i, t_j)A(x_i, t_{j+1}) - v(x_{i-1}, t_j)A(x_{i-1}, t_{j+1})}{h}$$

Now using the Taylor series expansions

$$A(x_i, t_{j+1}) = A + kA_t + \frac{k^2}{2!}A_{tt} + ... \tag{4.16a}$$

$$A(x_{i-1}, t_{j+1}) = A + (kA_t - hA_x) + \frac{1}{2!}\left(k^2A_{tt} - 2khA_{xt} + h^2A_{xx}\right) + ... \tag{4.16b}$$

$$v(x_{i-1}, t_j) = v - hv_x + \frac{h^2}{2!}v_{xx} + ... \tag{4.16c}$$

where $A := A(x_i, t_j)$ and $v := v(x_i, t_j)$.

and simplifying we get

$$TE_{h,k}^A = A_t + (vA)_x + k\left[v_xA_t + vA_{xt} + \frac{1}{2}A_{tt}\right] - \frac{h}{2}\left[vA_{xx} + 2A_xv_x + Av_{xx}\right] + \mathcal{O}(h^2) + \mathcal{O}(k^2)$$

Now since $A_t + (vA)_x = 0$, we have

$$TE^A_{h,k} = \mathcal{O}(h) + \mathcal{O}(k) \ \rightarrow 0 \text{ as } h, k \rightarrow 0$$

Next we consider the finite difference equation (4.4) and replace the approximate solutions with the true solutions to get

$$\begin{aligned} TE^R_{h,k} =& \frac{1}{k}\left[R^2(x_i, t_{j+1}) - R^2(x_i, t_j)\right] + \frac{1}{h}\Big[v(x_i, t_j)R^2(x_i, t_{j+1}) - v(x_{i-1}, t_j) \\ & \times R^2(x_{i-1}, t_{j+1})\Big] - \frac{\pi c_1 p}{\mu(T(x_i, t_j))A(x_i, t_j)}\left[R^4(x_i, t_{j+1}) - \frac{A^2(x_i, t_j)}{(4\pi c_1)^2}\right]. \end{aligned}$$

Again using Taylor series expansions about $(x_i, t_j)$ and simplifying we get

$$\begin{aligned} TE^R_{h,k} =& (R^2)_t + \left(vR^2\right)_x - \frac{\pi c_1 p}{\mu(T)A}\left(R^4 - \frac{A^2}{(4\pi c_1)^2}\right) + k\Big[v_x(R^2)_t + v(R^2)_{xt} \\ & + \frac{1}{2}(R^2)_{tt} + \frac{\pi c_1 p}{\mu(T)A}(R^4)_t\Big] - \frac{h}{2}\Big[v(R^2)_{xx} + 2(R^2)_x v_x + (R^2)v_{xx}\Big] \\ & + \mathcal{O}(h^2) + \mathcal{O}(k^2) \end{aligned}$$

Using the continuous equations (2.20c) we arrive at

$$TE^R_{h,k} = \mathcal{O}(h) + \mathcal{O}(k) \ \rightarrow 0 \text{ as } h, k \rightarrow 0 \tag{4.17}$$

Applying the same procedure to the finite difference equations (4.5) and (4.6) we respectively get the following truncation errors

$$\begin{aligned} TE^T_{h,k} =& k\left[c_2(T^4)_t + \left(\frac{b_1 R}{A} + \frac{b_2}{R}\right)T_t + vT_{xt} + \frac{1}{2}T_{tt}\right] \\ & + h\left(-\frac{v}{2}T_{xx}\right) + \mathcal{O}(h^2) + \mathcal{O}(k^2) \end{aligned}$$

and

$$\begin{aligned} TE^v_h = h^2\Big[&\frac{1}{8}A\mu_{xxx}v_x + \frac{3}{8}A_x\mu_{xx}v_x + \frac{3}{8}A_{xx}\mu_x v_x + \frac{1}{8}A_{xxx}\mu v_x \\ & + \frac{3}{8}A\mu_{xx}v_{xx} + \frac{3}{4}A_x\mu_x v_{xx} + \frac{3}{8}A_{xx}\mu v_{xx} + \frac{1}{2}A\mu_x v_{xxx} \\ & + \frac{1}{2}A_x\mu v_{xxx} + \frac{1}{4}A\mu v_{xxxx}\Big] + \mathcal{O}(h^4). \end{aligned}$$

Hence

$$TE^T_{h,k} \rightarrow 0, \ TE^v_h \rightarrow 0 \text{ as } h, k \rightarrow 0.$$

□

In order to prove the grid consistency of the linearized state equations (3.39a)-(3.39d), we give the following theorem.

**Theorem 4.11** *(grid consistency of linearized state equations) Let $V_A$, $V_v$, $V_R$, $V_T$ are sufficiently smooth functions of independent variables $x$ and $t$. Then the finite difference methods* (4.7)-(4.9) *are respectively consistent with the differential equations* (3.39a)-(3.39d). *Furthermore, the schemes* (4.7)-(4.9) *are accurate of order* 1 *both in time and space and the scheme* (4.10) *is accurate of order* 2 *in space.*

*Proof*: Consider the finite difference equation (4.7) and replace the approximate solutions $(V_A)_i^j$, $(V_v)_i^j$, $A_i^j$, $v_i^j$ respectively by $V_A(x_i,t_j)$, $V_v(x_i,t_j)$, $A(x_i,t_j)$, $v(x_i,t_j)$ to get the truncation error

$$TE_{h,k}^{V_A} = \frac{1}{k}\Big[V_A(x_i,t_{j+1}) - V_A(x_i,t_j)\Big] + \frac{1}{h}\Big[v(x_i,t_{j+1}V_A(x_i,t_{j+1}) - v(x_{i-1},t_{j+1}) \times V_A(x_{i-1},t_{j+1}))\Big] + \frac{1}{h}\Big[A(x_i,t_{j+1})V_v(x_i,t_j) - A(x_{i-1},t_{j+1})V_v(x_{i-1},t_j)\Big].$$

Using the Taylor series expansions

$$\begin{aligned} V_A(x_i,t_{j+1}) =& V_A + k(V_A)_t + \frac{k^2}{2!}(V_A)_{tt} + ... \\ V_A(x_{i-1},t_{j+1}) =& V_A + (k(V_A)_t - h(V_A)_x) + \frac{1}{2!}\Big[k^2(V_A)_{tt} \\ & - 2kh(V_A)_{xt} + h^2(V_A)_{xx}\Big] + ... \end{aligned}$$

$$\begin{aligned} V_v(x_i,t_{j+1}) =& V_v + k(V_v)_t + \frac{k^2}{2!}(V_v)_{tt} + ... \\ V_v(x_{i-1},t_{j+1}) =& V_v + (k(V_v)_t - h(V_v)_x) + \frac{1}{2!}\Big[k^2(V_v)_{tt} \\ & - 2kh(V_v)_{xt} + h^2(V_v)_{xx}\Big] + ... \end{aligned}$$

and the expansions (4.16), and then cancelling out and rearranging the terms, we get

$$\begin{aligned} TE_{h,k}^{V_A} =& k\Big[(V_vA_t)_x + (v(V_A)_x)_t + (V_Av_x)_t + \frac{1}{2}(V_A)_{tt}\Big] \\ & + h\Big[-\frac{1}{2}\left(v(V_A)_{xx} + V_Av_{xx} + A(V_v)_x x + V_vA_{xx}\right) \\ & + v_x(V_A)_x + A_x(V_v)_x\Big] + \mathcal{O}(h^2) + \mathcal{O}(k^2). \end{aligned}$$

or

$$TE_{h,k}^{V_A} = \mathcal{O}(h) + \mathcal{O}(k) \to 0 \text{ as } h, k \to 0$$

Following the similar procedure for the other discretized equations (4.8)-(4.10), we reach at the following truncation errors

$$\begin{aligned} TE_{h,k}^{V_R} = k\Bigg[&\frac{1}{2}R(V_R)_{tt} + R_t(V_R)_t + \frac{1}{2}V_R R_{tt} + vR(V_R)_{xt} + (vR)_t(V_R)_x + (vR)_x \\ &\times (V_R)_t + V_R(vR_{xt} + v_t R_x + v_x R_t + Rv_{xt}) - \frac{2\pi c_1 p}{\mu A}(R^3 V_R)_t\Bigg] \\ -h\Bigg[&\frac{1}{2}vR(V_R)_{xx} + (vR)_x(V_R)_x + V_R(vR_{xx} + 2v_x R_x + Rv_{xx}) + \frac{1}{4}V_v \\ &\times (R^2)_{xx} + \frac{1}{2}(V_v)_x(R^2)_x + \frac{1}{4}R^2(V_v)_{xx}\Bigg] + \mathcal{O}(h^2) + \mathcal{O}(k^2) \end{aligned}$$

$$\begin{aligned} TE_{h,k}^{V_T} = k\Bigg[&\frac{1}{2}(V_T)_{tt} + v(V_T)_{xt} + v_t(V_T)_x + \left(4c_2T^3 + \frac{b_1 R}{A} + \frac{b_2}{R}\right)(V_T)_t \\ &+ (T_a - T)\left(\frac{b_1(V_R)_t}{A} - \frac{b_1 R(V_A)_t}{A^2} - \frac{b_2(V_R)_t}{R^2}\right)\Bigg] \\ &+ h\Bigg[-\frac{1}{2}v(V_T)_{xx} - \frac{1}{2}V_v T_{xx}\Bigg] + \mathcal{O}(k^2) + \mathcal{O}(h^2). \end{aligned}$$

$$\begin{aligned} TE_h^{V_v} = h^2\Bigg[&\frac{1}{4}\left\{A\mu(V_v)_{xxxx} + v_{xxxx}\left(\mu V_A - \beta\mu A V_T\right)\right\} + \frac{1}{8}(V_v)_x(\mu A)_{xxx} \\ &+ \frac{3}{8}\left\{(V_v)_{xx}(\mu A)_{xx} + v_{xx}\left((\mu V_A)_{xx} - \beta(\mu A V_T)_{xx}\right)\right\} \\ &+ \frac{1}{2}\left\{(V_v)_{xxx}(\mu A)_x + v_{xxx}\left((\mu V_A)_x - \beta(\mu A V_T)_x\right)\right\} \\ &+ \frac{1}{8}v_x\left((\mu V_A)_{xxx} - \beta(\mu A V_T)_{xxx}\right)\Bigg] + \mathcal{O}(h^4). \end{aligned}$$

Hence

$$TE_h^{V_v} \to 0,\ TE_{h,k}^{V_R} \to 0,\ TE_{h,k}^{V_T} \to 0 \text{ as } h, k \to 0.$$

□

# Chapter 5

# Numerical Results

In this chapter we present the numerical results for the control problems defined in Chapter 3 and in Appendix A. To obtain these results, we use the solution algorithms and the discretization defined in Chapter 4. The parameters appearing in the equations (state equations, adjoint equations, linearized state equations, linearized adjoint equations) use values given in the tables 2.1 and 5.1. Specific heat, density and thermal conductivity are assumed to be constant.

In the following sections, numerical results both for the isothermal and the non-isothermal tube drawing models are presented, discussed and compared. Performance comparison of the solution algorithms and the analysis of the Newton-CG algorithm is discussed in subsection 5.1.2.

| Parameters | Symbols | Values |
|---|---|---|
| length of hot-forming zone | $L$ | $1\ m$ |
| final time | $t_f$ | 1 |
| input temperature | $T_0$ | $1300\ K$ |
| input viscosity | $\mu_0$ | $5 \times 10^5\ Pa\ sec.$ |
| temperature-viscosity parameter. | $\beta$ | 13 |
| inside pressure | $p$ | $420\ Pa$ |
| feeding speed | $v_0$ | $1\ mm/sec.$ |
| drawing speed | $v_L$ | $12\ mm/sec.$ |

Table 5.1: Parameter values involved in simulations [18, 49]

| Opt. Algorithms | $s_2$ | |
|---|---|---|
| | Isothermal | Non-isothermal |
| SD | 0.9 | 0.9 |
| NCG | 0.87 | 0.87 |
| BFGS | 0.56 | 0.6 |
| Newton-CG | 0.9 | 0.65 |

Table 5.2: Value of parameter used in strong Wolfe conditions

## 5.1 Control of Area for the entire Time Domain

We consider the control problems (3.4) and (A.3) with $w_1 = 1$, $w_2 = 0$ with the aim to find the time dependent optimal drawing speed $v_d(t)$ of the drawing machine such that the glass tubes of the desired cross-sectional area $A_d$ are obtained. Here $A_d$ is defined as constant both in space and time. The parameters $s_1$ and $s_2$ used in the strong Wolfe conditions (4.1) are defined as $s_1 = 10^{-4}$ and for $s_2$ see the table 5.2.

### 5.1.1 Comparison of Isothermal and Non-isothermal Processes

We started the optimization process with the constant drawing speed $v_d = 12$ and reached the optimal speed that varies over the time and minimizes the cost functional (3.1) with $w_1 = 1$ and $w_2 = 0$. The profile of the drawing speed before and after optimization is shown in the figure 5.1. From this figure we conclude that the process starts with a high drawing speed and then after $t = 0.1$ the drawing speed becomes almost constant over time except very near to the final time $t = t_f$ where it is approaching zero. The profiles of drawing speed both for the isothermal and the non-isothermal processes are quite similar except at the start where the isothermal process starts with a little bit higher speed than that of the non-isothermal process.

In figures 5.2-5.4, we have plotted the cross-sectional area $A(x, t)$ before and after optimization at different times both for the isothermal and the non-isothermal processes. We notice here how the optimal drawing speed $v_d$ is forcing the cross-sectional area $A$ to converge to the desired state $A_d$ in the very start of the processes. For the non-isothermal process, cross-sectional

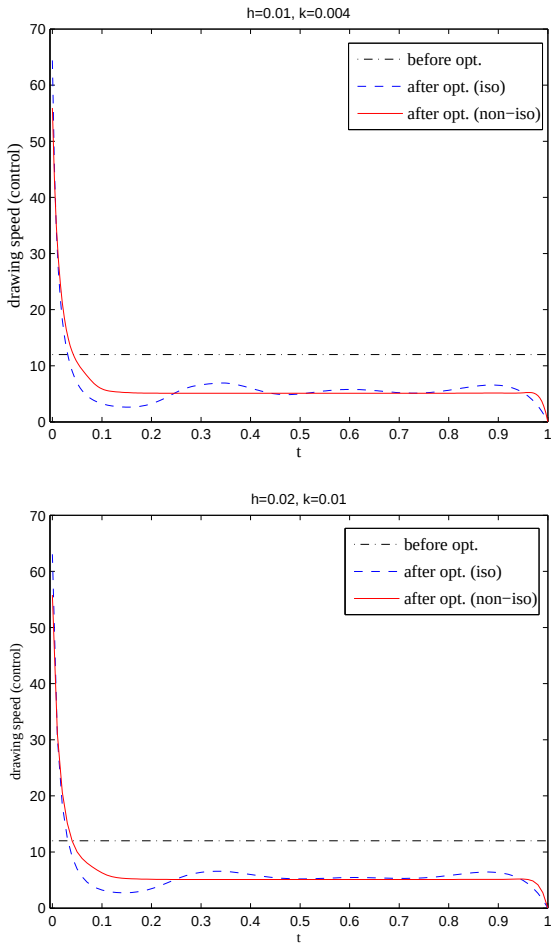


Figure 5.1: Drawing speed (control) before and after optimization. Isothermal: $\lambda = 1.4 \times 10^{-4}$, Non-isothermal: $\lambda = 1.8 \times 10^{-4}$ (SD algorithm).

area has almost reached the desired state at time $t = 0.35$ and we don't observe any change afterwards in the area. However in the isothermal process, it takes more time to match the desired state.

Mean radius $R(x,t)$ of the tube, the temperature $T(x,t)$ and the viscosity $\mu(T)$ of the fluid (glass) before and after optimization at time $t = t_f$ are shown in figure 5.5. Figure 5.6 shows the tube geometry before and after optimization at $t = t_f$ where one can observe that the optimized tube is matching to the desired one.

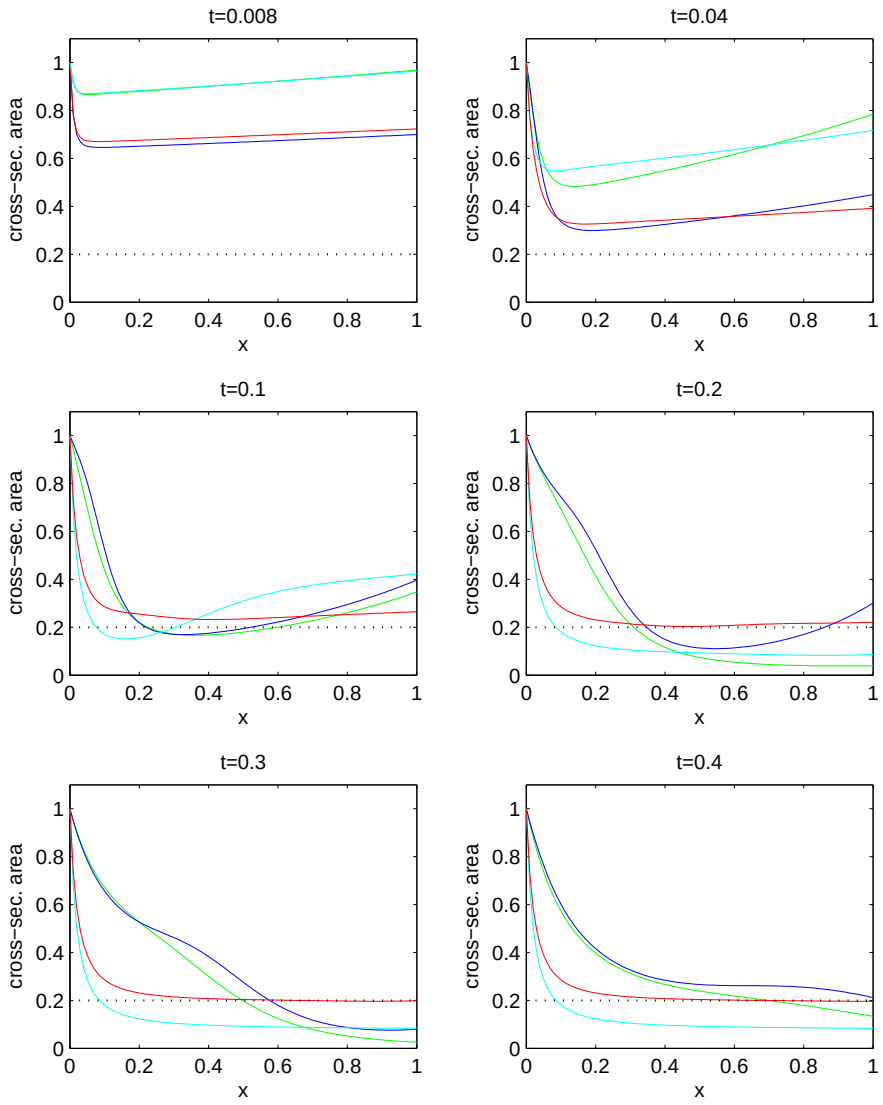


Figure 5.2: Cross-sectional area $A$ before and after optimization at different times for $h = 0.01$, $k = 0.004$, Isothermal: before opt.- green, after opt.- blue and $\lambda = 1.4 \times 10^{-4}$. Non-isothermal: before opt.- cyan, after opt.- red and $\lambda = 1.8 \times 10^{-4}$. (SD algorithm).

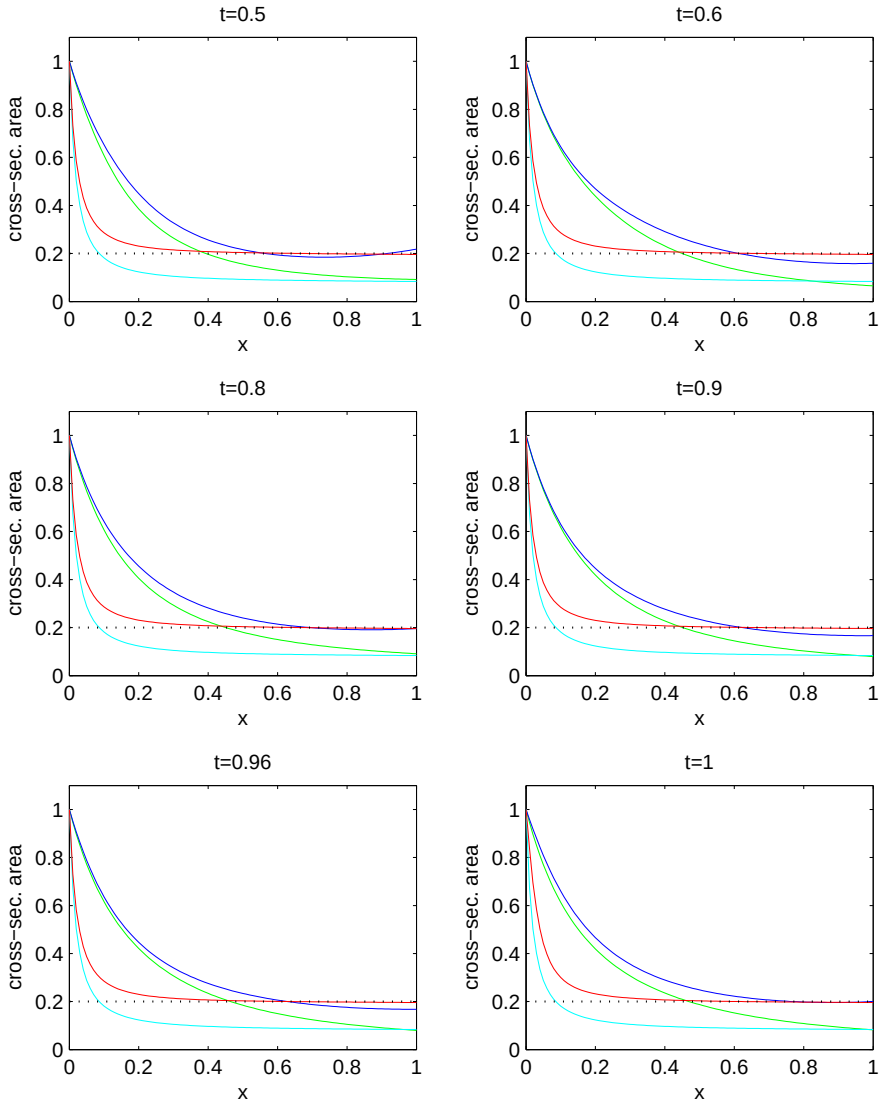


Figure 5.3: Cross-sectional area $A$ before and after optimization at different times for $h = 0.01$, $k = 0.004$, Isothermal: before opt.- green, after opt.- blue and $\lambda = 1.4 \times 10^{-4}$. Non-isothermal: before opt.- cyan, after opt.- red and $\lambda = 1.8 \times 10^{-4}$. (SD algorithm).

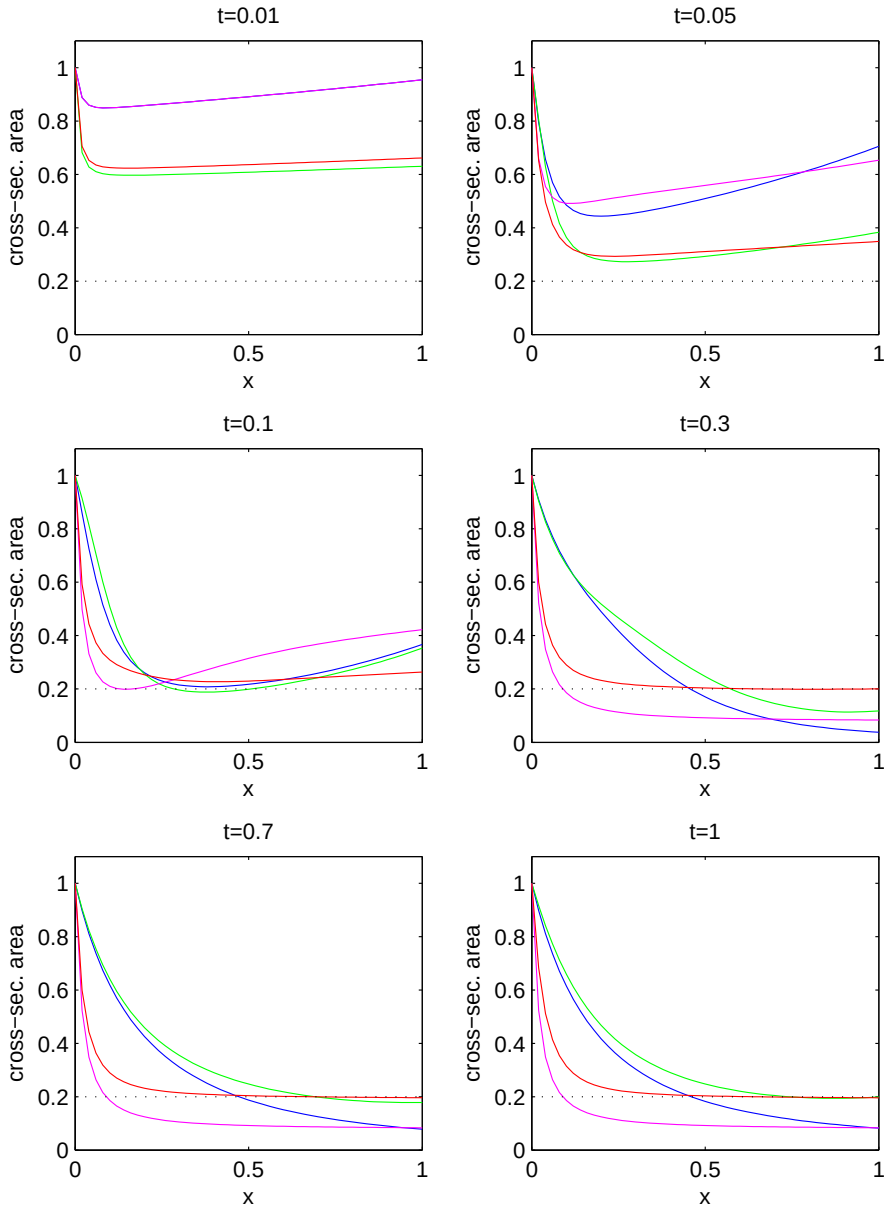


Figure 5.4: Cross-sectional area $A$ before and after optimization at different times for $h = 0.02$, $k = 0.01$, Isothermal: before opt.- blue, after opt.- green and $\lambda = 1.4 \times 10^{-4}$. Non-isothermal: before opt.- magenta, after opt.- red and $\lambda = 1.8 \times 10^{-4}$. (SD algorithm).

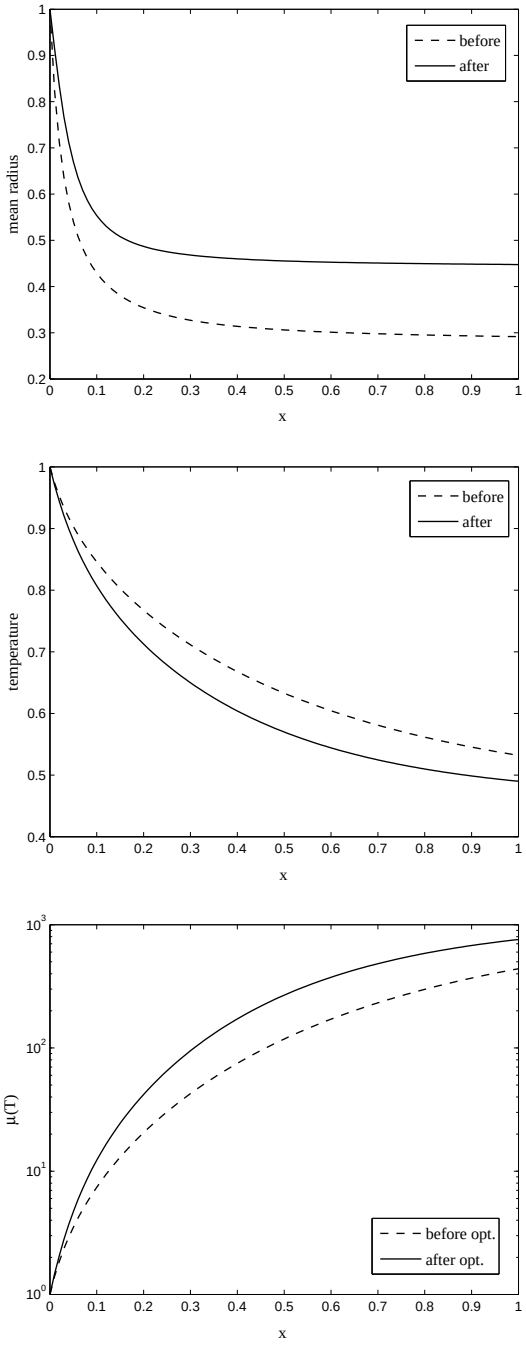


Figure 5.5: Mean radius $R$ (top), temperature $T$ (middle) and viscosity $\mu(T)$ (bottom) before and after optimization at time $t = t_f$ for $h = 0.01$, $k = 0.004$ and $\lambda = 1.8 \times 10^{-4}$ (SD algorithm - non-isothermal tube drawing).

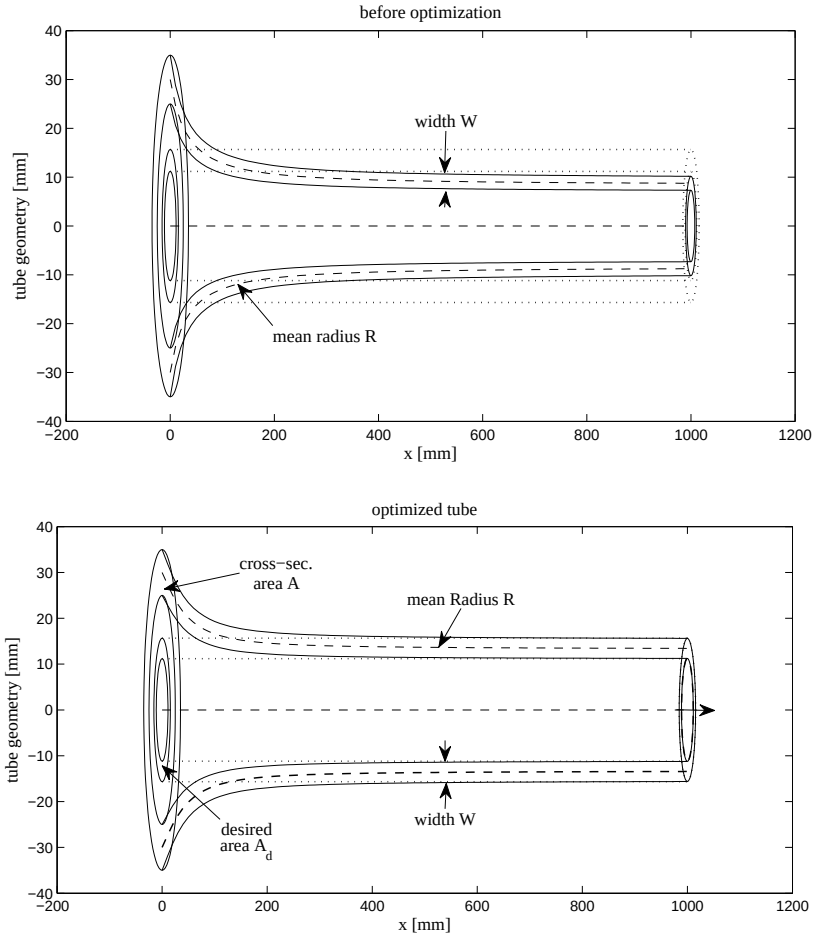


Figure 5.6: Tube geometry before and after optimization at $t = t_f$. (for $h = 0.01$, $k = 0.004$ and $\lambda = 1.8 \times 10^{-4}$)

Convergence of the cost functional to the minimum under four different optimization algorithms is shown in figures 5.7 (non-isothermal) and 5.8 (isothermal). We observe decrease in the cost functional with the iterations, indicating that the objective functional has been minimized. Figures 5.10 and 5.11 show the decrease of the $L^2$ norm of the gradient against the number of iterations for each of the solution algorithms. Observations are shown in the figure 5.9. From these figures, we also conclude that our iterative schemes for the minimization problems (3.4) and (A.3) converge.

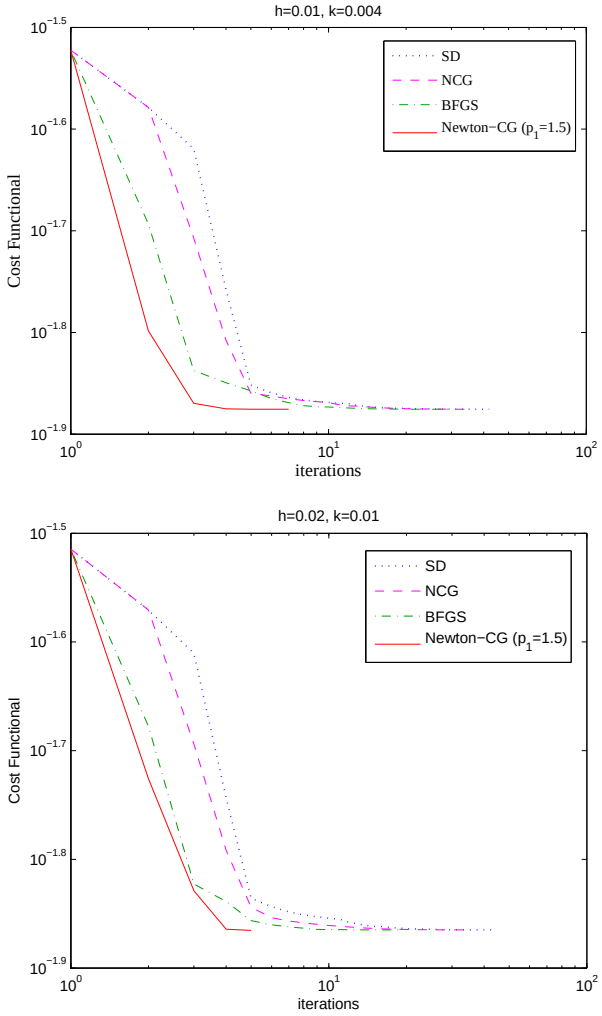


Figure 5.7: Evaluation of Cost Functional under SD, NCG, BFGS, Newton-CG ($p_1 = 1.5$) optimization algorithms (non-isothermal tube drawing). $\lambda = 1.8 \times 10^{-4}$

| Opt. Algo. | Comp. Time (min) | Itrs. | Func. Evaluations |
|---|---|---|---|
| SD | 36.96 | 42 | 196 |
| NCG | 31.77 | 36 | 173 |
| BFGS | 23.3 | 30 | 118 |
| Newton-CG ($p_1 = 1.5$) | 7.54 | 6 (30) | 9 |

Table 5.3: Performance evaluations of optimization algorithms when $h = 0.01$, $k = 0.004$ and $\lambda = 1.8 \times 10^{-4}$ (non-isothermal tube drawing)

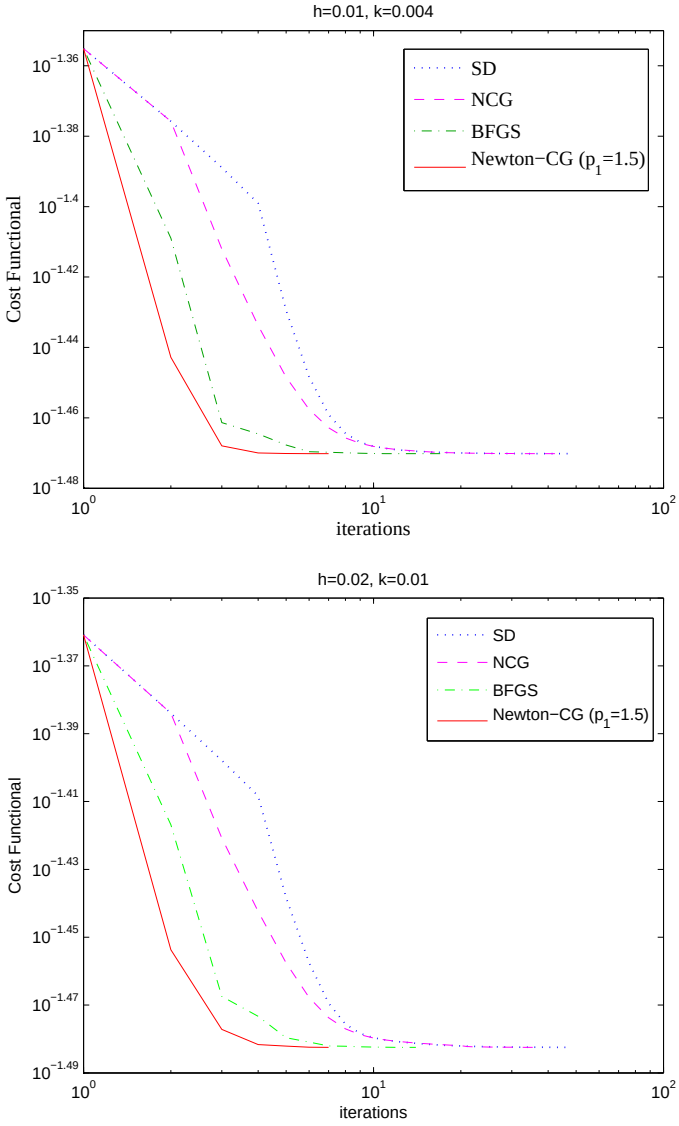


Figure 5.8: Evaluation of Cost Functional under SD, NCG, BFGS, Newton-CG ($p_1 = 1.5$) optimization algorithms (isothermal tube drawing). $\lambda = 1.4 \times 10^{-4}$

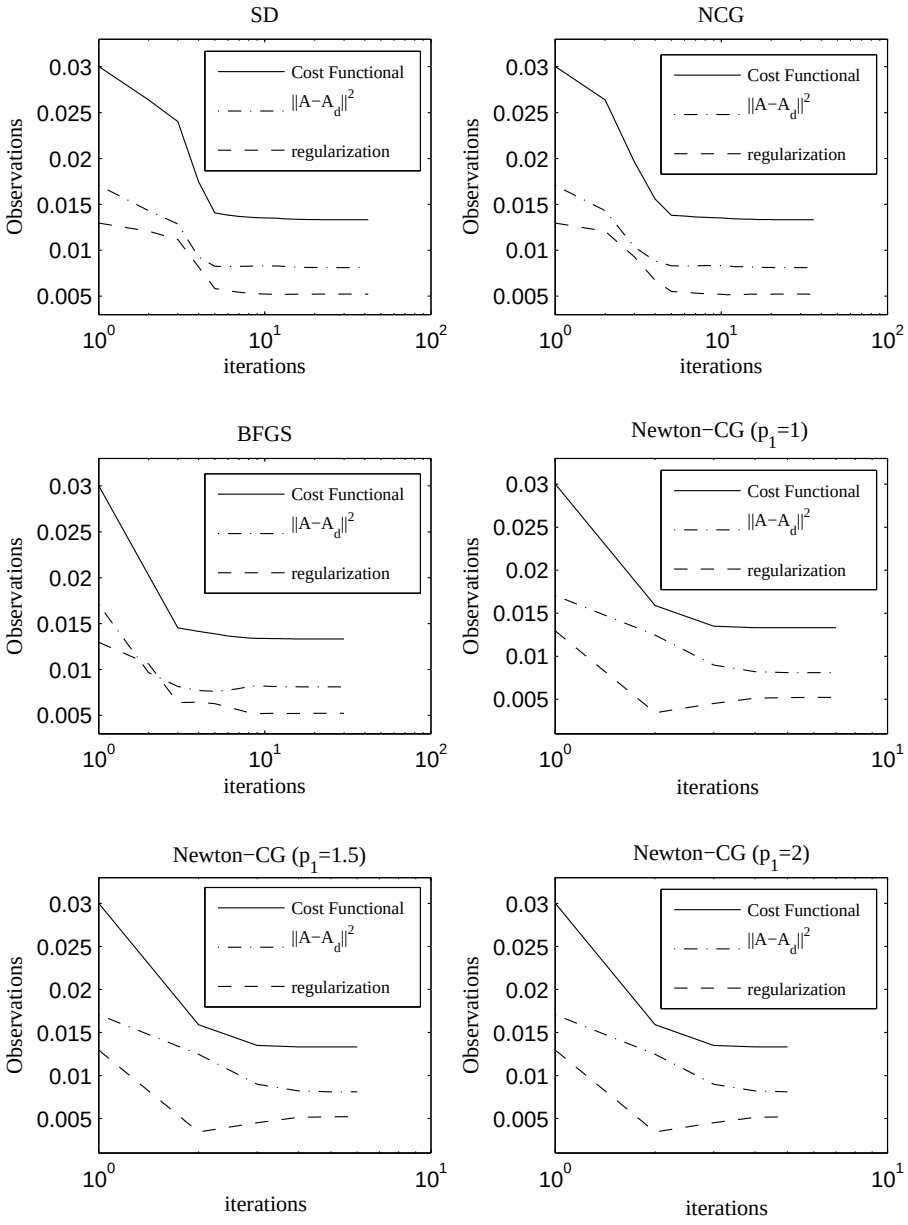


Figure 5.9: Cost functional and observations under SD, NCG, BFGS, and Newton-CG optimization algorithms for $h = 0.01$, $k = 0.004$ and $\lambda = 1.8 \times 10^{-4}$ (non-isothermal tube drawing) .

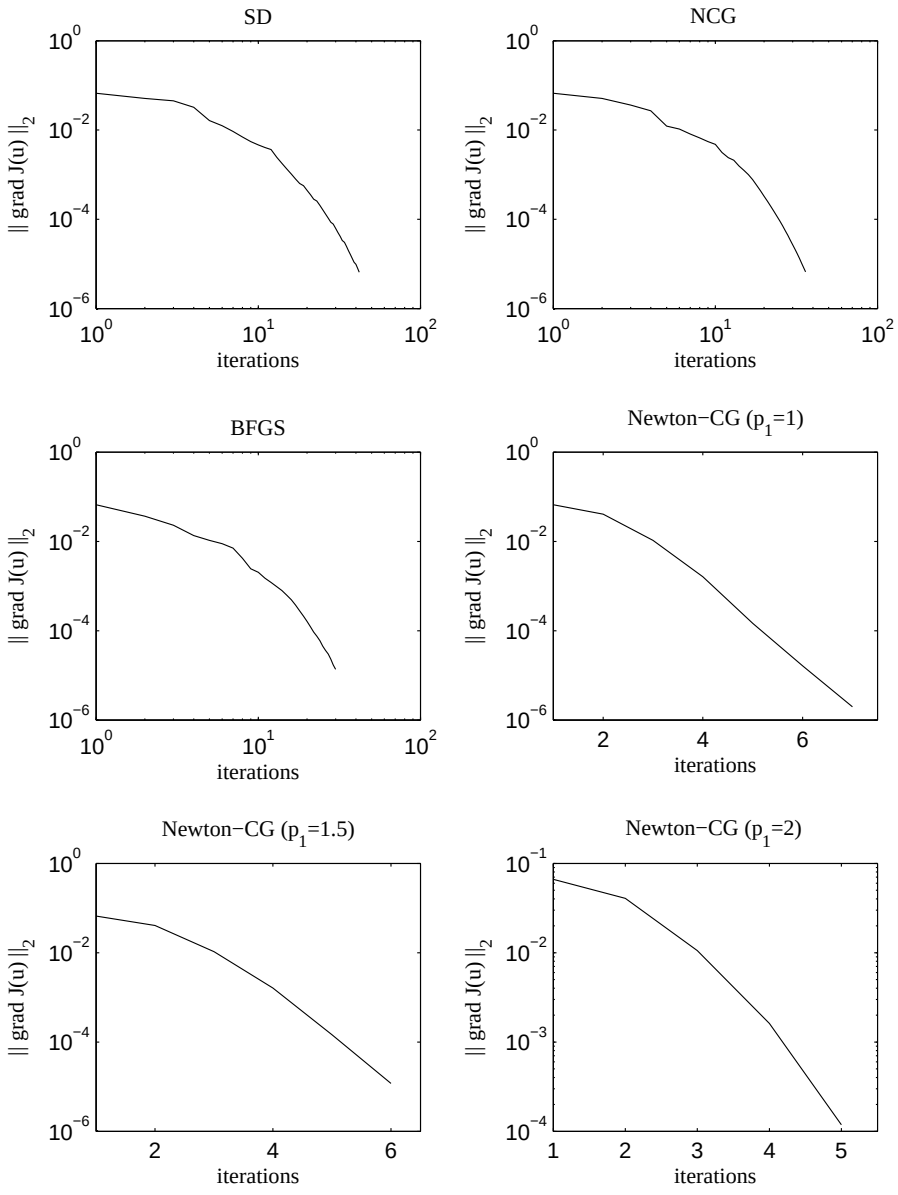


Figure 5.10: Evaluation of $\|\hat{J}'(u)\|_2$ under different optimization algorithms for $h = 0.01$, $k = 0.004$ and $\lambda = 1.8 \times 10^{-4}$ (non-isothermal tube drawing).

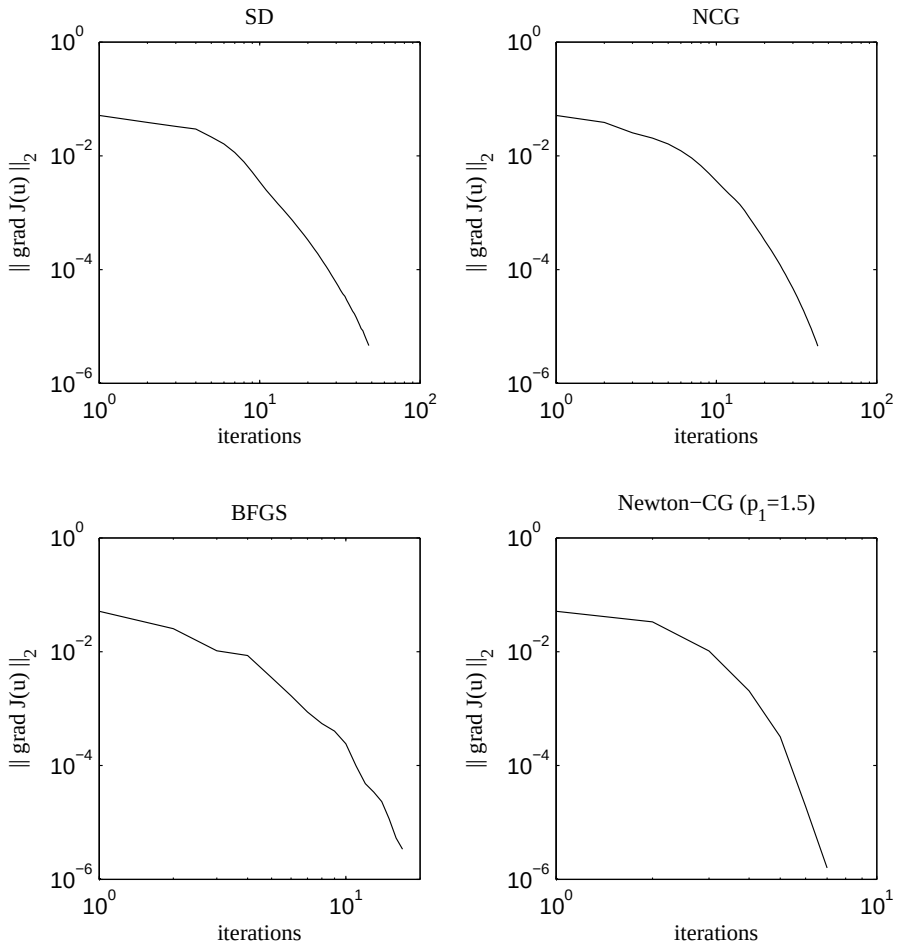


Figure 5.11: Evaluation of $\|\hat{J}'(u)\|_2$ under different optimization algorithms for $h = 0.01$, $k = 0.004$ and $\lambda = 1.4 \times 10^{-4}$ (isothermal tube drawing).

### 5.1.2 Comparisons of Algorithms

We used the first order (SD, NCG), the superlinear (BFGS) and the second order (Newton-CG) optimization algorithms to find the optimal control (drawing speed) for the control problems (3.4) and (A.3). From the obtained results, we notice that less number of optimization iterations are needed in the case of superlinear Algorithm 4.5 and the second order Algorithm 4.4 as compared to the first order Algorithms 4.1-4.2 (see the tables 5.3 and 5.5). Further comparisons of these algorithms in terms of number of solution iterations can be seen in figures 5.7 and 5.8 where the cost functional is plotted against the solution iterations.

Because of the quadratic convergence of the Newton-CG Algorithm 4.4, very few iterations are needed to reach the optimal solution as compared to the others. We present the figures 5.12 and 5.13 to see the convergence behaviour of the Newton-CG algorithm. In figure 5.12, decrease of the residual $r_k^j$ is shown for different values of $p_1 = 1, 1.5, 2$ (see stopping criterion in inner CG loop of the Algorithm 4.4). For all of the three cases we observe a linear convergence at the beginning of the iterations but later on the superlinear convergence (for $p_1 = 1.5$) and the quadratic convergence (for $p_1 = 2$) behaviour are also noticed. From figure 5.13, we also observe the influence of the parameter $p_1$ on the number of CG steps. For $p_1 = 1$ we have almost constant amount of CG steps in each Newton iteration and for $p_1 = 2$ we get a sudden increase towards the end of the iterations. However, overall number of CG steps are almost the same in both of the cases.

To study the influence of the grid spacing $h$ on the performance of the Newton-CG Algorithm 4.4, we keep the parameter $p_1 = 1.5$ and the regularization parameter $\lambda = 1.8 \times 10^{-4}$ fixed and vary only the grid spacing from 1/80 through 1/125 to 1/225. We, from the figure 5.14, don't observe any dependence of the residuals on the grid spacing $h$. However a small dependence of the CG iterations on the grid spacing $h$ is observed in figure 5.15.

Finally we perform the numerical test for three different values of the regularization parameter $\lambda$ to see its influence on the algorithm. In figure 5.16(*top*) where observations are plotted against number of Newton iterations, we notice a significant reduction after two steps. For the smallest value of $\lambda$, this reduction is comparatively more but on the other hand one more Newton iteration and more CG iterations are needed to meet the stopping criterion, e.g. see the figure 5.16(*middle*). We also observe bad convergence of the algorithm in figure 5.16(*bottom*) with the decrease of the regularizing param-

| Opt. Algo. | Comp. Time (min) | Itrs. | Func. Evaluations |
|---|---|---|---|
| SD | 9.51 | 43 | 202 |
| NCG | 6.92 | 34 | 169 |
| BFGS | 3.06 | 19 | 90 |
| Newton-CG ($p_1 = 1.5$) | 1.21 | 5 (20) | 8 |

Table 5.4: Performance evaluations of the optimization algorithms when $h = 0.02$, $k = 0.01$ and $\lambda = 1.8 \times 10^{-4}$ (non-isothermal tube drawing)

eter $\lambda$.

We end our discussion on results for the isothermal and the non-isothermal tube drawing with the tables 5.3, 5.4, 5.5 and 5.6 that show the performance comparison of all of the four algorithms for optimal control problems (3.4) and (A.3) in terms of the solutions iterations, the functional evaluations, and the computation time. From these tables we can conclude that Newton-CG algorithms is more efficient than the others.

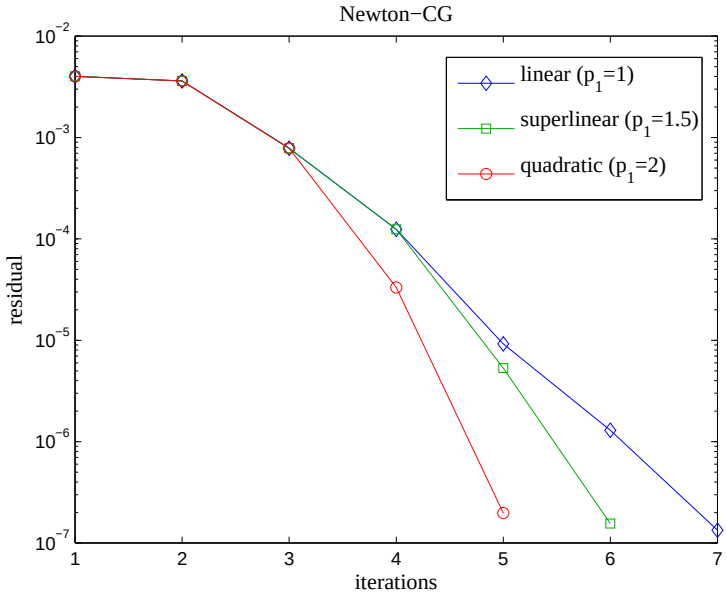


Figure 5.12: Dependence of the residuals on $p_1$. Here $h = 0.01$, $k = 0.004$ and $\lambda = 1.8 \times 10^{-4}$ (non-isothermal tube drawing)

| Opt. Algo. | Comp. Time (min) | Itrs. | Func. Evaluations |
|---|---|---|---|
| SD | 14.66 | 48 | 234 |
| NCG | 13.29 | 43 | 214 |
| BFGS | 6.56 | 17 | 99 |
| Newton-CG ($p_1 = 1.5$) | 2.24 | 7 (32) | 8 |

Table 5.5: Performance evaluations of the optimization algorithms when $h = 0.01$, $k = 0.004$ and $\lambda = 1.4 \times 10^{-4}$ (isothermal tube drawing)

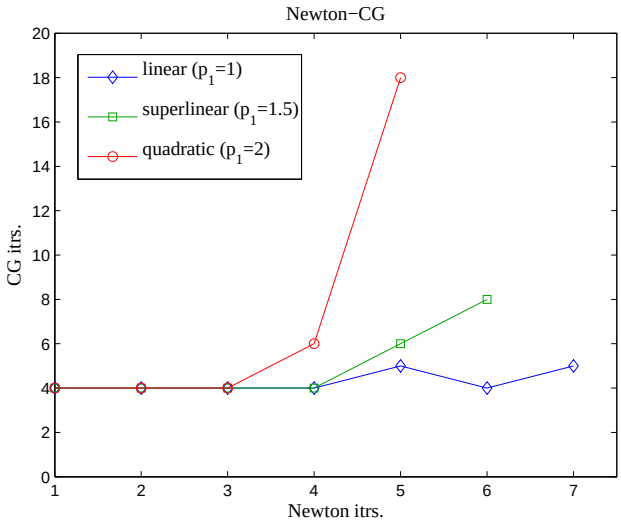


Figure 5.13: Dependence of CG iterations on $p_1$. Here $h = 0.01$, $k = 0.004$ and $\lambda = 1.8 \times 10^{-4}$ (non-isothermal tube drawing)

| Opt. Algo. | Comp. Time (min) | Itrs. | Func. Evaluations |
|---|---|---|---|
| SD | 3.49 | 46 | 227 |
| NCG | 2.05 | 37 | 186 |
| BFGS | 1.13 | 14 | 80 |
| Newton-CG ($p_1 = 1.5$) | 0.34 | 7 (26) | 8 |

Table 5.6: Performance evaluations of the optimization algorithms when $h = 0.02$, $k = 0.01$ and $\lambda = 1.4 \times 10^{-4}$ (isothermal tube drawing)

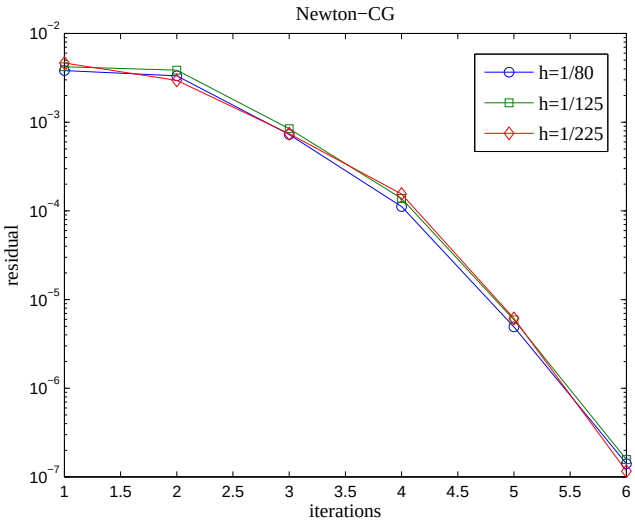


Figure 5.14: Dependence of the residuals on grid spacing $h$ with $k = 0.004$. (non-isothermal tube drawing)

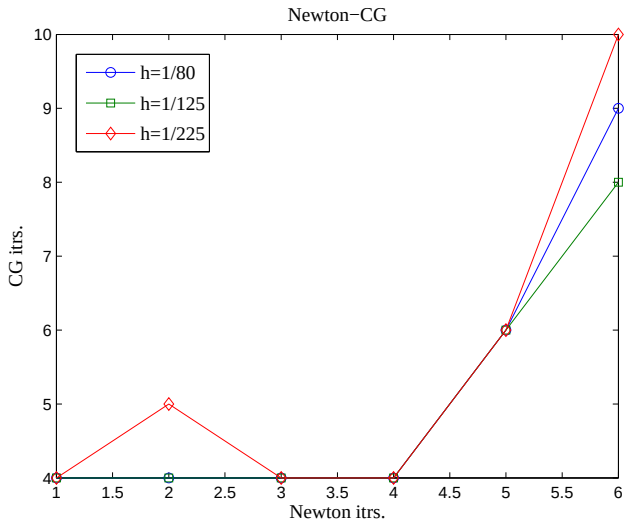


Figure 5.15: Dependence of the CG iterations on $h$ with $k = 0.004$. (non-isothermal tube drawing)

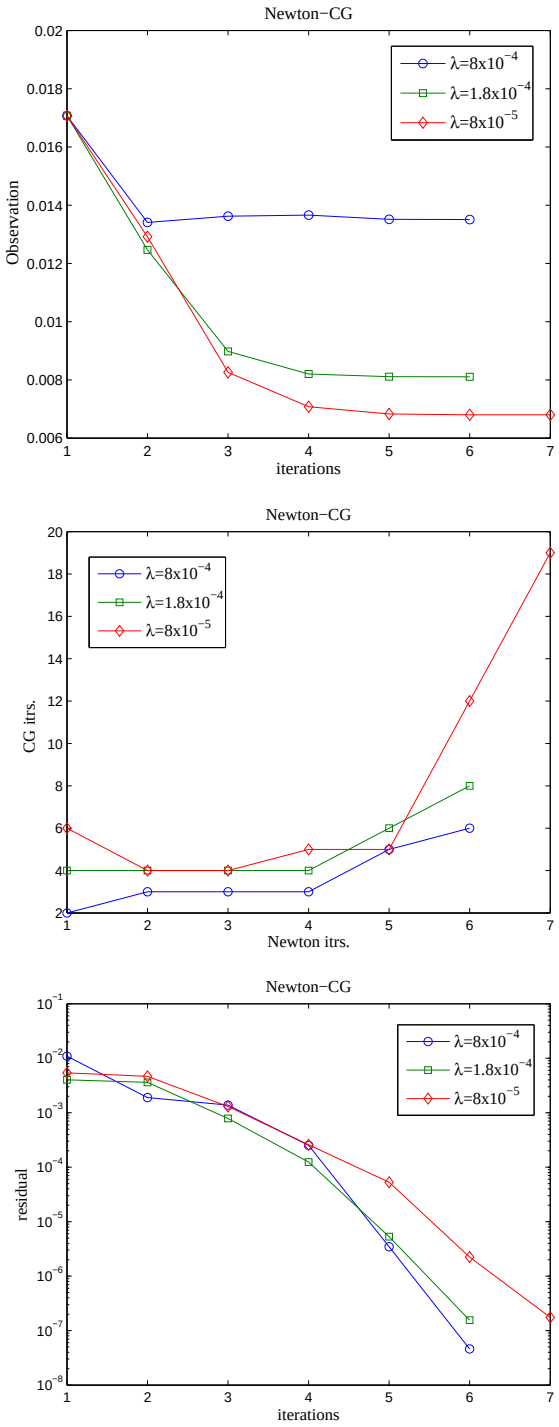


Figure 5.16: Dependence of the observations on $\lambda$ (top), dependence of the CG iterations on $\lambda$ (middle), dependence of the residuals on $\lambda$ (bottom), Here $h = 0.01, k = 0.004$ and $p_1 = 1.5$. (non-isothermal tube drawing)

## 5.2 Control of Area at Final Time

Here we consider the control problems (3.4) and (A.3) with $w_1 = 0$, $w_2 = 1$ and try to find the optimal drawing speed $v_d(t)$ such that the cross-sectional area at final time $t = t_f$ matches the desired area $A_d$ defined as

$$A_d(x) = \begin{cases} -\frac{7}{2}x + 1, & 0 \leq x \leq 0.2, \\ -\frac{1}{4}x + \frac{7}{20}, & 0.2 \leq x \leq 0.6, \\ 0.2, & 0.6 \leq x \leq 1. \end{cases}$$

The parameters $s_1$ and $s_2$ used in the strong Wolfe conditions (4.1) are given as $s_1 = 10^{-4}$, $s_2 = 0.9$ (for isothermal) and 0.78 (for non-isothermal).

### 5.2.1 Comparison of Isothermal and Non-isothermal Processes

Optimal profiles of the drawing speed $v_d(t)$ both for the isothermal and the non-isothermal processes are shown in the figure 5.17. We observe that both of the processes start with almost similar drawing speeds which remain constant till $t = 0.6$ and then change with time. We notice a high increase in the drawing speed near $t = 1$ for the isothermal process as compared to the non-isothermal process. This behaviour of the drawing speed is quite different from that of the optimal speed determined in the previous section where the processes start with high drawing speeds. The reason is the profile of the area to be controlled.

Cross-sectional area $A(x, t)$ before and after optimization at different times is shown in the figures 5.18 and 5.19. From these figures, we can observe how the increase in the drawing speeds near the final time $t = t_f$ is forcing

| Processes | Comp. Time (min) | Itrs. | Func. Evaluations |
|---|---|---|---|
| Isothermal | 4.58 | 19 | 96 |
| non-isothermal | 40.5 | 89 | 355 |

Table 5.7: Performance evaluations of the NCG algorithm for control problems (3.4) and (A.3) with $w_1 = 0$, $w_2 = 1$

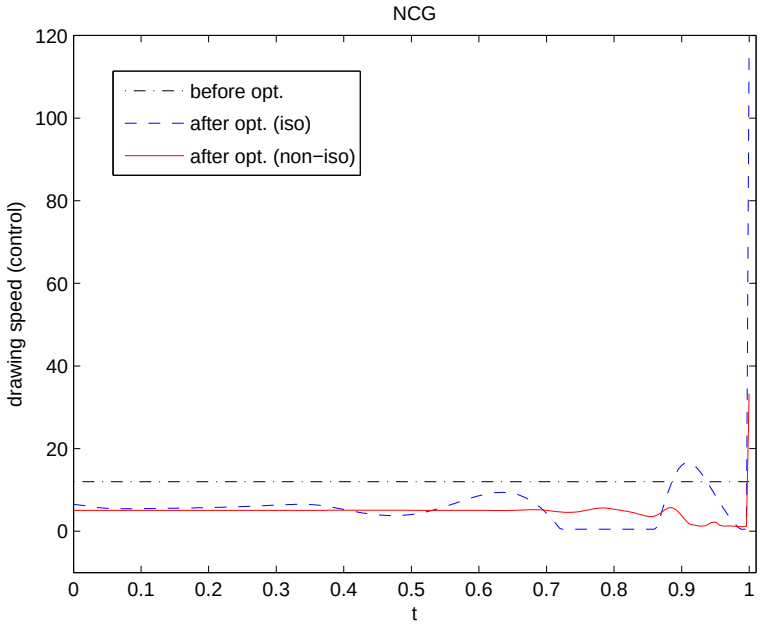


Figure 5.17: Drawing speed (control) before and after optimization. Isothermal: $\lambda = 1.6 \times 10^{-5}$, Non-isothermal: $\lambda = 5.8 \times 10^{-5}$.

the cross-sectional area to meet the desired area. In the non-isothermal case, matching at the final time is more accurate as compared to the isothermal case.

Tube geometry before and after optimization is shown in figure 5.20. Convergence of the cost functional to the minimum and the observations both for the isothermal and non-isothermal processes are shown in figure 5.21. Mean radius $R(x,t)$ of the tube, temperature $T(x,t)$ and viscosity $\mu(T)$ of the fluid (glass) before and after optimization at time $t = t_f$ are shown in the figure 5.22.

The results presented in this section are obtained by using the NCG Algorithm 4.2 whose performance evaluation is given in table 5.7.

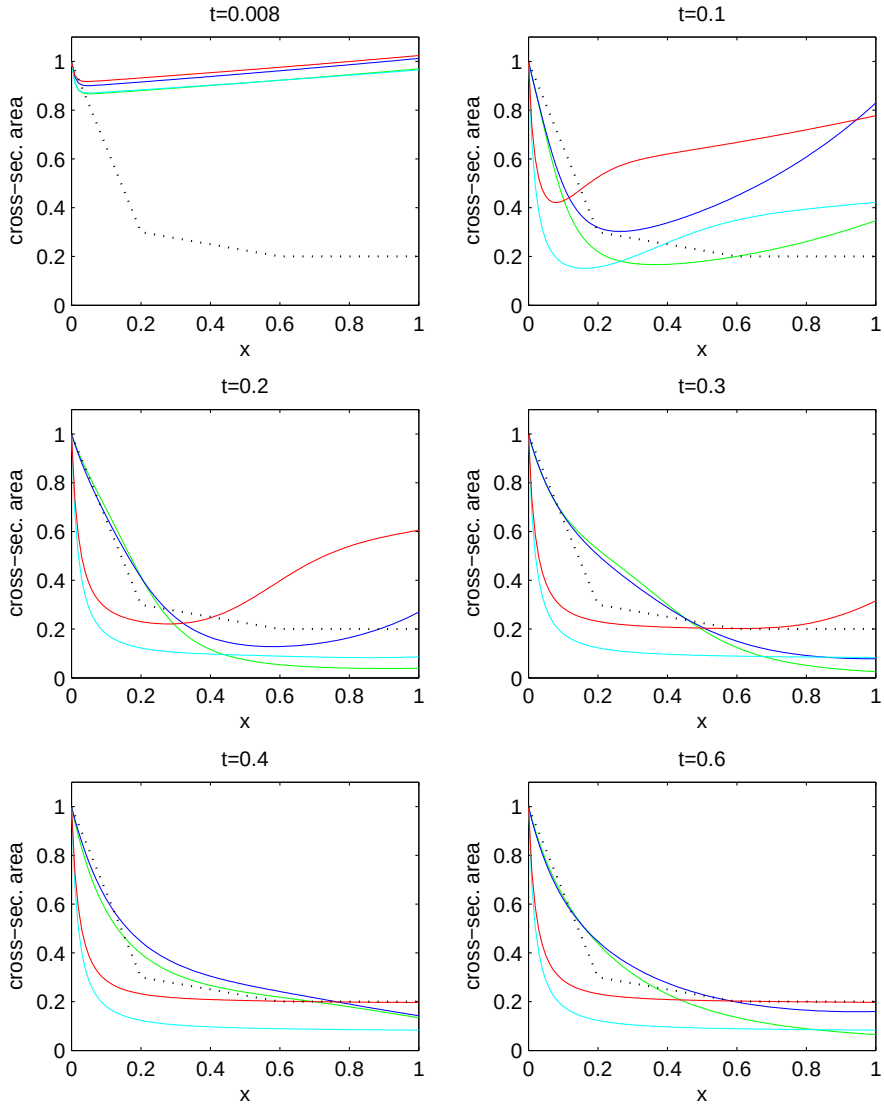


Figure 5.18: Cross-sectional area $A$ before and after optimization at different times for $h = 0.01$, $k = 0.004$, Isothermal: before opt.- green, after opt.- blue and $\lambda = 1.6 \times 10^{-5}$. Non-isothermal: before opt.- cyan, after opt.- red and $\lambda = 5.8 \times 10^{-5}$. (NCG algorithm).

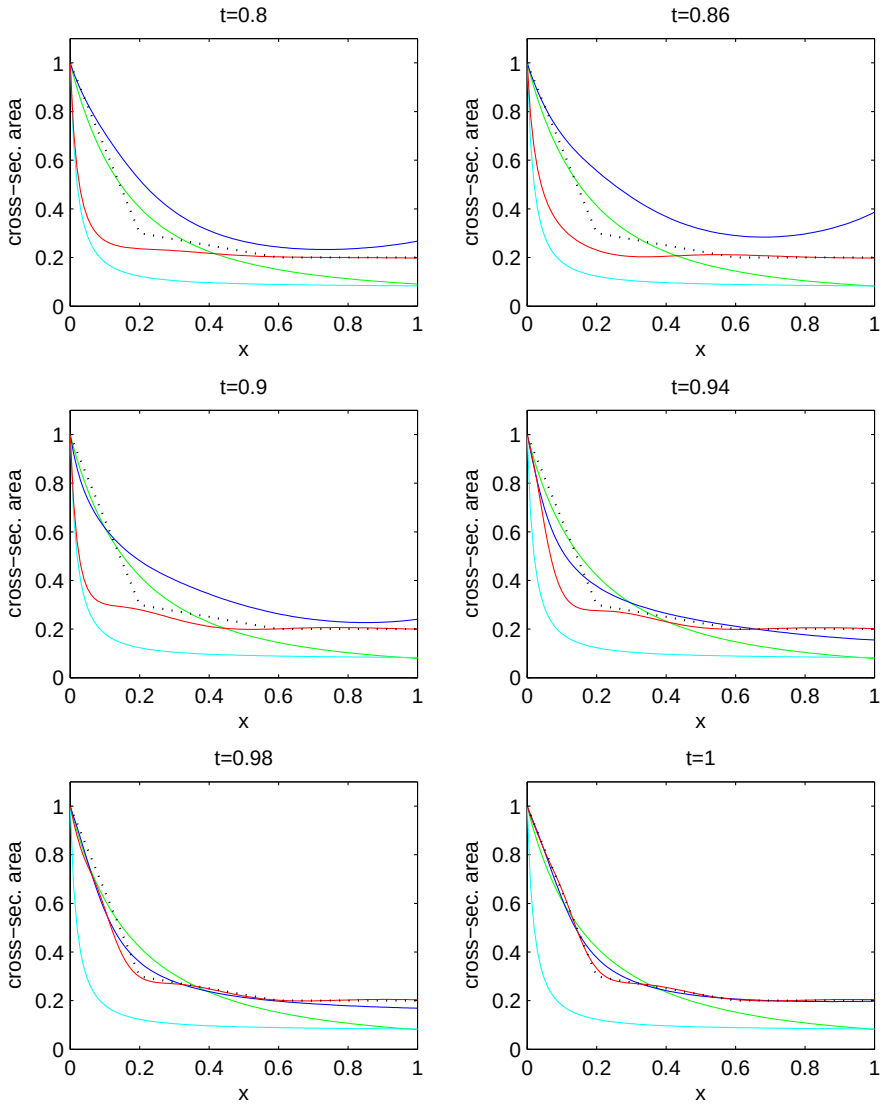


Figure 5.19: Cross-sectional area $A$ before and after optimization at different times for $h = 0.01$, $k = 0.004$, Isothermal: before opt.- green, after opt.- blue and $\lambda = 1.6 \times 10^{-5}$. Non-isothermal: before opt.- cyan, after opt.- red and $\lambda = 5.8 \times 10^{-5}$. (NCG algorithm).

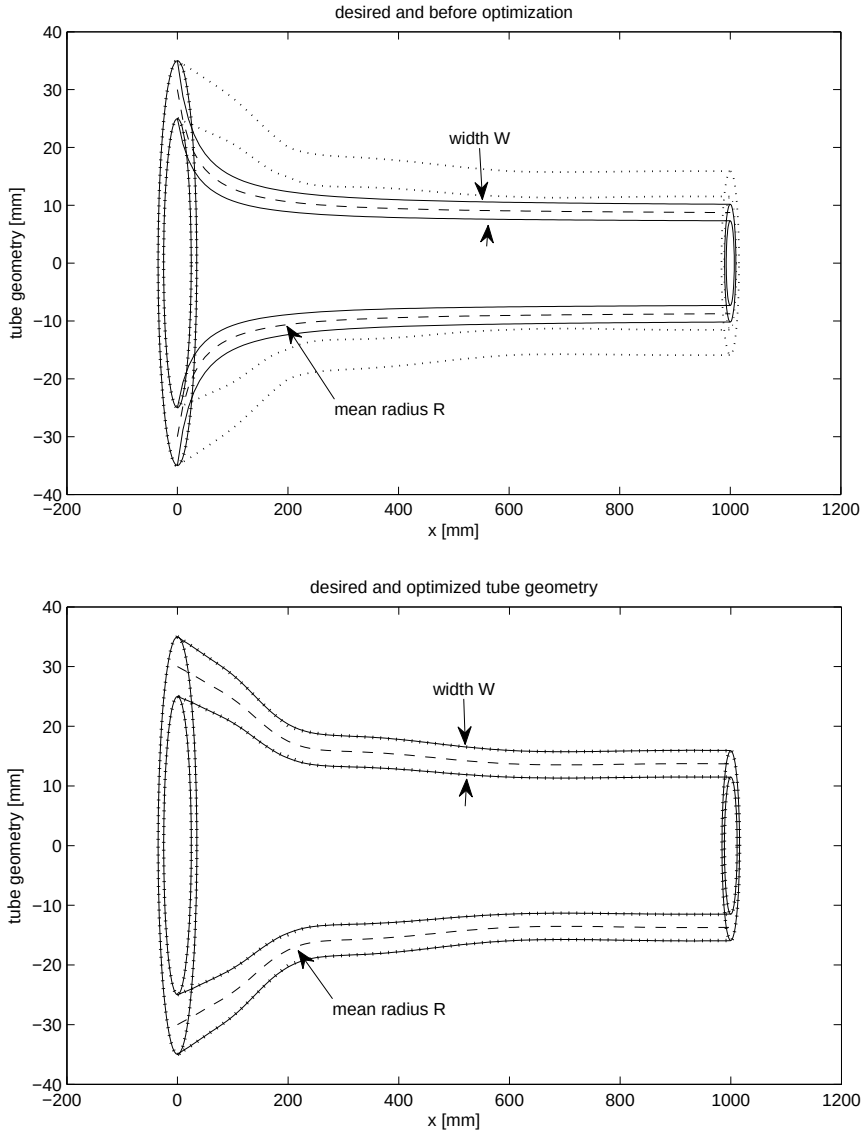


Figure 5.20: Tube geometry before and after optimization at $t = t_f$. (for $h = 0.01$, $k = 0.004$ and $\lambda = 5.8 \times 10^{-5}$- NCG algorithm)

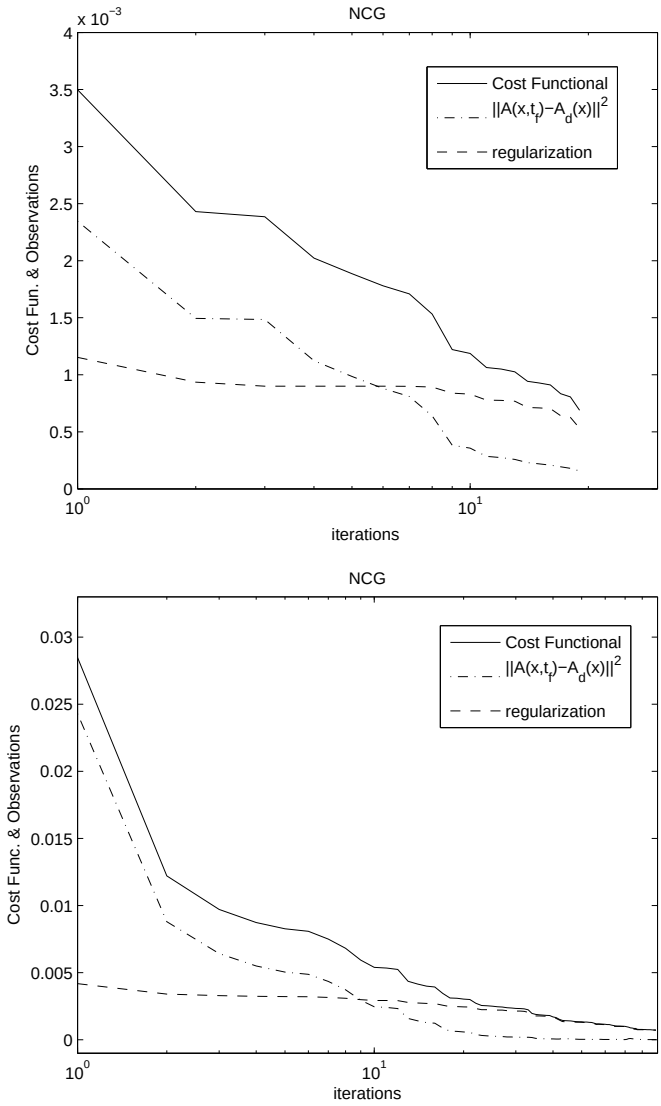


Figure 5.21: Cost functional and observations for $h = 0.01$, $k = 0.004$, Isothermal (top): $\lambda = 1.6 \times 10^{-5}$, Non-isothermal (bottom): $\lambda = 5.8 \times 10^{-5}$ .

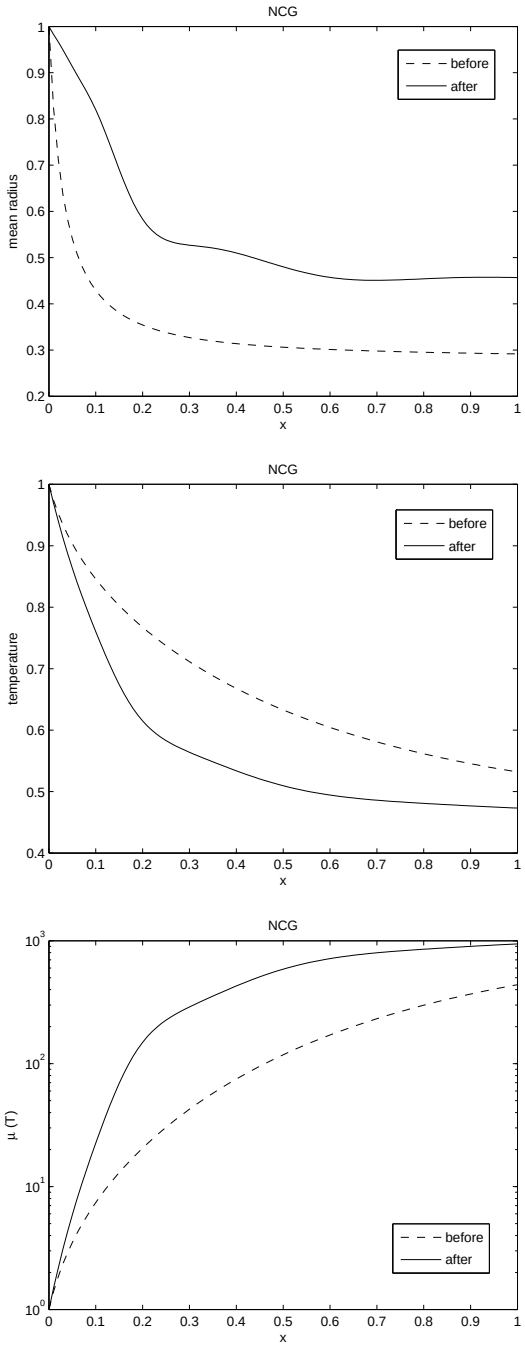


Figure 5.22: Mean radius $R$ (top), temperature $T$ (middle) and viscosity $\mu(T)$ (bottom) before and after optimization at time $t = t_f$ for $h = 0.01$, $k = 0.004$ and $\lambda = 5.8 \times 10^{-5}$ (NCG algorithm - non-isothermal tube drawing).

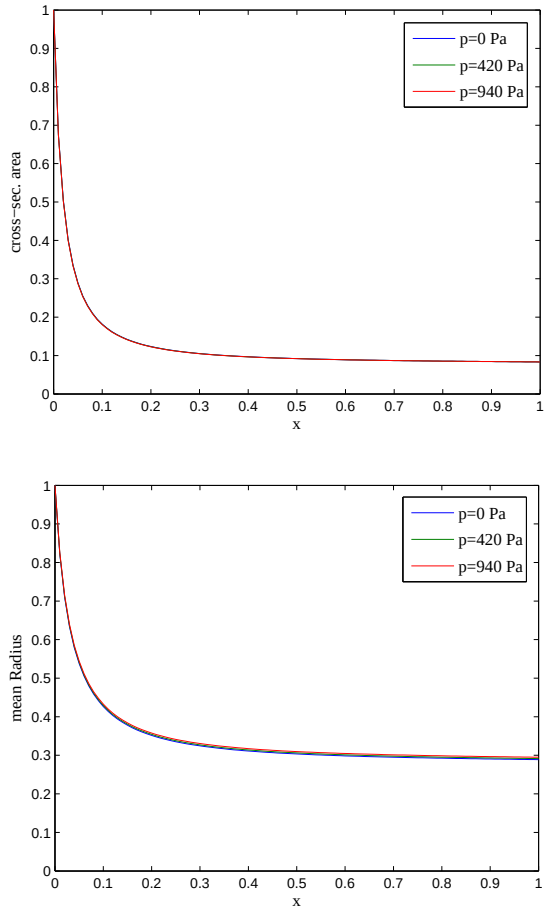


Figure 5.23: Cross-sec. Area (top) and mean radius (bottom) under different pressures (non-isothermal tube drawing).

**Remark 5.1** *For the simulations presented above, we did not consider the inside blowing pressure as a control variable. The reason is that it does not have any effect on the cross-sectional area $A$, as shown in figure 5.23(top) where one cannot see any change in the area under different blowing pressures. However depending upon the physical parameters used for the simulations, it may only affect the mean radius $R$ and the width $W$ of the tube. But for the physical parameters used in our numerical simulations, we don't observe any significant change in the mean radius $R$ under different blowing pressures (see the figure 5.23(bottom)).*

# Chapter 6

# Conclusions

In this thesis we studied the optimal control problems of the tube drawing process with the aim to control the circular cross-sectional area of the tube. Since pulling speed of the drawing machine greatly influences the cross-sectional area, we considered it as the control variable. We derived the model equations both for the isothermal and the non-isothermal tube drawing processes. In section 2.1, we considered the Stokes equations and the energy equation to describe the slow flow of the molten glass and then by exploiting the large aspect ratio of the flow, we derived the simplified model equations. In section 2.2 we described the isothermal model of the tube drawing and proved the existence and the uniqueness of the solutions of the stationary nonlinear equations of the model.

Based on our goal and the derived model equations, we formulated the constrained optimization problem to determine the optimal drawing speed which in turn led us to the desired cross-sectional area. To solve the problem, we used the adjoint variable approach. We introduced the Lagrangian functional associated with the minimization problem and derived the first order and the second order optimality conditions both for the isothermal (see appendix A) and the non-isothermal models. In section 3.4.1.1, we presented the existence and uniqueness results for the solution of the stationary adjoint equations for isothermal tube drawing process.

To solve the optimality conditions, we defined the solution algorithms based on the steepest descent, nonlinear conjugate gradient, BFGS and the Newton approaches. In the Newton method, we introduced the CG iterations to solve the Newton equation in order to avoid more numerical efforts involved in computing the Hessian matrix. To stop these CG iterations, the criterion

defined in [33, 37, 44] was used, which (depending upon the parameters involved) also gave us the linear, the superlinear and the quadratic convergence of the algorithm (Newton-CG). In each of the solution algorithms, we used the strong Wolf conditions to find the optimal step length.

Numerical results are obtained for two different cases. In the first case, we controlled the area for the entire time domain. In this case, we observed that the isothermal process starts with a higher drawing speed as compared to the non-isothermal process and after time $t = 0.1$ both have a significant decrease in speed and become almost similar. We also noticed that the cross-sectional area in the non-isothermal case reaches the desired state earlier than the isothermal case. However the overall computing time for the isothermal process is less than that of the non-isothermal process. In the second case, we controlled the area at the final time $t = t_f$. Our observation in this case is that both the isothermal and the non-isothermal processes start with the same low drawing speeds which remain constant till $t = 0.6$ and afterwards start varying with time and get a significant increase in the speed at the end. The isothermal process stops with a higher drawing speed as compared to the non-isothermal process. This sudden increase in the speed near the final time is because of our objective to control area at the final time. We also notice in this case that the cross-sectional area exactly matches to the desired area in non-isothermal tube drawing.

For our optimal control problems, we also compared the performance of the optimization algorithms in terms of the solution iterations, functional evaluations and the computation time. From the performance comparisons shown in the tables 5.3 and 5.5, we can conclude that the Newton-CG method is better than the others for our optimal control problems. However, to implement this algorithm we have to collect the second derivative informations.

# Appendix A

# Control Problem for Isothermal Tube Drawing

We define here the optimal control problem for the isothermal tube drawing process and give a brief derivation of the first order and the second order optimality conditions necessary for solving the control problem. The detailed procedure of derivation is given in Chapter 3.

The isothermal model (2.21) in dimensionless form is given as:

$$(A)_t + (vA)_x = 0, \tag{A.1a}$$

$$(3Av_x)_x + StA = 0, \tag{A.1b}$$

$$\left(R^2\right)_t + \left(vR^2\right)_x = \frac{\pi c_1 p}{A}\left(R^4 - \frac{A^2}{\left(4\pi c_1\right)^2}\right) \tag{A.1c}$$

$$\tag{A.1d}$$

where dimensionless parameters are

$$St = \frac{\rho g L^2}{v_0 \mu}, \quad c_1 = \frac{R_0^2}{A_0}.$$

The initial and boundary conditions are respectively given as:

$$A(x,0) = 1,\ R(x,0) = 1,\ for\ x \in [0,1] \tag{A.1e}$$

and

$$A(0,t) = 1,\ R(0,t) = 1,\ v(0,t) = 1,\ v(1,t) = v_d,\ for\ t \in [0,t_f] \tag{A.1f}$$

where $v_d = \dfrac{v_L}{v_0}$.

## A.1 Optimal Control Problem

The integration domains used in the weak formulation are $Q := \Omega \times (0, t_f)$, $\Sigma_0 := 0 \times (0, t_f)$ and $\Sigma_1 := 1 \times (0, t_f)$ where $\Omega = (0, 1)$ is the space domain. The appropriately chosen spaces are the Hilbert space $U$ and the Banach spaces $Y$ and $Z$ where $U$ is the space of controls $u = (v_d)$, $Y$ is the space of states $y = (A, v, R)$ and $Z$ is the space of test functions.

**Definition A.1** *The weak formulation of the state system* (A.1) *is given by*

$$E(y, u) = 0, \tag{A.2a}$$

*where the operator*

$$E = (E_1, E_2, E_3, E_{A_0}, E_{R_0}) : Y \times U \to Z^*$$

*is defined as*

$$\begin{aligned}\langle E_1(y,u), \xi_A \rangle := &\int_0^{t_f} \langle A_t, \xi_A \rangle dt - \int_Q vA(\xi_A)_x dx dt - \int_{\Sigma_0} \xi_A dt \\ &+ \int_{\Sigma_1} v_d(t) A \xi_A dt = 0,\end{aligned} \tag{A.2b}$$

$$\begin{aligned}\langle E_2(y,u), \xi_v \rangle := &\int_Q (3A(\xi_v)_x)_x v dx dt + \int_Q (St) A \xi_v dx dt + \int_{\Sigma_0} 3(\xi_v)_x dt \\ &- \int_{\Sigma_1} 3Av_d(t)(\xi_v)_x dt - \int_{\Sigma_0} 3v_x \xi_v dt + \int_{\Sigma_1} 3Av_x \xi_v dt = 0,\end{aligned} \tag{A.2c}$$

$$\begin{aligned}\langle E_3(y,u), \xi_R \rangle := &\int_0^{t_f} \langle (R^2)_t, \xi_R \rangle dt - \int_Q \frac{\pi c_1 p}{A} \left( R^4 - \frac{A^2}{(4\pi c_1)^2} \right) \xi_R dx dt \\ &- \int_Q vR^2 (\xi_R)_x dx dt - \int_{\Sigma_0} \xi_R dt + \int_{\Sigma_1} v_d(t) R^2 \xi_R dt = 0\end{aligned} \tag{A.2d}$$

*with*

$$E_{A_0} = A(0) - 1, \quad E_{R_0} = R(0) - 1 \tag{A.2e}$$

*for all test functions* $(\xi_A, \xi_v, \xi_R) \in Z$.

Now the minimization problem subject to cost functional (3.1) reads

$$\min_{(y,u) \in Y \times U} \quad J(y, u) \quad \textit{subject to } E(y, u) = 0. \tag{A.3}$$

## A.2 Derivatives

**Lemma A.1** *Let the mapping $E : Y \times U \to Z^*$ be twice continuously Fréchet differentiable. Then the action of the first two derivatives of $E = (E_1, E_2, E_3)$ at $(y, u) \in Y \times U$ in directions $\tilde{y} = (\tilde{A}, \tilde{v}, \tilde{R})$ and $(\tilde{y}, \hat{y}) = \left((\tilde{A}, \tilde{v}, \tilde{R}), (\hat{A}, \hat{v}, \hat{R})\right) \in (Y \times U)^2$ are respectively given by*

$$\begin{aligned}
\langle E_{1y}(y,u)\tilde{y}, \xi_A\rangle &= \int_0^{t_f} \langle (\tilde{A})_t, \xi_A\rangle dt - \int_Q (v\tilde{A} + \tilde{v}A)(\xi_A)_x dxdt + \int_{\Sigma_1} v_d \tilde{A}\xi_A dt,\\
\langle E_{2y}(y,u)\tilde{y}, \xi_v\rangle &= \int_Q St\tilde{A}\xi_v dxdt - \int_Q 3\left(\tilde{A}v_x + A\tilde{v}_x\right)(\xi_v)_x dxdt\\
&\quad + \int_{\Sigma_1} 3\left(\tilde{A}v_x + A\tilde{v}_x\right)\xi_v dt - \int_{\Sigma_0} 3\tilde{v}_x\xi_v dt,
\end{aligned}$$

$$\begin{aligned}
\langle E_{3y}(y,u)\tilde{y}, \xi_R\rangle &= \int_0^{t_f} \langle (2R\tilde{R})_t, \xi_R\rangle dt + \int_Q \pi c_1 p\left(\frac{R^4}{A^2} + \frac{1}{(4\pi c_1)^2}\right)\tilde{A}\xi_R dxdt\\
&\quad - \int_Q 2vR\tilde{R}(\xi_R)_x dxdt - \int_Q \frac{4\pi c_1 p R^3 \tilde{R}}{A}\xi_R dxdt\\
&\quad - \int_Q \tilde{v}R^2(\xi_R)_x dxdt + \int_{\Sigma_1} 2v_d R\tilde{R} dt
\end{aligned}$$

*and*

$$\begin{aligned}
\langle E_{1yy}(y,u)\left[\tilde{y},\hat{y}\right], \xi_A\rangle &= -\int_Q (\tilde{v}\hat{A} + \hat{v}\tilde{A})(\xi_A)_x dxdt,\\
\langle E_{2yy}(y,u)\left[\tilde{y},\hat{y}\right], \xi_v\rangle &= \int_{\Sigma_1} 3\left(\hat{A}\tilde{v}_x + \tilde{A}\hat{v}_x\right)\xi_v dt - \int_Q 3\left(\hat{A}\tilde{v}_x + \tilde{A}\hat{v}_x\right)(\xi_v)_x dxdt,
\end{aligned}$$

$$\begin{aligned}
\langle E_{3yy}(y,u)\left[\tilde{y},\hat{y}\right], \xi_R\rangle &= \int_0^{t_f} \langle (2\hat{R}\tilde{R})_t, \xi_R\rangle dt - \int_Q \frac{12\pi c_1 p R^2 \hat{R}\tilde{R}}{A}\xi_R dxdt\\
&\quad + \int_Q \frac{4\pi c_1 p R^3 \hat{R}\tilde{A}}{A^2}\xi_R dxdt + \int_Q 2\pi c_1 p R^3\left(\frac{2\tilde{R}}{A^2} - \frac{R\tilde{A}}{A^3}\right)\\
&\quad \times \hat{A}\xi_R dxdt - \int_Q 2\left(v\hat{R}\tilde{R} + \tilde{v}R\hat{R} + \hat{v}R\tilde{R}\right)(\xi_R)_x dxdt\\
&\quad + \int_{\Sigma_1} 2v_d\hat{R}\tilde{R}\xi_R dt,
\end{aligned}$$

□

## A.3 First order conditions

The Lagrange functional $L : Y \times U \times Z \to \mathbb{R}$ associated with the problem (A.3) is defined as

$$L(y, u, \xi) = J(y, u) + \langle E(y, u), \xi \rangle_{Z^*, Z}$$

where $\xi = (\xi_A, \xi_R, \xi_v) \in Z$ are the adjoint variables.

The first-order optimality conditions are then computed by setting the directional derivatives of $L$ with respect to $(y, u, \xi)$ equal to zero in all admissible directions. Taking variation of $L$ with respect to $y$ in direction $\tilde{y}$ leads us to the following system of adjoint equations.

$$\begin{aligned} -(\xi_A)_t - v(\xi_A)_x =& 3v_x(\xi_v)_x - St(\xi_v) - w_1(A - A_d) \\ & - \pi c_1 p \xi_R \left( \frac{R^4}{A^2} + \frac{1}{(4\pi c_1)^2} \right), \qquad \text{(A.4a)} \\ (3A(\xi_v)_x)_x =& A(\xi_A)_x + R^2(\xi_R)_x, \qquad \text{(A.4b)} \\ -(\xi_R)_t - v(\xi_R)_x =& \frac{2\pi c_1 p R^2}{A} \xi_R. \qquad \text{(A.4c)} \end{aligned}$$

with the boundary conditions

$$\xi_A(1, t) = 0,\ \xi_R(1, t) = 0,\ \xi_v(1, t) = 0,\ \xi_v(0, t) = 0,\ for\ t \in [0, t_f] \quad \text{(A.4d)}$$

and the terminal conditions

$$\xi_A(x, t = t_f) = -w_2 \left( A(x, t_f) - A_d \right),\ \xi_R(x, t_f) = 0,\ for\ x \in [0, 1] \quad \text{(A.4e)}$$

Then taking variation of $L$ with respect to $u$ in the direction $\tilde{u}$ and assuming sufficient regularity and the uniqueness of the solution of (A.1), we write the gradient of the reduced cost functional $\hat{J}(u) = J(y(u), u)$ as

$$\hat{J}'(u) = \lambda u - 3A(\xi_v)_x, \qquad on \quad \{1\} \times [0, t_f] \qquad \text{(A.5)}$$

## A.4 Second order conditions

To implement the Newton Algorithm 4.4, we need to collect the second derivative information of the reduced cost functional $\hat{J}(u) := J(y(u), u)$.

By using the definition of the Lagrange functional, for arbitrary $\xi \in Z$,

$$L\left(y(u),u,\xi\right) = J\left(y(u),u\right) + \left\langle E\left(y(u),u\right),\xi\right\rangle_{Z^*,Z} = J\left(y(u),u\right) = \hat{J}(u). \tag{A.6}$$

the second derivative of $\hat{J}$ is given as

$$\begin{aligned}\hat{J}''(u)\delta u =& y'(u)^* L_{yy}\left(y(u),u,\xi(u)\right) y'(u)\delta u + y'(u)^* L_{yu}\left(y(u),u,\xi(u)\right)\delta u \\ &+ L_{uy}\left(y(u),u,\xi(u)\right) y'(u)\delta u + L_{uu}\left(y(u),u,\xi(u)\right)\delta u.\end{aligned} \tag{A.7}$$

We use the following procedure to compute $\hat{J}''(u)\delta u$.

1. compute the solution

$$V = y'(u)\delta u = -E_y(y(u),u)^{-1} E_u(y(u),u)\delta u$$

for linearized state variables $V := (V_A, V_v, V_R)$ i.e.,

$$(V_A)_t + (vV_A)_x = -\left(AV_v\right)_x, \tag{A.8a}$$

$$(3A(V_v)_x)_x = -\left(3V_A v_x\right)_x - StV_A, \tag{A.8b}$$

$$\begin{aligned}(RV_R)_t + (vRV_R)_x - \frac{2\pi c_1 p R^3}{A}V_R =& -\frac{1}{2}(R^2 V_v)_x \\ &- \frac{\pi c_1 p V_A}{2}\left(\frac{R^4}{A^2} + \frac{1}{(4\pi c_1)^2}\right),\end{aligned} \tag{A.8c}$$

with boundary conditions

$$V_A(0,t) = 0,\ V_R(0,t) = 0,\ V_v(0,t) = 0,\ V_v(1,t) = \delta u,\ t \in [0,t_f] \tag{A.8d}$$

and initial conditions

$$V_A(x,0) = 0,\ V_R(x,0) = 0,\ x \in [0,1] \tag{A.8e}$$

2. compute

$$\begin{pmatrix} s_1 \\ s_2 \end{pmatrix} = \begin{pmatrix} (J_{yy} + \langle E_{yy},\xi\rangle)(V,.) + (J_{yu} + \langle E_{yu},\xi\rangle)(\delta u,.) \\ (J_{uy} + \langle E_{uy},\xi\rangle)(V,.) + (J_{uu} + \langle E_{uu},\xi\rangle)(\delta u,.) \end{pmatrix}$$

where $s_2$ is computed as

$$s_2 = -3(\xi_v)_x V_A + \lambda\delta u, \quad on \quad \{1\}\times(0,t_f)$$

3. compute the solution

$$W = E_y(y(u), u)^{-*} s_1$$

where $W := (W_A, W_v, W_R)$ i.e., solve

$$\begin{aligned} -(W_A)_t - v(W_A)_x =& \pi c_1 p \left[ \frac{2R^3 \xi_R}{A^3} (2AV_R - RV_A) - W_R \left( \frac{R^4}{A^2} + \frac{1}{(4\pi c_1)^2} \right) \right] \\ &+ 3 \left\{ (W_v)_x v_x - (\xi_v)_x (V_v)_x \right\} + w_1 V_A - (St) W_v - V_v (\xi_A)_x \end{aligned}$$

$$(3A(W_v)_x)_x = A(W_A)_x + R^2 (W_R)_x - 2RV_R (\xi_R)_x + (3V_A (\xi_v)_x)_x - V_A (\xi_A)_x,$$

$$\begin{aligned} -R(W_R)_t - vR(W_R)_x - \frac{2\pi c_1 p R^3}{A} W_R =& - RV_v (\xi_R)_x \\ &+ \frac{2\pi c_1 p R^2 \xi_R}{A^2} (RV_A - 2V_R A) . \end{aligned}$$

with boundary conditions

$$W_A(1,t) = 0,\ W_R(1,t) = 0,\ W_v(0,t) = 0,\ W_v(1,t) = 0,\ t \in [0, t_f]$$

and terminal conditions

$$W_A(x, t_f) = w_2 V_A(x, t_f),\ W_R(x, t_f) = 0,\ x \in [0, 1]$$

4. compute

$$s_3 = -E_u(y(u), u)^* W = 3A(W_v)_x, \quad on \quad \Sigma_1$$

5. and set

$$\hat{J}''(u)\delta u = s_2 + s_3$$

which reads as

$$\hat{J}''(u)\delta u = 3A(W_v)_x - 3V_A(\xi_v)_x + \lambda \delta u, \quad on \quad \Sigma_1 \tag{A.10}$$

# Appendix B

# Basic Definitions and Theorems

We introduce here some basic definitions, lemmas and theorems that are needed and used in defining and solving the optimal control problems.

**Definition B.1** *[37] Let $F : U \subset X \to Y$ be an operator with Banach spaces $X$, $Y$ and $U \neq \emptyset$ open. Then*

*(a) $F$ is called directionally differentiable at $x \in U$ if the limit*

$$dF(x,h) = \lim_{t \to 0^+} \frac{F(x+th) - F(x)}{t} \in Y$$

*exist for all $h \in X$. In this case, $dF(x,h)$ is called directional derivative of $F$ in the direction $h$.*

*(b) $F$ is called Gâteaux differentiable (G-differentiable) at $x \in U$ if $F$ is directionally differentiable at $x$ and the directional derivative $F'(x) : X \ni h \mapsto dF(x,h) \in Y$ is bounded and linear,i.e., $F'(x) \in \mathcal{L}(X,Y)$.*

*(c) $F$ is called Fréchet-differentiable at $x \in U$ if $F$ is G-differentiable at $x$ and if the following approximation condition holds:*

$$\|F(x+h) - F(x) - F'(x)h\|_Y = o\left(\|h\|_X\right) \quad for \quad \|h\|_X \to 0.$$

*(d) If $F$ is Fréchet-differentiable in a neighbourhood $V$ of $x$, and $F' : V \to \mathcal{L}(X,Y)$ is itself Fréchet-differentiable at $x$, then $F$ is called twice Fréchet-differentiable at $x$ and is written as $F''(x) \in \mathcal{L}(X, \mathcal{L}(X,Y))$.*

**Remark B.1** *Fréchet-differentiability of $F$ at $x$ implies continuity of $F$ at $x$. Furthermore $F$ is $k$-times continuously Fréchet-differentiable if $F$ is $k$-times Fréchet-differentiable and $F^k$ is continuous [37].*

**Theorem B.2** *[37] (Riesz representation theorem) The dual space $H^*$ of a Hilbert space $H$ is isometric to $H$ itself. More precisely, for every $v \in H$ the linear functional $u^*$ defined by*

$$\langle u^*, u\rangle_{H^*,H} := (v,u)_H \ \forall\ u \in H$$

*is in $H^*$ with norm $\|u^*\|_{H^*} = \|v\|_H$. Vice versa, for any $u^* \in H^*$ there exists a unique $v \in H$ such that*

$$\langle u^*, u\rangle_{H^*,H} = (v,u)_H \ \forall\ u \in H$$

*and $\|u^*\|_{H^*} = \|v\|_H$.*

**Theorem B.3** *[37](Implicit Function Theorem) Let $Y$, $Y$, $Z$ be Banach spaces and let $F : G \to Z$ be a continuously Fréchet-differentiable map from an open set $G \subset X \times Y$ to $Z$. Let $(\bar{x}, \bar{y}) \in G$ be such that $F(\bar{x}, \bar{y}) = 0$ and that $F_y(\bar{x}, \bar{y}) \in \mathcal{L}(Y, Z)$ has a bounded inverse.*
*Then there exists an open neighbourhood $U_X(\bar{x}) \times U_Y(\bar{y}) \subset G$ of $(\bar{x}, \bar{y})$ and a unique continuous function $w : U_X(\bar{x}) \to Y$ such that*

1. *$w(\bar{x}) = \bar{y}$,*
2. *For all $x \in U_X(\bar{x})$ there exists exactly one $y \in U_Y(\bar{y})$ with $F(x, y) = 0$, namely $y = w(x)$.*

*Moreover, the mapping $w : U_X(\bar{x}) \to Y$ is continuously Fréchet-differentiable with derivative*

$$w'(x) = F_y\left(x, w(x)\right)^{-1} F_x\left(x, w(x)\right).$$

*If $F : G \to Z$ is m-times continuously Fréchet-differentiable then also $w : U_X(\bar{x}) \to Y$ is m-times continuously Fréchet-differentiable.*

**Proof:** see for example [13].

**Definition B.2** *[37] Let $X$ be a Banach space. A sequence $(x_k)_{k\in\mathbb{N}} \subset X$ converges weakly to $x \in X$ i.e., $x_k \rightharpoonup x$ if*

$$\langle x^*, x_k\rangle_{X*,X} \to \langle x^*, x\rangle_{X*,X} \text{ as } k \to \infty \quad \forall x^* \in X^*$$

*where $\langle x^*, x\rangle_{X*,X} := x^*(x)$ denotes the functional value of $x^*$ at $x$.*

**Definition B.3** *[37] A Banach space $X$ is called reflexive if the mapping $x \in X \mapsto \langle ., x\rangle_{X*,X} \in (X^*)^*$ is surjective, i.e., if for any $x^{**} \in (X^*)^*$ there exists $x \in X$ with*

$$\langle x^{**}, x^*\rangle_{(X*)^*,X^*} \to \langle x^*, x\rangle_{X*,X} \quad \forall x^* \in X^*$$

**Remark B.4** *$L^p$ spaces, because of isometric isomorphisms property $(L^p)^* = L^q$ where $1 < p, q < \infty, \frac{1}{p} + \frac{1}{q} = 1$, are reflexive. Moreover, any Hilbert space is reflexive by the Riesz representation theorem.*

**Theorem B.5** *[37] (Weak sequential compactness) Let $X$ be a reflexive Banach space. Then the following holds*

1. *Every bounded sequence $(x_k) \subset X$ contains a weakly convergent subsequence, i.e., there are $(x_{k_i}) \subset (x_k)$ and $x \in X$ with $x_{k_i} \rightharpoonup x$.*
2. *Every bounded, closed and convex subset $C \subset X$ is weakly sequentially compact, i.e., every sequence $(x_k) \subset C$ contains a weakly convergent subsequence $(x_{k_i}) \subset (x_k)$ with $x_{k_i} \rightharpoonup x$, where $x \in C$.*

For proof see for example [25, 17].

**Definition B.4** *[37] Let $X$ be a Banach space, $M \subset X$. A function $F : M \to \mathbb{R}$ is weakly lower semicontinuous if $x_k \in M$ and $x_k \rightharpoonup x \in M$ imply*

$$F(x) \leq \liminf_{k\to\infty} F(x_k)$$

**Theorem B.6** *[37] Let $X$ be a Banach space. Then any continuous, convex functional $F : X \to \mathbb{R}$ is weakly lower semicontinuous, i.e.,*

$$x_k \rightharpoonup x \quad \Longrightarrow \quad F(x) \leq \liminf_{k\to\infty} F(x_k)$$

**Theorem B.7** *[51] If the functions $p(t)$ and $g(t)$ are continuous on an open interval $I$: $\alpha < t < \beta$ containing the point $t = t_0$, then there exists a unique solution $y = \phi(t)$ that satisfies the differential equation*

$$\frac{dy}{dt} + p(t)y = g(t), \tag{B.1a}$$

*for each $t$ in $I$, and that also satisfies the initial condition*

$$y(t_0) = y_0, \tag{B.1b}$$

*where $y_0$ is an arbitrary prescribed initial value.* □

**Theorem B.8** *[51] Let the functions $f$ and $\partial f/\partial y$ be continuous in some rectangle $\alpha < t < \beta$, $\gamma < y < \delta$ containing the point $(t_0, y_0)$. Then, in some interval $t_0 - h < t < t_0 + h$ contained in $\alpha < t < \beta$, there is a unique solution $y = \phi(t)$ of the initial value problem,*

$$\frac{dy}{dt} = f(t, y), \quad y(t_0) = y_0.$$

□

**Lemma B.9** *[37] (Lax-Milgram lemma) Let $V$ be a real Hilbert space with inner product $(.,.)_V$ and let $a : V \times V \to \mathbb{R}$ be a bilinear form that satisfies with constants $\alpha_0, \beta_0 > 0$*

$$\begin{aligned} |a(y, v)| &\leq \alpha_0 \|y\|_V \|v\|_V \quad \forall\ y, v \in V, && (boundedness) \\ a(y, y) &\geq \beta_0 \|y\|_V^2 \quad \forall\ y \in V && (V - coercivity) \end{aligned}$$

*Then for any bounded linear functional $F \in V^*$, the variational equation*

$$a(y, v) = F(v) \quad \forall v \in V$$

*has a unique solution $y \in V$. Moreover, $y$ satisfies*

$$\|y\|_V \leq \frac{1}{\beta_0} \|F\|_{V^*}$$

*For proof see [41].*

# List of Figures

# List of Tables

# Bibliography


[1] A.A. Goldstein, On Steepest Descent, SIAM J. Control, 1965, 3: 147-151.

[2] A. Cohen, Rate of Convergence of Several Conjugate Gradient Algorithms, SIAM J. Numer. Anal., 1972, 9: 248-259.

[3] A.D. Fitt, K. Furusawa, T.M. Monro, C.P. Please, Modelling the Fabrication of Hollow Fibers: Capillary Drawing, Journal of lightwave Technology, December 2001, vol. 19, No. 12.

[4] A.D. Fitt, K. Furusawa, T.M. Monro, C.P. Please, D.J. Richardson, The mathematical Modelling of Capillary Drawing for Holey Fiber Manufacture, Journal of Engineering Mathematics, 2002, 43: 201-227.

[5] B. Dayanand Reddy, Functional Analysis and Boundary-value Problems: an Introductory Treatment. Longman Scientific & Technical, 1986.

[6] Christian Grossmann, Hans-Grg Roos, Martin Stynes, Numerical Treatment of Partial Differential Equations, Springer-Verlag Berlin Heidelberg, 2007.

[7] C. A. Tobias Schulze, Minimizing Thermal Stress in Glass Production Processes: Model Reduction and Optimal Control, PhD thesis, Shaker Verlag Aachen 2007.

[8] C.T.Kelly, Iterative Methods for Linear and Nonlinear Equations. SIAM Philadelphia, 1995.

[9] C.T.Kelly, Iterative Methods for Optimization. SIAM Philadelphia, 1999.

[10] D. Krause, H. Loch (Eds.) Mathematical Simulation in Glass Technology , Springer-Verlag: 293-307, Berlin, Heidelberg, 2002.

[11] D.F. Shanno, On the Convergence of a New Conjugate Gradient Algorithm, SIAM J. Numer. Anal., 1978, 15: 1247-1257.

[12] E. Polak, G. Ribière, Note Sur la Convergence de Directions Conjuguées, Rev. Fransaise Infomat Recherche Operatonelle, 3e Année, 1969, 16: 35-43.

[13] E. Zeidler, Nonlinear Functional Analysis and its applications I, Fixed-Point Theorems. Springer, Berlin, 1986.

[14] F. Abergel, R. Temam, On Some Control Problems in Fluid Mechanics, Theoretical and Computational Fluid Dynamics, 1990, 1: 303-325.

[15] G. Murad, I. Postlethwaite, D.-W. Gu and J.F. Whidborne, Robust Control of a Glass Tube Production Process, IEE, Syvoy Place, London UK, 1994.

[16] H. Huang, R.M. Miura, W.P. Ireland and E. Puil, Heat-induced Stretching of a Glass Tube under Tension: Application to glass microelectrodes. SIAM J. Appl. Math., 2003, vol. 63, No. 5. 1499-1519.

[17] H.W. Alt, Lineare Funktionalanalysis, Springer, 1999.

[18] I.M. Griffiths, P.D. Howell, Mathematical Modelling of Non-axisymmetric Capillary Tube Drawing, J. Fluid Mechanics 2008, 605: 181-206 Cambridge University Press.

[19] J.C. Gilbert, J. Nocedal, Global Convergence Properties of Conjugate Gradient Methods for Optimization, SIAM J. Optim., 1992, 2(1): 21-42.

[20] John C. Strikwerda, Finite Difference Schemes and Partial Differential Equations, 2nd Edit. SIAM, 2004.

[21] J.M. Ortega and W.C. Rheinboldt, Iterative Solution of Nonlinear Equations in Several Variables, Academic Press, New York, 1970.

[22] J. Nocedal, S.J. Wright, Numerical Optimization, Springer Series in Operations Research, 1999.

[23] K. Ito, S.S. Ravindran, Optimal Control of Thermally Convected Fluid Flows. SIAM Journal on Scientific Computing, 1998, 19(6): 1847-1869.

[24] K. Selvanayagam, T. Gtz, S. Sundar, V. Vetrivel, Optimal Control of Film Casting Processes. Int. J. for Num. Math. in Fluids., 2008.

[25] K. Yosida, Functional Analysis. Springer 1980.

[26] L. Armijo, Minimization of Functions having Lipschitz Continuous Partial Derivatives, Pacific J. Math. 1966, 16:1-3.

[27] L.Grippo, S. Lucidi, A globally Convergent Version of the Polak-Ribière Conjugate Gradient Method, Math. Programming, 1997, 78: 375-392.

[28] L.J. Cummings, P.D. Howell, On the Evolution of Non-axisymmetric Viscous Fibers with Surface Tension, Inertia and Gravity. J. Fluid Mech., 1999, 389, pp:361-389.

[29] L.S. Hou, S.S. Ravindran, Computations of Boundary Optimal Control Problems for an Electrically Conducting Fluid. Journal Computational Physics 1996; 128: 319-330.

[30] M.D. Gunzburger, S. Manservisi, The velocity Tracking Problem for Navier-Stokes Flows with Boundary Controls. SIAM J. Cont. Optim., 2000, 39: 594-634.

[31] M.D. Gunzburger, L.S. Hou, S. Manservisi, Y. Yan, Computations of Optimal Controls for Incompressible Flows, International Journal of Computational Fluid Dynamics, 1998, 11: 181-191.

[32] M. Herty, R. Pinnau, M. Seaïd, Optimal Control Problems in Radiative Transfer. Optimization Methods & Software, 2007, 22(6): 917-936.

[33] M. Hinze, Optimal and Instantaneous Control of the Instationary Navier-Stokes equations. Habilitationsschrift, Fachbereich Math. TU Berlin 2000.

[34] M. Hinze, R. Pinnau. An Optimal Control Approach to Semiconductor Design., Math. Models Methods Appl. Sci., 2002 12: 89-107.

[35] M. Hinze, R. Pinnau. Second-Order Approach to Optimal Semiconductor Design. J. Optim Theory Appl, 2007, 133: 179-199.

[36] M. Hinze, R. Pinnau. Mathematical Tools in Optimal Semiconductor Design. Bull. Inst. Math. Acad. Sin. (New Series) Vol 2 (2007), No. 2: 569-586.

[37] M. Hinze, R. Pinnau, M. Ulbrich, S. Ulbrich: Optimization with PDE Constraints. Springer, 2009.

[38] M. Hinze, S. Volkwein, Instantaneous Control for the Instationary Burgers Equation - Convergence Analysis & Numerical Implementations. Nonlinear Analysis, Theory, Methods & Applications, 2002, 50: 1-26.

[39] M.Kh. Karapet'yants, The Viscosity-Temperature Relationship for Silicate Glass. Glass and Ceramics, 1960, 15: 26-32.

[40] M.R. Hestenes, E. Stiefel, Method of Conjugate Gradient for Solving Linear Systems, J. Res. Nat. Bur. Stand., 1952 49: 409-436.

[41] M. Renardy, R.C. Rogers, An introduction to Partial Differential Equations. Springer, Berlin, 1993.

[42] P.D. Howell: Extensional Thin Layer Flows, PhD thesis, St. Catherine's College, Oxford, 1994.

[43] R. Fletcher, C.M. Reeves, Function Minimization by Conjugate Gradients, Computer Journal, 1964, 7: 149-154.

[44] R. Pinnau, A. Schulze, Newton's Method for Optimal Temperature Tracking of Glass Cooling Processes, Inverse problems in Sc. and Eng., 2007, 15(4): 303-323.

[45] R. Pinnau, G. Thömmes, Optimal Boundary Control of Glass Cooling Processes. Mathematical Methods in the Applied Sciences 2004; 27: 1261-1281.

[46] S.D. Sarboh, S.A. Milinkovic, & D.L.J. Debeljkovic, Mathematical Model of the Glass Capillary Tube Drawing Process. 1998 Glass Technol. 39, 53-67.

[47] S. H-K. Lee, Y. Jaluria, Simulation of the Transport Process in the Neck-Down Region of a Furnace Drawn Optical Fiber. Int. J. Heat Mass Transfer, 1997, 40, pp:843-856.

[48] S.J. Graham, Mathematical modelling of glass flow in container manufacture. PhD thesis, 1987.

[49] T. Bernard, E. Ebrahimi Moghaddam, Nonlinear Model Predictive Control of a Glass Forming Process based in a Finite Element Model, IEEE International Conference on Control Applications, Munich, 2006. Proceedings. Vol.2, pp:960-965

[50] U.B. Paek, R.B. Runk, Physical Behaviour of the Neck-Down Region during Furnace Drawing of Silica Fibers. J. App. Phys., 1978, 40, pp: 4417-4422.

[51] William E. Boyce, Richard C. Diprima, Elementary Differential Equations, 6th Edit. John Wiley & Sons, Inc. 1997.

[52] Zhen-Jun Shi, Jie Shen, Convergence of the Polak-Ribiére-Polyak Conjugate Gradient Method. Nonlinear Analysis, 2007, 66: 1428-1441.